

**DEVELOPMENT AND EVALUATION OF AN ADVANCED REAL-TIME
ELECTRICAL POWERED WHEELCHAIR CONTROLLER**

by

Hongwu Wang

BS, Biomedical Engineering, Xi'an Jiaotong University, 2003

MS, Biomedical Engineering, Xi'an Jiaotong University, 2005

Submitted to the Graduate Faculty of

School of Health and Rehabilitation Science in partial fulfillment

of the requirements for the degree of

PhD in Rehabilitation Science and Technology

University of Pittsburgh

2012

UNIVERSITY OF PITTSBURGH
SCHOOL OF HEALTH AND REHABILITATION SCIENCE

This dissertation was presented

by

Hongwu Wang

It was defended on

December 2, 2011

and approved by

Ding, Dan, PhD, Assistant Professor

Jonathan, L. Pearlman, PhD, Assistant Professor

Emmanuel, Collins, PhD, Professor

Dissertation Director: Rory A. Cooper, PhD, Professor

Copyright © by Hongwu Wang

2012

DEVELOPMENT AND EVALUATION OF AN ADVANCED REAL-TIME ELECTRICAL POWERED WHEELCHAIR CONTROLLER

Hongwu Wang, PhD

University of Pittsburgh, 2012

Advances in Electric Powered Wheelchairs (EPW) have improved mobility for people with disabilities as well as older adults, and have enhanced their integration into society. Some of the issues still present in EPW lie in the difficulties when encountering different types of terrain, and access to higher or low surfaces. To this end, an advanced real-time electrical powered wheelchair controller was developed. The controller was comprised of a hardware platform with sensors measuring the speed of the driving, caster wheels and the acceleration, with a single board computer for implementing the control algorithms in real-time, a multi-layer software architecture, and modular design. A model based real-time speed and traction controller was developed and validated by simulation. The controller was then evaluated via driving over four different surfaces at three specified speeds. Experimental results showed that model based control performed best on all surfaces across the speeds compared to PID (proportional-integral-derivative) and Open Loop control. A real-time slip detection and traction control algorithm was further developed and evaluated by driving the EPW over five different surfaces at three speeds. Results showed that the performance of anti-slip control was consistent on the varying surfaces at different speeds. The controller was also tested on a front wheel drive EPW to evaluate a

forwarding tipping detection and prevention algorithm. Experimental results showed that the tipping could be accurately detected as it was happening and the performance of the tipping prevention strategy was consistent on the slope across different speeds. A terrain-dependent EPW user assistance system was developed based on the controller. Driving rules for wet tile, gravel, slopes and grass were developed and validated by 10 people without physical disabilities. The controller was also adapted to the Personal Mobility and Manipulation Appliance (PerMMA) Generation II, which is an advanced power wheelchair with a flexible mobile base, allowing it to adjust the positions of each of the four casters and two driving wheels. Simulations of the PerMMA Gen II system showed that the mobile base controller was able to climb up to 8” curb and maintain passenger’s posture in a comfort position.

TABLE OF CONTENTS

PREFACE.....	xvii
1.0 INTRODUCTION	1
1.1 EPW USAGE AND CURRENT STATE OF CONTROLLERS	1
1.2 FOCUS GROUP STUDIES ON EPW USERS	5
1.3 OBJECTIVE.....	8
2.0 RELATION BETWEEN WHEELCHAIR DURABILITY AND WHEELCHAIR TYPE AND YEARS OF TEST	11
2.1 WHEELCHAIR STANDARD AND DURABILITIES	12
2.2 OUR APPROACHES	14
2.2.1 Variables Definition.....	14
2.2.2 Study Design.....	16
2.2.3 Data Analysis	16
2.3 WHEELCHAIR TESTED.....	17
2.4 HOW DURABILITIES HAD BEEN CHANGED	19
2.5 SUMMARIES	21

3.0	3-D MATHEMTAICAL MODELING OF AN ELECTRIC POWERED WHEELCHAIR AND SIMULATION RESULTS.....	22
3.1	MODELING AN ELECTRIC-POWERED WHEELCHAIR ON A SLOPE.....	22
3.1.1	Why a mathematical model of wheelchair?.....	22
3.1.2	Development of the Model	23
3.2	AN EXPERIMENTAL METHOD FOR MEASURING THE MOMENT OF INERTIA OF AN ELECTRIC POWERED WHEELCHAIR.....	30
3.2.1	Why moment of inertia is important?	31
3.2.2	Methodological approach.....	32
3.2.3	Measurement results	38
3.2.4	Evaluation of the method	40
3.2.5	Summary	41
3.3	SIMULATION OF MODEL BASED FEEDBACK CONTROL OF AN ELECTRIC POWERED WHEELCHAIR.....	42
3.3.1	Kinematic Model of an EPW	42
3.3.2	Dynamic Model	44
3.3.3	Control Algorithm.....	47
3.3.4	Simulation results.....	48
3.3.5	Summary	53
3.4	DEVELOPMENT OF AN ADVANCED REAL-TIME EPW CONTROLLER	53

3.4.1	Electronic Design.....	54
3.4.2	Mechanical Design.....	58
3.4.3	Software Design.....	60
3.4.4	How the smart controller could be used?.....	62
4.0	REAL-TIME MODEL BASED ELECTRIC POWERED WHEELCHAIR VELOCITY, TRACTION AND TIP-OVER CONTROL.....	64
4.1	CONTROLLER FOR EPWS.....	64
4.2	DEVELOPMENT OF A 3-D HYBRID ADVANCED CONTROL SYSTEM.....	66
4.2.1	Robust Velocity Control.....	67
4.2.2	Traction Control.....	69
4.3	EXPERIMENTAL TESTS.....	71
4.3.1	Test Wheelchair.....	71
4.3.2	Software Algorithms.....	71
4.3.3	Experimental Protocol.....	72
4.3.4	Experimental results.....	74
4.3.5	Effectiveness of the controller.....	82
4.4	Real-time Slip Detection and Traction Control of Electrical Powered Wheelchairs.....	86
4.4.1	Traction control of EPWs.....	86
4.4.2	Set-up for the slip detection.....	87
4.4.3	Experimental results.....	88

4.4.4	Summary	91
4.5	Real-Time Forwarding Tipping Detection and Prevention of a Front Wheel Drive Electric Powered Wheelchair.....	92
4.5.1	What is the problem of EPW tipping?	92
4.5.2	Experimental approach	93
4.5.3	What we got	97
4.5.4	Summary.....	100
5.0	DEVELOPMENT AND EVALUATION OF ELECTRICAL POWERED WHEELCHAIR DRIVING RULES ON DIFFERENT TERRAINS.....	101
5.1	EPW PERFORMANCES ON DIFFERENT TERRIANS.....	102
5.2	DEVELOPMENT OF THR DRIVING RULES.....	105
5.2.1	Phase I.....	105
5.2.2	Phase II.....	109
5.3	RESULTS.....	113
5.3.1	Phase I results	113
5.3.2	Phase II Results.....	117
5.4	THE DRIVING RULES.....	126
6.0	DEVELOPMENT OF AN ADVANCED MOBILE BASE FOR PERSONAL MOBILITY AND MANIPULATION APPLIANCE GENERATION II (PERMMA GEN II).....	133
6.1	WHY PERMMA GENII	134

6.2	SYSTEM DESCRIPTION	138
6.2.1	Electrical system	139
6.2.2	Software system	140
6.2.3	Description of different kinds of motion	142
6.2.4	Climbing strategies	143
6.3	MOBILE BASE CONTROL SYSTEM.....	145
6.3.1	Sensor system.....	145
6.3.2	Actuator system	145
6.3.3	Mathematical model of PerMMA Gen II.....	146
6.3.4	Control Development.....	149
6.4	SIMULATIONS AND RESULTS.....	152
6.5	SUMMARIES	155
7.0	RECOMMENDATIONS FOR FUTURE WORK	158
	APPENDIX A.....	163
	Questionnaires of Demographics	163
	APPENDIX B	166
	Self-Scoring Sheet	166
	BIBLIOGRAPHY.....	169

LIST OF TABLES

Table 1-1: Strategies summarized from EPW users interviews.....	7
Table 2-1: Test results of different types of wheelchairs.....	17
Table 2-2: Summary of logistic regression analysis for variables predicting test results by year of tested and wheelchair type	18
Table 3-1: Parameters of the EPW used in the modeling and simulation work	25
Table 3-2: Parameters required for validating the mathematical model of the EPW	29
Table 3-3: Definition of variables.....	33
Table 3-4: Parameters of the torsional pendulum.....	37
Table 3-5: Parameters onf metal disk	38
Table 3-6: Parameters of the cylinder.....	38
Table 3-7: Parameters of the EPW.....	38
Table 3-8: Periods of the torsional pendulum.....	39
Table 3-9: Measurement results of the inertias and calculating results	39
Table 3-10: Parameters of the mathematical model of an EPW.....	43
Table 4-1: Physical parameters for the test EPW and test surface	75
Table 4-2: Test results of the mean, standard deviation and variance of the wheels speed NRMSE of all the three control methods	76

Table 4-3: Slip coefficient of all the tests with and without traction control	88
Table 4-4: Performance of the wheelchair for all the experiment tests with and without tip-prevention control applied	99
Table 5-1: Driving parameters used in Phase I testing	107
Table 5-2: The four driving settings used in Phase II studies.....	110
Table 5-3: Demographic information of the participants	118
Table 5-4: Mean rank of users' overall rating on the four driving settings.....	119
Table 5-5: Mean rank of user ratings on the four drive settings at each testing surface	119
Table 5-6: Means and standard deviation of time to complete the trials, number of direction changes and critical slip ration for the four drive settings	121
Table 5-7: Mean rank of time to complete each trial, number of direction changes and critical slip ratio for the four driving settings	122
Table 5-8: Mean rank of maximum angular velocity about the longitudinal, lateral and vertical axes for the four driving settings	125
Table 5-9: Mean rank of maximum angular velocity regarding to longitudinal, lateral and vertical axes for the four driving settings on all slopes	125
Table 5-10: Recommended driving rules for novice and experience EPW users.....	131
Table 6-1: Wheelchair dimension comparison	152

LIST OF FIGURES

Figure 1-1: User responses about ease of 23 driving conditions and prevalence of common accidents.....	6
Figure 2-1: Tests setup for all four types of wheelchairs on double drum and curb drop	15
Figure 3-1: 3-D mathematical model of wheelchair system on the slope.....	24
Figure 3-2: Wheelchair axes systems on a slope	26
Figure 3-3: Mathematical representatives of different views of a wheelchair on a slope	27
Figure 3-4: The principle of torsional pendulum used in the experiment.....	35
Figure 3-5: Photographs of the motion of the bottom plate with the EPW on the plate and the devices (gradienter, stopwatch, rulers, etc.) and materials (metal disks, cylinder) used in the experiment.....	37
Figure 3-6: Free body diagram of an EPW	42
Figure 3-7: Output Feedback Control Diagram of the System	48
Figure 3-8: Three desired paths for the simulation: Case i: $Y=10$, Case ii: $Y=X$ and Case iii: $Y=X^2/60$	48
Figure 3-9: Trajectory of wheelchair for Case i.....	49
Figure 3-10: Trajectory errors between center of mass and desired path for case i	49
Figure 3-11: Trajectory of wheelchair for Case ii	50

Figure 3-12: Trajectory errors between center of mass and desired path for case ii	50
Figure 3-13: Trajectory of wheelchair for Case iii	51
Figure 3-14: Trajectory errors between center of mass and desired path for case iii	51
Figure 3-15: Trajectory errors between center of mass and desired path for case ii with different [Kp Kd] values.....	52
Figure 3-16: Components of the wheelchair control platform.....	57
Figure 3-17: Layout schematic of electrical components	57
Figure 3-18: Core components installed in chassis.....	59
Figure 3-19: Layout of components in chassis	59
Figure 3-20: Control architecture of the advanced real-time controller platform	61
Figure 4-1: Open-loop and closed-loop control systems for the model based control of a wheelchair	68
Figure 4-2: Five difference surfaces on which the experiment was conducted.....	74
Figure 4-3: Example figures of two driving wheels and caster speeds with different controllers applied at low and high speeds on a grass surface.....	77
Figure 4-4: Slip coefficients of three controllers with the wheelchair driving on grass at 2 m/s. .	78
Figure 4-5: Wheelchair performances with three controllers at three different speeds	79
Figure 4-6: Wheelchair performances with three controllers on five different surfaces	80
Figure 4-7: Slip measurements with three different controllers: open loop, PID and model based control	82
Figure 4-8: Slip coefficients with and without traction control during the tests across three speeds	89
Figure 4-9: Slip coefficients with and without traction control during the test on five surfaces..	89

Figure 4-10: The desired speed, left and right driving wheel speed and caster speed for the wheelchair driving at 1meter per second on a Teflon surface without traction control when slip happened	90
Figure 4-11: The desired speed, left and right driving wheel speed and caster speed for the wheelchair driving at 1 meter per second on Teflon surface with traction control when slip happened	91
Figure 4-12: Diagram of EPW on Slope.....	94
Figure 4-13: Experimental setup of the EPW	96
Figure 4-14: Inertial data and residuals after filtering at slow speed when the wheelchair transitioned from level ground to the downward slope	97
Figure 4-15: Inertial data and residuals after filtering at the slow speed when the wheelchair transitioned from the slope to level ground	98
Figure 4-16: Angular velocities about the wheel axes at the three test speeds when the wheelchair transitioning from level ground to the slope	98
Figure 5-1: The EPW with encoders and inclinometer for data collection.....	106
Figure 5-2: Three surfaces selected for Phase I test	107
Figure 5-3: Driving protocol for dry and wet tile (left) slopes and gravel (right)	108
Figure 5-4: Driving surfaces for the Phase II study	111
Figure 5-5: Distributions of critical slip values for different driving speeds over wet tile surface	114
Figure 5-6: Distributions of critical slip values for different acceleration/deceleration combinations over wet tile surface	114

Figure 5-7: Distributions of critical slip values for different driving speeds over gravel surface	115
Figure 5-8: Distribution of critical slip for different acceleration and deceleration combinations over gravel surface	115
Figure 5-9: Measured angles of the EPW from inclinometer; correction angles with encoder values and real slope angle	116
Figure 6-1: PerMMA Gen II system overview	138
Figure 6-2: Electrical system diagram of PerMMA Gen II	140
Figure 6-3: PerMMA Gen II software modules.....	141
Figure 6-4: PerMMA Gen II in automatic climbing mode	142
Figure 6-5: PerMMA Gen II step climbing sequences	144
Figure 6-6 Mathematical model of PerMMA Gen II mobile base.....	147
Figure 6-7: PerMMA Gen II control states.....	150
Figure 6-8: Block diagram of the state feedback feed-forward controller.....	151
Figure 6-9: 3-D simulation environment of PerMMA Gen II on a slope using ODE	153
Figure 6-10: Simulation setup for PerMMA Gen II posture control	154
Figure 6-11: Simulation results for PerMMA Gen II posture control	154

PREFACE

First, I would like to thank my dissertation committee: Dr. Ding Dan, Dr. Jonathan Perlman, and Dr. Emmanuel Collins. The support and guidance that each of you has given me over the years is immeasurable and I will be forever grateful. Special thanks are reserved for my dissertation advisor Dr. Rory Cooper. I cannot begin to thank you enough for not only my past five years at HERL, but also for giving me the tools to succeed in the future. You have contributed to all that I have learned about conducting research and being a mentor and advisor, and you have fueled my passion for rehabilitation research and engineering as a discipline.

I would like to thank all of the students whom I have met during my time at HERL who have provided me with not only their knowledge and wisdom, but with their friendship. Additionally, I would like to thank all of the staff at HERL. Without the shop technicians and clinical coordinators, it would have been impossible for me to finish my studies. Thanks to all the administrators and Amy Donovan. They offered assistance whenever it was requested.

Last but not least I must thank my family. Through all of the good times and the bad my Mother, Father, and my Sister have been unwavering in their support and have given me strength when I had none left. They have sacrificed more than their fair share for me and I love them very much. To my wife Lidan, your love and support has shown me what is truly important.

1.0 INTRODUCTION

In this chapter, the statistics of electrical powered wheelchair (EPW) usage and problems of current EPW are presented. In addition, focus group study results from active EPW users are discussed to introduce the problems which will be addressed throughout the dissertation work. At the end of the chapter, the objectives of this dissertation are listed.

1.1 EPW USAGE AND CURRENT STATE OF CONTROLLERS

Over 200,000 people in the United States used electric-powered wheelchairs (EPWs) as their primary means of mobility by 2000 [1] and, according to 2010 United States Census figures, there are 3.3 million wheelchair users age 15 or over [2]. Worldwide, an estimated 100-130 million people with disabilities need wheelchairs, though less than 10 percent own or have access to one. While these numbers are staggering, experts predict that the number of people who need wheelchairs will increase by 22 percent over the next ten years [1]. Medicare reimbursement for power wheelchairs grew from less than US\$150 million in 1997 to more than US\$1.1 billion in 2003 [3]. More and more people with mobility impairments utilize EPWs for their functional mobility because there are many positive reasons to use an EPW. For example,

EPW users' mobility range and freedom are increased, and this improved mobility independence facilitates user social interaction, motivation, and community participation [4-6]. A study conducted to investigate how assistive devices affected the daily life of persons with stroke and their spouses found that the outdoor powered wheelchair improved quality of life for its user in the form of increased competence, independence, well-being, happiness and self-esteem [7, 8]. Some young people's experiences using EPWs also reported increased independence and social activities like wheelchair football. Most young people and their families were fairly satisfied with the service and provision of their wheelchairs [9]. Older adults of EPW users also reported moderate satisfaction with their chairs [10]. However, even those who were satisfied reported only moderate use of the EPW outdoors due to an infrequent need for outings, outdoor barriers, feelings of insecurity over EPW safety and lengthy waiting times for chair delivery and required modifications [10]. Therefore, the need for wheelchairs, and the research and development required to make them durable, more effective, and widely available are overwhelming.

Advances have been made in the design of EPWs over the past 20 years, such as advances in user interfaces, navigation, obstacle avoidance, and improved battery life [11]. However, there are issues with current EPWs' control systems. A study of able-body adults driving EPW found that 66% percent participants failed at least one test item (the tests including basic driving skills like driving straight, turning, u-turns etc; traffic tests like avoiding unexpected pedestrians; and multiple tasks of driving, such as reading signs at eye height and at the same time avoiding obstacles in the path) [12]. EPW users complained about the response of the system to the movement of the joystick [13]. EPW users were often limited in their ability to adjust to hazardous surfaces [14, 15]. The controller was adequate in meeting the needs of highly skilled operators, but a large majority found difficulties in traversing surfaces such as bathroom tile,

grassy surfaces, slopes, and snow/ice that caused problems of wheel slip, wheel sink, and tipping. An individual's inability to handle these terrains may be caused by a number of factors such as inexperience, injury, or mental fatigue. Additionally, new users are given a limited amount of training on how to properly use a new EPW. As a result of these factors, incidents in which the user loses some or all control of their wheelchair are frequent, and device and control failures account for about 60% of injuries each year [16]. In 2003, more than 100,000 wheelchair related injuries were treated in emergency departments in the US, and tips and falls accounted for 65-80% of injuries [17]. According to the FDA MAUDE database, the incidents were problems with the electric-drive/controlled to uncontrolled movements (47%), collisions (17%) and falls and tips (15%) during one year. Incidents outdoors were more frequent than those that happened indoors. For the most severely injured individuals, even slight disturbances can induce a problem during PMDs driving [18]. PMD users with insufficient strength and/or slow movement responses in their upper extremities are more likely to have accidents. The addition of computer-controlled systems that constantly monitor and correct for position, attitude, and terrain variations may solve the problem [19].

Control systems research has achieved broad application in other areas, such as telecommunications, robotics, automation, and medicine. For EPWs, there are several research studies working on the development of smart wheelchairs with functions like obstacle avoidance, path planning, trajectory generation and manipulation [20]. A smart wheelchair usually consists of either a standard EPW to which a computer and a collection of sensors have been added, or a mobile robot base to which a seat has been attached [21]. Smart wheelchairs could provide users more assistance if necessary based on advanced sensory and control techniques. An example of one such assistive feature of a smart wheelchair is the obstacle avoidance feature: wheelchair

users with visual impairments may not see obstacles, but are able to navigate without visual cues. People who could benefit from the smart wheelchair are users with physical impairments that may cause them to temporarily lose control of the chair. Smart wheelchairs could also be advantageous for wheelchair users with cognitive impairments that may perform unsafe driving (e.g., poor impulse control) [22].

Although a smart wheelchair could provide assistance to users, there are limitations for these kinds of technologies. First of all, there are few smart wheelchairs on the market as they are mainly developed for research use (e.g. AAI TAO-7 [23], CALL CENTER smart wheelchair [24], and TopChair [25]). Secondly, limited commercial availability results in limited clinical impact of smart wheelchairs. And lastly, little attention has been paid to evaluating their performance since no smart wheelchair had been subjected to a rigorous, controlled evaluation that involves extensive use in real-world settings. In addition, some users complain about design of the smart wheelchairs which lack consideration from their perspective [26, 27].

Most EPW users may have several driving profiles with different control parameters (e.g., indoor driving, outdoor driving, tight corner driving), allowing them to select the most appropriate profile for a specific terrain condition to optimize wheelchair performance. However, no previous work has investigated how to set the control parameters for different terrain conditions especially adverse conditions (e.g. inclines, slippery surfaces, and rough terrain), as well as how to make it convenient for the users to use the different driving profiles. Most of the time the control parameters are set based on the experience of clinical professionals after observing the driving performance of an EPW user during a short training session. In addition, current approaches mentioned above are not applied in real-time. Real-time environment reconstruction has been applied for virtual reality training tools [28] and a wheelchair system for

EPW users with Cerebral Palsy [29]. One project [30] uses a camera for goal selection and tracking. The system used template matching vision techniques to track the selected goal. Sonar sensors were retained for local sensing and obstacle avoidance. Another robotic wheelchair [31] employed vision techniques through two cameras. Sonar sensors were still retained for obstacle avoidance. Both projects could detect the obstacle in real-time and avoid them base on them during moving. However, for those projects, the results were either based on simulation or lacking real life evaluation.

1.2 FOCUS GROUP STUDIES ON EPW USERS

As discussed in the previous section, the currently available driving profiles for EPWs are not sufficiently able to traverse different terrains. To further investigate the problems, a series of semi-structured interviews with 31 EPW users were conducted to help identify difficult terrains encountered by EPW users on a daily basis and driving strategies under such conditions by our research group [32]. Participants rated 23 driving conditions as to their ease of navigation. **Figure 1-1** showed how participants rated the ease of navigation for the 23 different driving conditions and the prevalence of common accidents. The most common categories were (1) getting stuck due to loss of traction, (2) ran into person in crowded place, and (3) tipping over sideways. These EPW users were most concerned about slipping (loss of traction on the drive wheels) and getting stuck (immobilized) on difficult terrain such as gravel, sand, ice, etc. Also a unique concern with EPW users is wheelchair tipping (loss of stability), which usually happens

on cross slopes, at transitions from a slope to horizontal surfaces such as curb cuts, and when driving up and down steep slopes.

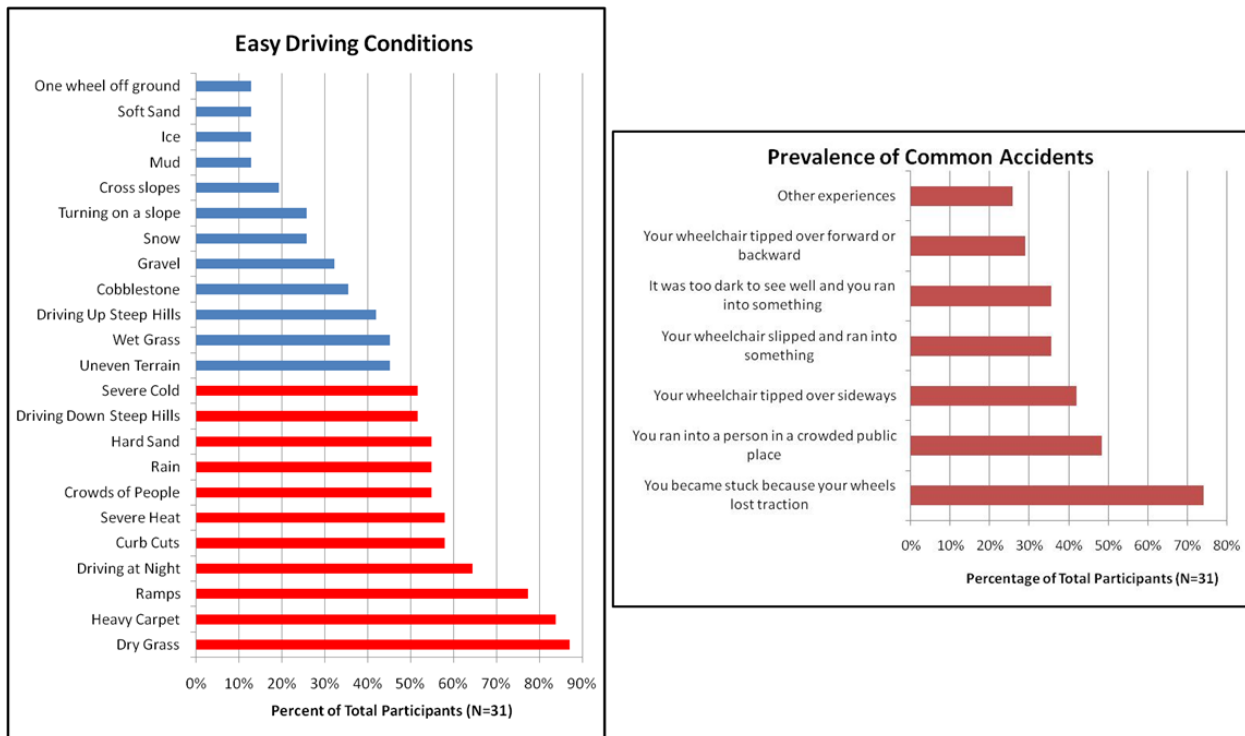


Figure 1-1: User responses about ease of 23 driving conditions and prevalence of common accidents

When we asked how users dealt with difficult surfaces, the EPW users in the interviews shared some useful driving strategies learned through years of experience using EPWs. For example, it is important not to drive too slowly or make sudden starts/stops when driving on gravel. However, driving fast over gravel was also a problem as the bouncing could set off very uncomfortable spasms in the user or cause their hand to be jostled off the joystick control. The best strategy is to drive as fast as one can tolerate over gravel or sand to avoid bogging down.

Ice, snow or other slippery surfaces were identified as requiring similar strategies, such as not making sudden changes in speed and direction. EPW users also suggested driving strategies for slopes and cross-slopes, which from were shown to be difficult terrains that are often avoided. Strategies for these terrains were as follows: 1) when driving down a steep slope, tilt the seat back (if possible) so that the seat is level with the horizon instead of the slope; 2) sit in an upright position when driving up a steep slope; and 3) avoid sharp turns on steep slopes. Additionally, it was suggested that EPW users drive along a steep side slope (along the transverse axes) with their joystick pointing somewhat towards the top of the slope in order to avoid causing the lighter uphill drive wheel to slip. A brief summary of the strategies collected from the EPW users were listed in **Table 1-1**.

Table 1-1: Strategies summarized from EPW users interviews

Obstacles	Strategies
Sidewalks	Drive fast without obstacles, no quick turns to be safe
Potholes & Cobblestone	Drive fast as possible without causing discomfort
Curb cuts	approaching at an angle helps to lift one wheel at a time
Sand & Gravel	Must maintain momentum and not turn
Grass: Slippery	Drive slowly or avoid
Hills	Drive straight up & down hills slowly
Snow & Ice	Don't turn on ice, let inertia carry you over
Rain / Wet	Slow down and drive more carefully

1.3 OBJECTIVE

The primary goal of this work was to advance the EPWs control with maximum assistance and safety for users to function independently to improve their quality of life. These included two layers of work: one was to integrate technology and knowledge to advance EPW control; another was to dynamically provide users with maximum safety and independence. To approach these goals, first we developed a real-time controller that could be used for control algorithms development and testing, then we integrated prototypes that were developed and evaluated in real-world settings with users including people with disabilities, clinicians and researchers. Lastly we utilized the controller for two research projects. The specific aims for this study were:

- 1) To build an EPW platform and incorporate a network of sensors and controller which includes the following specifications:
 - a. Flexibility to be implemented with customized control algorithms
 - b. Robust and reliable enough to conduct field tests
 - c. Smooth response in real-time. The controller should not require any offline processing, nor should it halt to evaluate information whilst operationally engaged
 - d. Powerful to handle multiple tasks and flexible to be used as a mobile base controller for development of different research projects.
 - e. Safe/reliable enough to be evaluated in community
- 2) To develop a real-time model based velocity control algorithm, a real-time slip detection and traction control algorithm, a real-time tip over detection and prevention control algorithm.
 - a. To identify the terrain dependent EPW driving rules

- b. To validate the terrain dependent EPW driving rules with user testing

In the following sections, the development and evaluation of the controller platform as well as the control algorithms were detail introduced.

The purpose of section two was to find the relationship between the durability of wheelchairs according to ANSI/RESNA Wheelchair Standards and wheelchair type as well as year of test. The collection of this data was important to find out whether the problems raised by users were caused by EPW durability or control failure.

The purpose of section three was to build a 3-D mathematical model of an EPW to measure the inertia of the EPW and other parameters for the model, to validate the model by simulation, and to develop the advanced real-time EPW controller platform. The controller platform included a single board computer providing the computational power and storage space needed to execute normal operations, complex safety algorithms, and extensive data logging. An array of sensors connected to the computer, providing feedback on velocity, inertia, and caster angle. A rugged aluminum enclosure protected the electronics and provided connectors for all the sensors. A real-time operating system was used as the basis for programming. The software architecture used a multiple level hierarchical structure that organized tasks based on periodicity, priority, and computational load.

The purpose of section four was to evaluate the 3-D model based real-time control algorithm using the advanced real-time EPW controller platform in experimental settings. The advanced real-time EPW platform was used to record wheel speeds and to calculate the slip. The model based, a proportional-integral-derivative (PID) and an open-loop controller were applied with the EPW driving on four different surfaces at three specified speeds. The speed errors, variation, rise time, settling time and slip coefficient were calculated and compared for a speed

step-response input. Experimental results showed that model based control performed best on all surfaces across the speeds. A real-time slip detection and traction control algorithm and a real-time forward-tipping prevention algorithm were then developed. The EPW was driven over five different surfaces at three speeds to evaluate the performance of the slip detection control algorithm. The EPW was driven over a ramp at different speeds to evaluate the effectiveness of the tipping detection and prevention control algorithm.

The purpose of section five was to use the advanced real-time controller to develop a terrain dependent EPW driving assistant system (TD-EDAS). We conducted a two phases study: at phase 1, we developed driving rules when EPW was driven on wet tile, gravel and slopes surfaces at experimental settings. Then at phase 2, we recruited 10 able-body subjects to validate the driving rules on the three surfaces as well as grass surface. The driving rules varying the driving speed, acceleration, and deceleration when EPW was driven on different surfaces.

The purpose of section six was to use and evaluate a mobile base controller for the Personal Mobility and Manipulation Appliance (PerMMA) using the advanced real-time controller. The advance real-time controller was modified and adapted as a robotic mobile base controller. The mechanical and electrical system of the mobile controller was tested on the current PerMMA prototype. A feedback, feed-forward posture stability control algorithms was developed based on the kinematic model of current PerMMA, and simulation results showed that the with the controller, user could keep their posture at same with driving on flat surface when driving over 3” curbs and on a 10 degree slope.

2.0 RELATION BETWEEN WHEELCHAIR DURABILITY AND WHEELCHAIR TYPE AND YEARS OF TEST

This study investigated the relationship between the durability of wheelchairs according to American National Standard for Wheelchairs/Rehabilitation Engineering and Assistive Technology Society of North America (ANSI/RESNA) Wheelchair Standards and wheelchair type as well as test year. A retrospective study design was implemented with a sample of 246 wheelchairs that were tested in accordance with the ANSI/RESNA standards from 1992 to 2008 including four types of wheelchairs: (1) manual wheelchair, (2) electrical powered wheelchair, (3) scooter, and (4) pushrim-activated power-assisted wheelchair (PAPAW). Unconditional binary logic regression analysis was chosen to evaluate the relationship between test results and test year as well as wheelchair type. No relationship was identified between the standards durability test results and the year that the testing was conducted. A significant relation was found between test results and wheelchair type. Scooters and electrical powered wheelchairs had significantly higher odds ratios to pass the standards test than manual wheelchairs and PAPAWs, indicating that scooters and electrical powered wheelchairs may be more durable than manual wheelchairs and PAPAWs. No significant difference on pass ratio was found between manual wheelchairs and PAPAWs. The overall durability of wheelchairs in this broad sample did not improve over the course of 17 years. The authors conclude that, although ANSI/RESNA

wheelchair durability test procedures have remained consistent, it does not appear that the introduction of new materials and designs and the availability of test data have improved wheelchair fatigue life.

2.1 WHEELCHAIR STANDARD AND DURABILITIES

Wheelchairs, including scooters, are required to have considerable reliability, since they are typically used most hours of the day, every day of the year [33]. A broken wheelchair can leave the user stranded for long periods of time while the wheelchair is being repaired. Moreover, a failure of a wheelchair may lead to injury of its occupant. A recent study conducted by Xiang et al. stated that wheelchair related injuries treated in emergency departments in the US may have increased during the past decade [34]. In 2003, more than 100,000 wheelchair related injuries were treated in emergency departments in the US, double the number reported in 1991. Their results showed one of the triggering factors of injury was the failure of wheelchair components which accounted for 62.9% for 2-5 years old young kids and at least 20% for adults [34]. Safety and durability are critical factors when a wheelchair is prescribed. Durability is an important factor that can potentially either contribute to or prevent common tip- and fall-related injuries [35]. When wheelchair failures occur, not only are the user's ability to perform daily tasks compromised, but serious physical injuries may result. Component failure related to wheelchair design as a cause of user injuries had been discussed in [35]. Durability of the wheelchair should be sufficient that it does not fail within a 3-5 year period, which is the typical time span

Medicare (and thus other insurance companies) expects wheelchairs to last before they will fund a replacement.

ANSI/RESNA and ISO have developed more than 18 standards that test for performance, safety, and dimensions of wheelchairs [36, 37]. However, meeting these standards is voluntary for wheelchairs, and their manufacturers rarely provide information on fatigue testing of their products to consumers. When tested by the manufacturer, bias or misinterpretation of the ANSI/RESNA standards may lead to inaccurate outcomes. Previous studies showed that Electric Power Wheelchairs (EPWs) [38, 39], scooters [39], pushrim activated power assisted wheelchair (PAPAW) [40] and manual wheelchairs [41-44] on the market do not necessarily pass the ANSI/RESNA testing standards when evaluated independently. Cooper et al discussed the importance of knowing a wheelchair's reliability and life expectancy for the growing number of individuals who rely upon these devices [34]. As wheelchair related technologies such as manufacturing, materials and control technology progress and more attention is focused on the comfort and functions of wheelchairs, a recent article by Wright emphasized the importance of wheelchair safety [45]. In this study, we investigated whether the durability of wheelchairs has improved since 1992 with developments of technologies and increasing function of wheelchairs.

The Human Engineering Research Laboratories has a database of wheelchair standards testing dating back to 1992. The wheelchairs HERL has tested include many commercially available manual, power, and power assisted wheelchairs as well as scooters. The test results and comments have been logged in a database and a sample of them has been published in peer review journals and proceedings [38-44]. In this study, we retrospectively examined testing data to determine if there have been changes in durability of different types of wheelchairs over 17 years.

2.2 OUR APPROACHES

2.2.1 Variables Definition

Wheelchair durability was evaluated using the double-drum and curb-drop tests (section 8 of the ANSI/RESNA standards, see **Figure 2-1**). All of the selected wheelchairs were tested according to the ANSI/RESNA standard for static, impact and fatigue strength. A wheelchair that completed 200,000 cycles on the double-drum machine was considered to have passed the double drum Test (DDT). Only wheelchairs that passed the DDT would continue on to the curb-drop test (CDT). In the CDT, each wheelchair was dropped freely from a 5 centimeter height repetitively onto a concrete floor to simulate a wheelchair going down small curbs. A wheelchair passes the standards tests when it survives 200,000 cycles on the DDT and 6,666 cycles in the CDT without visible damage that affects function or safety [37]. The durability of the wheelchairs was evaluated by using the equivalent cycles (EC) for fatigue life calculated by this following equation:

$$\text{Total Cycles} = (\text{Double-Drum Tester Cycles}) + 30 \times (\text{Curb-Drop Tester Cycles})$$

The EC represents the number of cycles before the occurrence of a Class III failure in the fatigue tests. A wheelchair that obtained an equivalent cycle of 400,000 cycles was denoted as passing the minimum durability requirements. Since some of the test results were only recorded pass or instead of the total equivalent cycles, we could not use the equivalent cycles as our main outcome measure. The main outcome variable in this study was whether the wheelchair passed or failed the fatigue tests. The wheelchairs that passed the standards tests were categorized into one group and those that failed the fatigue tests were assigned to the other group. The test year

(from 1992 to 2008) was used as an independent variable. The type of wheelchair was another independent variable. Tested wheelchairs were divided into four groups: manual wheelchair (MWC), electrical powered wheelchair (EPW), scooters and pushrim activated power assisted wheelchair (PAPAW).



(a) A scooter set up on the DDT machine



(b) A EPW set up on the CDT machine



(c) A PAPAW set up on the DDT machine



(d) A MWC set up on the CDT machine

Figure 2-1: Tests setup for all four types of wheelchairs on double drum and curb drop

2.2.2 Study Design

This was a retrospective study. From the database, more than 300 wheelchairs were tested during the time frame, however, the results without complete data about EC or test year were excluded from the study. This resulted in 246 wheelchairs being chosen for inclusion in the study. Instead of considering survival cycles as in previous studies [38-44], we examined whether the year of conducting the tests and the type of wheelchair was significantly related to whether the wheelchairs would pass the standards durability tests.

2.2.3 Data Analysis

Unconditional binary logistic regression analyses were used to assess the association between the potential contributing factors (test year and wheelchair type) and wheelchair test result, where a binary variable (either pass the test or fail to pass the test) was used as the dependent variable and the potential contributing factors were used as independent variables. The Hosmer and Lemeshow test was used to check whether the model adequately fit the data. The odds ratios (ORs) and the corresponding 95% confidence intervals (CIs) were obtained with forward stepwise regression. All the data analyses were done using the SPSS 15. The alpha level was set at 0.05 *a priori*.

2.3 WHEELCHAIR TESTED

A total of 246 wheelchairs were included in this study incorporating MWC, EPW, scooter and PAPA W. **Table 2-1** gave the distribution of the test results by test year and wheelchair type.

Table 2-1: Test results of different types of wheelchairs

	Total	Pass No.	%	Fail No.	%
Wheelchair types					
MWC	154	79	51.3	75	48.7
EPW	61	41	67.2	20	32.8
Scooter	18	17	94.4	1	5.6
PAPA W	13	8	61.5	5	38.5
Test Year					
1993	12	4	33.3	8	66.7
1994	3	2	66.7	1	33.3
1995	13	8	61.5	5	38.5
1996	24	17	70.8	7	29.2
1997	16	10	62.5	6	37.5
1998	7	6	85.7	1	14.3
1999	14	10	71.4	4	28.6
2000	21	15	71.4	6	28.6
2001	24	20	83.3	4	16.7
2002	21	11	52.4	10	47.6
2003	22	9	40.9	13	59.1
2004	10	6	60.0	4	40.0
2005	11	7	63.6	4	36.4
2006	5	2	40.0	3	60.0
2007	19	8	42.1	11	57.9
2008	17	8	47.1	9	52.9

Table 2-2 showed the results for test result in association with test year and wheelchair type. The Hosmer and Lemeshow test indicated that the model adequately fit the data (Chi-square=4.197, degree of freedom=8, p=0.839).

Table 2-2: Summary of logistic regression analysis for variables predicting test results by year of tested and wheelchair type

Independent variables	Wald	df	Sig.	Odds Ratio	95.0% C.I.
Test Year	.587	1	.444	.977	.922-1.036
Wheelchair type	10.845	3	.013*		
Compare to					
EPW	4.456	1	.035*	1.953	1.049-3.636
Scooter	6.955	1	.008*	15.629	2.026-120.579
MWC					
PAPAW	.701	1	.403	1.657	.508-5.408

For the test year, the logistic regression model did not show a significant relation between test result and test year (Wald score=0.587, df=1, p=0.444). However, in the logistic regression model wheelchair type was significantly (Wald score=10.845, df=3, p=0.013) associated with test result. Specifically, scooters had a significantly higher pass ratio than MWC (OR=15.629, 95% CI=2.026-120.579). EPW also had significantly higher pass ratio than MWC (OR=1.953, 95% CI=1.049-3.636). No significant difference in pass ratio was found between PAPAW and MWC.

2.4 HOW DURABILITIES HAD BEEN CHANGED

While most previous studies focused on evaluating and comparing overall performance of groups of a certain type of wheelchair according to the ANSI /RESNA standards [39-45], this study investigated the relationship between wheelchair fatigue test results and wheelchair types as well as the year of testing. We found that there is a relationship between the test results and wheelchair types. Scooter and EPW had significantly higher Odds ratio to pass the standard test than MWC and PAPA W which means that scooters and EPWs had better durability than PAPA W and MWC. This result agrees with Fass et al [39] who also found that EPWs would expect fewer failures than MWC. This may be related to weight being less of a factor in the design of powered mobility products.

There was no relationship identified between test years and durability results. This result indicates that the durability has not significantly improved as expected in accordance with improvements in materials and technologies. One possible reason is that the design of the wheelchair may have deficiencies even when better materials and fabrication technologies were applied. Similar findings were reported by Liu H et al in a study of titanium wheelchairs [45]. Another reason may be that insufficient attention has been paid to wheelchair standards testing since it is not mandatory for manufactures. An interesting finding of this study is that from 1996-2001, more of the wheelchairs tested passed the fatigue tests than failed. This may be a result of more EPWs and scooters being tested during this period of time. Additionally, the adoption of the revised ANSI/RESNA standards in April 1998 may have contributed to better test results.

We only examined class III failures for the wheelchair standard fatigue test. During fatigue strength testing, many wheelchairs experience class I or II failures. These failures are

considered maintenance issues that can be easily fixed by the user or supplier. In this study, the wheelchair did not fail the test unless it experienced three of the same class I or II failures. However, in actual usage, consumers should be aware of maintenance that may be necessary for their wheelchair. Fitzgerald et al found that in a study involving 61 manual wheelchair users, there were 21 class I failures and 29 class II failures among their wheelchairs [43]. In the future, cost analysis may be another variable to examine as a result of fatigue testing. Studies have shown that certain wheelchairs may have a higher retail price than others, but because they last longer, they end up saving the user money in the long run [42]. Consumers and clinicians should examine the fatigue life and cycles/dollar of a wheelchair, not just the overall price.

There are some limitations to this study. There are factors that could affect the test results. For example, we did not test the same type of wheelchairs across all of the years. The type of wheelchairs is a factor that may affect the test results. We only had 18 scooters and 13 PAPAWS but 154 MWCs and 61 EPWs. There was some difference year-to-year in the chair types aslo. One possibility for this, especially for PAPAWS, may be that they have only been introduced on the market in the last decade. The large variances in the sample sizes may also introduce bias into the results. Although, all of the tests were performed by trained personnel very knowledgeable about the standards, all tests were not performed by the same person. There were some other factors that may have contributed to the test results such as manufacture and wheelchair materials. Future studies should consider testing more wheelchairs of each type to investigate the differences in the test results between different types of wheelchairs, or choose one type of wheelchair to follow the change of the durability with the passage of time. However, such studies are expensive and difficult to obtain funding for.

2.5 SUMMARIES

No relationship was identified between the standards durability test results and the year that the testing was conducted. There was a relationship between the test results and wheelchair type. Scooter and EPW had significantly higher odds ratio to pass the standards test than MWC and PAPA. This indicates that scooters and EPW may be more durable than PAPA and MWC. The overall durability of wheelchairs in our broad sample did not improve over the course of 17 years. More attention and focus should be addressed on wheelchair standards testing to assure quality and to improve the design of wheelchairs. We did not see PEW durability became better through testing years. There was also no evidence shown the durability was worsened. Further study is needed to look at whether EPW durability caused the failures and injuries discussed in background section. At the same time, we found that EPW controller did affected EPW users' driving experiences and related to the falls and injuries. Therefore, in the following sections, we were focus on the development and evaluation of the advanced real-time EPW controller.

3.0 3-D MATHEMATICAL MODELING OF AN ELECTRIC POWERED WHEELCHAIR AND SIMULATION RESULTS

This section presents a 3-d mathematical model of an electrical powered wheelchair on a slope to support the development of an advanced wheelchair controller. In order to validate the mathematical model, a simulation using an output feedback controller based on the model of the EPW was presented. An experiment measuring the moment of inertia of a wheelchair using a torsional pendulum method was developed for the simulation. The measured result of the moment inertia of the wheelchair was $5.2280 \text{ kg}\cdot\text{m}^2$. Feedback linearization approach was used to design the control algorithm for the simulation. Simulation results were presented to illustrate the efficacy of the model and control algorithm.

3.1 MODELING AN ELECTRIC-POWERED WHEELCHAIR ON A SLOPE

3.1.1 Why a mathematical model of wheelchair?

Increasingly people with disabilities, as well as old people, are compelled to make use of rehabilitation technology for their mobility. As one important means of mobility for people with

mobility impairments, performance of an EPW was related to its design usage in an outside environment. Most current commercial EPW controllers are very simple and do not take into consideration the wheelchair structure. Some research has considered a wheelchair kinematic model but ignored the affect of users and the dynamic model to ensure the same performance of wheelchairs in different circumstances [47].

Some research has presented dynamic mathematical models of wheelchairs and then showed that advanced controllers based on the model could be developed. Not only did the performance of the wheelchair improve via the advanced control method, but also the stability and safety of the wheelchair. However, most of the models were either 2-D models [47-49] or incomplete models which only considered a dynamic model of the drive wheels [50, 51]. To approach the motion control problem of an EPW, it is necessary to understand first its dynamics. This section presents a 3-D mathematical model of an EPW on a slope was built. The objective of modeling an EPW on a slope was to design a model-based controller to maintain the movement of wheelchair at the desired level in the circumstance of changes in dynamic of wheelchair and the operating environment.

3.1.2 Development of the Model

3.1.2.1 Deriving a 3-D model of the EPW An EPW could be viewed as a coupled electro-mechanical system in which two independent electrical motors produce torques that control rotation angle of the two drive wheels. **Figure 3-1** shows the schemed structure of the wheelchair with users on a slope.

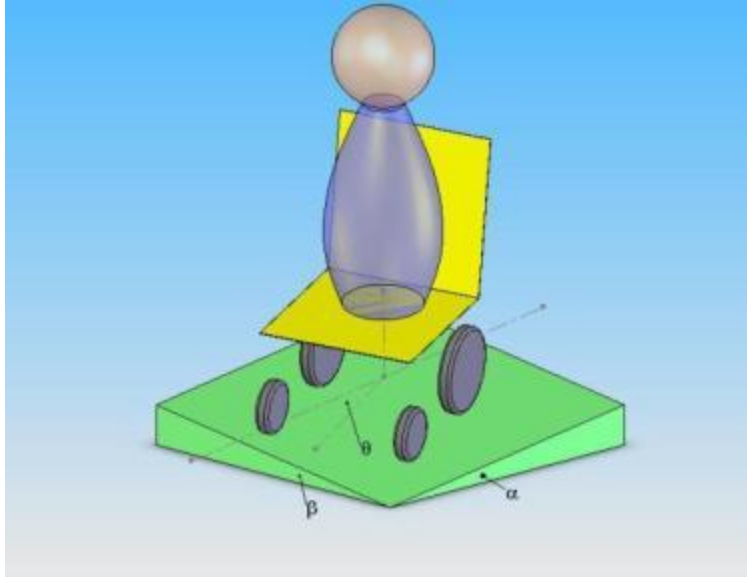


Figure 3-1: 3-D mathematical model of wheelchair system on the slope

3.1.2.2 Assumptions The wheelchair was composed of a rigid platform and non-deforming wheels, and it moved on a slope; the driving wheels rolled and did not slip; the changes of slopes along the path were gradual.

3.1.2.3 List of Variables Definitions Table 3-1 lists the parameters used in the modeling of the EPW.

3.1.2.4 3-D Mathematical Model of the EPW Select the coordinate system like **Figure 3-2**, $x'y'z'$ fixed on the earth ground, xyz on the wheelchair and z axes perpendicular to the earth, $x''y''z''$ also on the wheelchair with z axes perpendicular to the slope surface.

Table 3-1: Parameters of the EPW used in the modeling and simulation work

α =up/downhill slope of road
β =side slope of road associate with the surface
γ =slope along chair motion
ϕ =slope cross chair motion associate with the wheelchair
θ =chair direction
H =height of center of mass (m)
l =distance that center of mass is forward of rear axle (m)
I_z =moment of inertia about z'' axes ($\text{kg}\cdot\text{m}^2$)
L =chair length measured from front to rear axle (m)
M =total mass of chair and driver (kg)
W =width of chair measured between rear wheel footprints (m)
μ =friction coefficient of the surface of the slope
$F_x, F_y, F_z = x'', y'', z''$ component of total weight (N)
F_R, F_L =track force provided by the motor (N)
$F1 - F6$ =other forces acting on front or rear wheels (N)
$\dot{v}_x, \dot{v}_y = x'', y''$ component of velocity of center of mass (m/s)
v_R, v_L =right/left wheel velocity (m/s)
ω_z =chair angular velocity about z'' axes (degree/s)

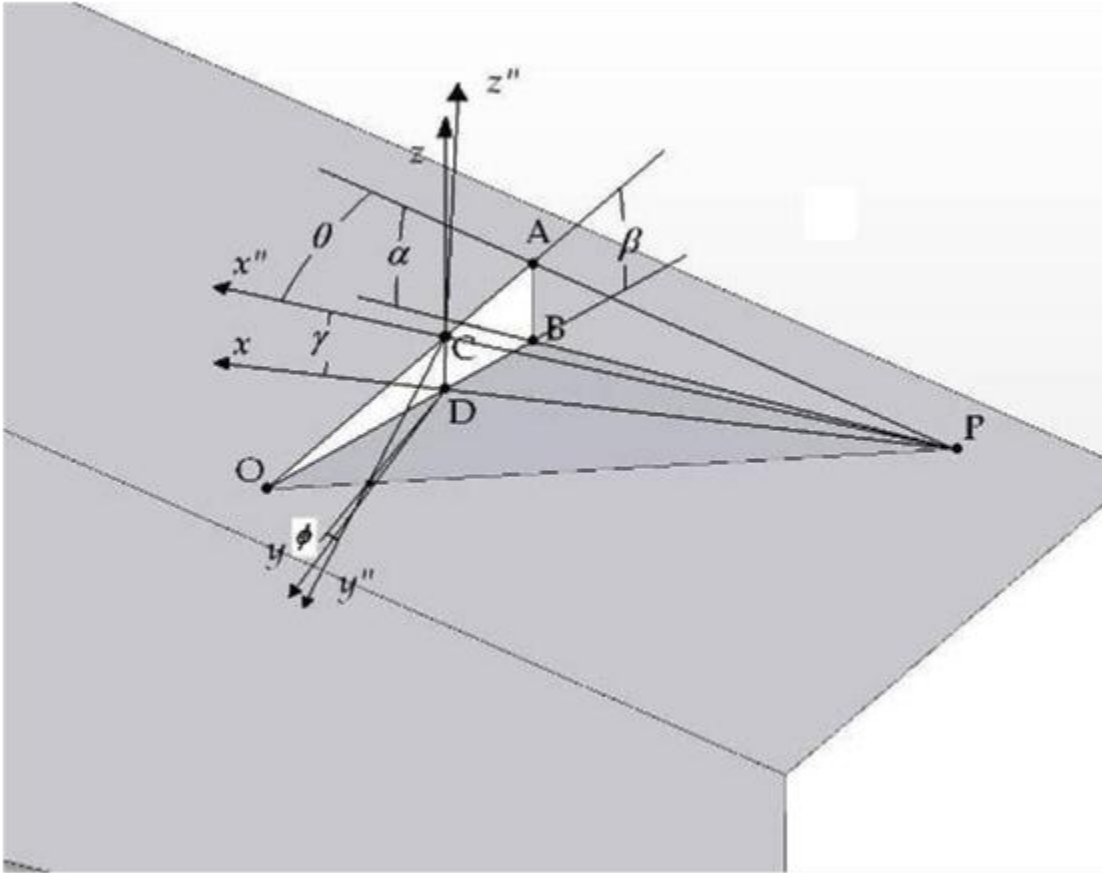


Figure 3-2: Wheelchair axes systems on a slope

Referring to **Figure 3-2**, wheelchair axes systems on a slope showing OAP as the slope surface, C represents the wheelchair, α (up/downhill slope of surface) and β (side slope of surface) associated with the surface, γ (slope along line of EPW motion) and ϕ (cross-slope to EPW motion) associated with the wheelchair, and the EPW direction θ the relations in equation 1 and 2 can be obtained among angles in these three coordinate systems.

$$\sin\gamma = \sin\alpha \cdot \cos\theta - \sin\beta \cdot \sin\theta \quad (1)$$

$$\sin\phi = \sin\alpha \cdot \sin\theta + \sin\beta \cdot \cos\theta \quad (2)$$

Define the track force provided by the drive wheel as F_L , F_R which were decided by the torque the motor provided to each wheel.

From **Figure 3-3**, we can get the force balance equations 3-10,

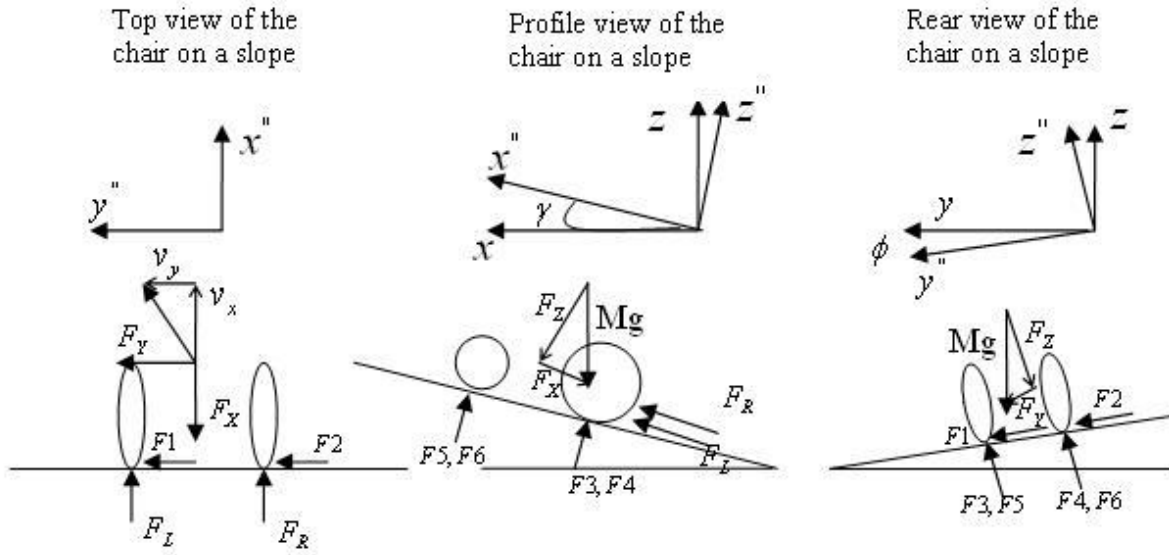


Figure 3-3: Mathematical representatives of different views of a wheelchair on a slope

$$F_L + F_R - \mu(F_3 + F_4 + F_5 + F_6) - F_x = M \cdot \dot{v}_x \quad (3)$$

$$F_1 + F_2 - \mu(F_3 + F_4 + F_5 + F_6) + F_y = M \cdot \dot{v}_y \quad (4)$$

$$F_3 + F_4 + F_5 + F_6 - F_z = M \cdot \dot{v}_z = 0 \quad (5)$$

Where

$$\dot{v}_x = \frac{\dot{v}_R + \dot{v}_L}{2} - \frac{l \cdot (v_R - v_L)^2}{W^2} \quad (6)$$

$$\dot{v}_y = \frac{(\dot{v}_R - \dot{v}_L) \bullet l}{W} + \frac{(v_R^2 - v_L^2)}{2 \bullet W} \quad (7)$$

$$F_x = \frac{M \bullet g \bullet \tan \gamma}{1 + \tan^2 \gamma + \tan^2 \beta} \quad (8)$$

$$F_y = \frac{M \bullet g \bullet \tan \beta}{1 + \tan^2 \gamma + \tan^2 \beta} \quad (9)$$

$$F_z = \frac{1}{1 + \tan^2 \gamma + \tan^2 \beta} \quad (10)$$

Moment balance about the center of mass of the system in **Figure 3-3** gives the equations 11-13,

$$(F_R - F_L) \bullet \frac{W}{2} - (F1 + F2) \bullet l = \frac{I_z \bullet \pi \bullet \dot{\omega}_z}{180} \quad (11)$$

$$(F3 + F5) \bullet \frac{W}{2} + (F1 + F2) \bullet H - (F4 + F6) \bullet \frac{W}{2} = 0 \quad (12)$$

$$(F5 + F6) \bullet (L - l) + (F_R + F_L) \bullet H - (F3 + F4) \bullet l = 0 \quad (13)$$

From equations (3) through (13), can be found that equations the results are 14-16

$$\dot{v}_R = \frac{A + B}{2} \quad (14)$$

$$\dot{v}_L = \frac{A - B}{2} \quad (15)$$

$$\omega_z = \frac{d\theta}{dt} = \frac{180 \bullet (v_R - v_L)}{\pi \bullet W} \quad (16)$$

Where 'A' and 'B' are given by equations 17 and 18, applying Euler's method, we can get the final results by equations 19-21.

$$A = \frac{2(F_L + F_R - \mu F_Z - F_X)}{M} + \frac{2 \bullet l \bullet (v_R - v_L)^2}{W^2} \quad (17)$$

$$B = \frac{\frac{2 \cdot (F_Y - \mu F_Z) \cdot l + (F_R - F_L) \cdot W}{2 \cdot M \cdot l} - \frac{v_R^2 - v_L^2}{2 \cdot W}}{\frac{l}{W} + \frac{I_Z}{M \cdot l \cdot W}} \quad (18)$$

Table 3-2: Parameters required for validating the mathematical model of the EPW

$F_R =$ (N) track force provided by the right side motor	Measured by the Smart ^{Hub} [52]
$F_L =$ (N) track force provided by the left side motor	
$\alpha =$ directly measured	
$\beta =$ directly measured	
$\theta =$ directly measured	
$H = 23.2304$ (cm) directly measured	
$l = 4.6256$ (cm) directly measured	
$I_Z = 5.2280$ (kg·m ²) (detail see next section)	
$L = 17.375$ (cm) directly measured	
$M = 200+$ (P) directly measured	
$W = 24.55$ (cm) directly measured	
$\mu =$ friction coefficient of the surface of the slope referred to [53]	
$\dot{v}_x, \dot{v}_y = \dot{x}, \dot{y}$ component of velocity of center of mass (m/s) measured from caster encoder	
$v_R, v_L =$ right/left wheel velocity (m/s) measured from wheel encoders	
$\omega_z =$ chair angular velocity about z axes (degree/s) measured from inertia sensor	

$$v_R(k) = \frac{(A+B) \bullet \Delta t}{2} + v_R(k-1) \quad (19)$$

$$v_L(k) = \frac{(A-B) \bullet \Delta t}{2} + v_L(k-1) \quad (20)$$

$$\theta(k) = \frac{180 \bullet (v_R - v_L) \bullet \Delta t}{\pi \bullet W} + \theta(k-1) \quad (21)$$

Validation of the Model

In order to validate the mathematical model, we planned to conduct some simulation first to test the model. Below **Table 3-2** lists the parameters required to determine or measure for the model.

Most of the parameters needed to validate the model could be either directly measured or calculated from the encoders. However, for the moment of inertia, we could not directly measure or calculate since the EPW is an irregularly shaped object. In the next section we present a lab-based method to measure the moment of inertia of the EPW.

3.2 AN EXPERIMENTAL METHOD FOR MEASURING THE MOMENT OF INERTIA OF AN ELECTRIC POWERED WHEELCHAIR

As stated in previous session, moment of inertia was one of the key factors for the 3D model and control. In this section, an experiment measuring the moment of inertia of an electric powered wheelchair (EPW) using a torsional pendulum method is presented. The experimental test platform consisted of a bottom circular wood plate, an upper metal plate, and four ropes. Materials with known moments of inertia such as a metal disk and cylinder were used to test the accuracy of the system. The EPW used in the experiment was an Invacare G3 Torque SP Storm

Series. The measured result of the moment inertia of the wheelchair was 5.2280 kg·m² and the errors of the system are less than 10% even if the object was only 25lbs. The results were consistent when compared with other approximation methods.

3.2.1 Why moment of inertia is important?

Accurate mathematical models are essential for the design of useful control systems. However, in electric powered wheelchair (EPW) modeling little attention has been paid to the parameters of these models. Much research has been conducted on the dynamic characteristics of wheelchairs, including dynamic stability [50, 51, 54, 55], velocity and traction control [47, 56], transportation, and vibration [57]. For the creation of mathematical models and design of control systems for wheelchairs, it is essential to know the moment of inertia. However, in the aforementioned studies, either an assumed mass moment of inertia for the wheelchair was used [50, 51, 54-57] or the wheelchair was simplified to regular cuboids. Ding et al [47] estimated the moment of inertia of the wheelchair by rotating the wheelchairs and occupant on a force plate and recording the angular velocity of the rotation. Euler equations were then applied to calculate the moment of inertia.

EPWs consist of motors, wheels, metal frames, and other components, which have different densities and irregular shapes. These factors make the direct computing of the inertia of the entire chair very difficult. The cuboid method of estimating moment of inertia does not account for irregular shapes and varying density and may not be sufficiently accurate for controller design. The methods described by Ding et al, are more accurate; however, a force plate to collect the ground reaction force and a motion capture device to record the angular velocity

are necessary. These pieces of equipments are expensive and may introduce error into the measurement.

The moment of inertia of any object can be experimentally measured by suspending the object through its center of mass with a single cable. The moment of inertia can be calculated by twisting the object about the axes of the cable and measuring the period of the oscillation [58]. However, for heavy, irregular objects, such as EPWs, suspending them through the center of mass with one cable is difficult. An addition problem is that in practice twisting the cable also results in a swinging motion, confounding the period measurement.

3.2.2 Methodological approach

3.2.2.1 Theory The following is the derivation of equation for calculating the mass moment of inertia of any given object from readily measurable quantities in the four cable system. A summary of the variables is given in **Table 3-3**.

For a group of objects, the combined moment of inertia is equal to the sum of the individual moments about a given axes. Given this, the difference between the moment of inertia of the bottom plate along with the wheelchair, I_1 , and bottom plate, I_0 , would yield moment of inertia of the wheelchair, I .

$$I = I_1 - I_0 \quad (22)$$

The equations used to calculate I_0 and I_1 were derived from the law of conservation of energy. Suppose the mass of the bottom plate is m_0 and it is rotated about its center axes, with a maximum height, h_m . During the rotation motion, the kinetic energy E_k and potential energy E_p of the plate are complimentary. At the highest point of the bottom plate:

$$E_p = m_0 g h_m \text{ \& } E_k = 0 \quad (23)$$

Table 3-3: Definition of variables

Symbol	Quantity	Unit
d	upper plate diameter	Cm 1cm=0.01m
D	wood plate diameter	Cm 1cm=0.01m
m_0	wood plate weight	pound 1 pound=0.4536kg
H_0	empty distance between upper plate and bottom plate	Cm 1cm=0.01m
m_m	Weight of metal disk	pound 1 pound=0.4536kg
m_c	Weight of the cylinder	pound 1 pound=0.4536kg
d_m	Inner diameter of metal disk	Cm 1cm=0.01m
D_m	Outer diameter of metal disk	Cm 1cm=0.01m
d_c	Diameter of cylinder	Cm 1cm=0.01m
m_w	Weight of the wheelchair	pound 1 pound=0.4536kg
d_{cr}	Distance between center of mass and rear wheel axes	Cm 1cm=0.01m
t_0 t_1 t_2	Ten periods time when bottom plate is empty, with metal disk, with cylinder and with wheelchair	s
\bar{t}	Average time of the two trials	s
I_0 I_1 I_2 I_3	Measured inertia of wood plate, metal disk, cylinder and wheelchair	kg·m ²

When the plate returns to equilibrium position:

$$E_k = 1/2 * I_0 \omega_m^2 \quad \& \quad E_p = 0 \quad (24)$$

As shown in **Figure 3-4**, I_0 is the moment of inertia of the plate with respect to the $00'$ axes and ω_m is the angular velocity of the plate when it passes the equilibrium position. By ignoring the resistance of the air and applying the conservation of mechanical energy:

$$1/2 * I_0 \omega_m^2 = m_0 g h_m \quad (25)$$

The parameter m_0 is readily measured with a scale. When the initial rotation angle of the bottom plate is very small, the movement of the plate is considered a harmonic vibration. Hence, the maximum angular displacement is

$$\theta = \theta_m \sin(2\pi / T_0)t \quad (26)$$

With an angular velocity of:

$$\omega = d\theta / dt = 2\pi\theta_m / T_0 \cos(2\pi / T_0)t, \quad \omega_m = 2\pi / T_0 \theta_m \quad (27)$$

From the geometric relations given in **Figure 3-4**:

$$h_m = \overline{OO_1} = \overline{BC} - \overline{BC'} = (\overline{BC}^2 - \overline{BC'}^2) / (\overline{BC} + \overline{BC'}) \quad (28)$$

$$\overline{BC}^2 = \overline{AB}^2 - \overline{AC}^2 = L^2 - (R-r)^2 \quad (29)$$

$$\overline{BC'}^2 = \overline{A'B}^2 - \overline{A'C'}^2 = L^2 - (R^2 + r^2 - 2Rr \cos \theta_m) \quad (30)$$

$$\overline{BC} + \overline{BC'} = 2H_0 - h_m \quad (31)$$

By substituting (29-31) into (28),

$$\begin{aligned} h_m &= 2Rr(1 - \cos \theta_m) / (2H_0 - h_m) \\ &= 4Rr \sin^2 \left(\frac{\theta_m}{2} \right) / (2H_0 - h_m) \end{aligned} \quad (32)$$

When θ_m is small ($\theta_m < 5^\circ$),

$$\sin \theta_m / 2 \approx \theta_m / 2 \text{ rad}, \quad 2H_0 - h_m \approx 2H_0 \quad (33)$$

Then,

$$h_m = Rr \theta_m^2 / (2H_0) \quad (34)$$

Substitute (27) and (34) into (25),

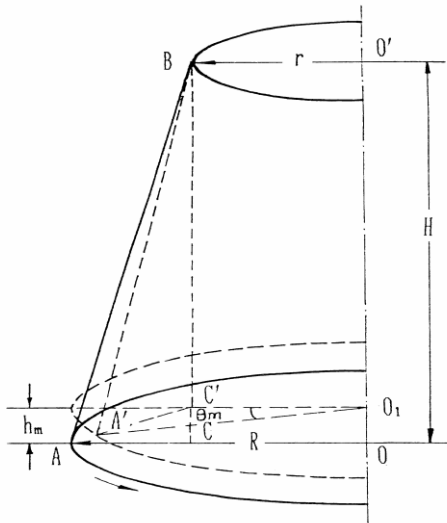


Figure 3-4: The principle of torsional pendulum used in the experiment

$$1/2 \cdot I_0 (2\pi/T_0 \cdot \theta_m)^2 = m_0 g R r / (2H_0) \theta_m^2 \quad (35)$$

Solving for I_0 ,

$$I_0 = m_0 g R r / (4\pi^2 H_0) T_0^2 \quad (36)$$

From (22), the mathematical model for measuring the moment of inertia about axes OO' to any object with mass m is obtained.

$$I_1 = (m + m_0) g R r / (4\pi^2 H_1) T_1^2 \quad (37)$$

From [55], the equations for the moment of inertia of metal disk and cylinder are:

$$I_d = 1/8m(D^2 + d^2) \ \& \ I_c = 1/8md^2 \quad (38)$$

Since the moment of inertia result is based on an experimental measurement, an average calculation can be incorporated.

$$I_0 = m_0 g R r / (4\pi^2 H_0) (t_0 / 10)^2 \quad (39)$$

$$I_1 = m_1 g R r / (4\pi^2 H_1) (t_1 / 10)^2 \quad (40)$$

In addition, the uncertainty of the measure of the moment inertia of the objects can be calculated.

$$u_r(I_0) = \sqrt{2^2 u_r^2(t_0) + u_r^2(H_0)} \quad u(I_0) = I_0 \cdot u_r(I_0) \quad (41)$$

$$u(I) = \sqrt{u(I_1)^2 + u(I_0)^2} \quad u(I_1) = I_1 \cdot u_r(I_1) \quad (42)$$

3.2.2.2 Experimental Protocol In order to implement the four cable torsional pendulum method, a circular wood bottom plate of uniform mass distribution was created. The bottom plate was connected to a small, circular top plate with four inelastic pieces of rope. The apparatus was set up in the wheelchair testing laboratory of the Human Engineering Research Labs (**Figure 3-5**). The frame used for curb drop testing was used to suspend the ropes and bottom plate with the EPW. The specifications for the torsional pendulum are given in **Table 3-4**.

The experiment commenced with the measuring of the moment of inertia of the bottom plate. A level was used to ensure the plate was horizontal. Then, the bottom plate was rotated to an angle of less than 5° and two trials of five rotation periods were recorded. A trial was considered invalid if the pendulum started to swing, instead of purely rotating.

An assumption of the moment of inertia derivation was that the torsion angle was not larger than 5°. The error, E, due to the angle estimation is given in equation (43) as a function of angle θ_m .

$$E = 2(\theta_m / 2 - \sin \theta_m / 2) / \sin(\theta_m / 2). \quad (43)$$



Figure 3-5: Photographs of the motion of the bottom plate with the EPW on the plate and the devices (gradienter, stopwatch, rulers, etc.) and materials (metal disks, cylinder) used in the experiment

Table 3-4: Parameters of the torsional pendulum

Efficiency diameter(cm)		Distance between up and bottom(cm)	Weight(pound)
Upper plate d	Bottom plate D	Empty plate H_0	Bottom plate m_0
6.312	110	199.15	29

During the experiment, to ensure θ_m was less than 5° , the bottom plate rotation was rotated a precise distance from a stationary marker.

Secondly, the accuracy of the experimental set-up was tested using two objects, a metal disk and a cylinder, whose theoretical mass moment of inertia could be readily calculated from the equations given in (38). The physical parameters of the metal disk and cylinder are given in **Table 3-5** and **Table 3-6** respectively. The testing procedure was complete in similar fashion as the exclusively bottom plate trial, only now each object was placed on the bottom plate with its

center of mass placed in line with the center of mass of the bottom plate. The measurements were recorded and compared to the theoretical values. Lastly, the test was completed a third time with an Invacare G3 Torque SP Storm Series, whose physical parameters are given in **Table 3-7**.

Table 3-5: Parameters onf metal disk

Weight m (pound)	Inner diameter d (cm)	Outer diameter D (cm)
25	3.842	29.296

Table 3-6: Parameters of the cylinder

Weight m (pound)	diameter d (cm)
27.5	15.4699

Table 3-7: Parameters of the EPW

Weight m (pound)	Center of mass from rear wheel axes d (cm)
200	4.6256

3.2.3 Measurement results

The raw results of the four conditions for the torsional pendulum experiment are given in **Table 3-8**. The time to complete the two trials of five time periods are given in the columns labeled trial 1 and 2, with the average given in \bar{t} . The distance between the top and bottom plates is given

in the last column. The time period decreased with increasing weight of the object while the distance between plates increased.

Table 3-8: Periods of the torsional pendulum

Order of the measurement	Trial 1	Trial 2	\bar{t}	Distance between top and bottom (cm)
The bottom plate only t_0 (s)	82.78	82.60	82.69	199.15
The bottom plate and metal disk t_1 (s)	62.64	62.74	62.69	199.18
The bottom plate and cylinder t_2 (s)	60.21	60.12	60.165	199.20
The bottom plate and wheelchair t_3 (s)	56.81	56.88	56.845	201.60

Table 3-9: Measurement results of the inertias and calculating results

Inertia I (kg·m ²)	Measured result	Calculated Result	Difference between the two results	Errors in percent (%)
The bottom plate only I_0	1.9461	1.9896	0.0435	2.1864
The metal disk I_1	0.1238	0.1362	0.0124	9.1042
The cylinder I_2	0.0413	0.0373	0.0040	10.3279
The wheelchair I_3	5.2280	NA		

Table 3-9 shows that all three objects for which the theoretical values were calculated had measurement errors of less than 10%. Errors tended to decrease with heavier objects. The Invacare EPW had a moment of inertia of $5.228 \text{ kg}\cdot\text{m}^2$.

Evaluation of equation (43) resulted in an error of +0.064% when $\theta_m=5^\circ$ and an error of +0.24 when $\theta_m=10^\circ$. The positive error indicates that over rotation will cause the measure moment of inertia to be larger than it should be.

3.2.4 Evaluation of the method

The four cables-torsional pendulum method for experimentally measuring the moment of inertia of an EPW proved to be successful. The method utilized low cost, readily available materials which could allow for wider usage as compared to methods that depend on expensive instrumentation [55, 59]. The set up was also able to support the weight and size and an EPW.

Of objects measured whose theoretical value was calculated, a low percentage error was found. The data suggested that heavier object had lower percentage errors than lighter ones, a favor condition for measuring the inertia of heavy objects like EPWs. The results were further validated when compared to the values measured by Ding et al [47], who reported EPWs had a moment of inertia of $3 \text{ kg}\cdot\text{m}^2$ (Quickie P100), $6 \text{ kg}\cdot\text{m}^2$ (Quickie P200) and $8 \text{ kg}\cdot\text{m}^2$ (Invacare). The $5.228 \text{ kg}\cdot\text{m}^2$ measured in this study falls within this range.

Despite these promising results, this method does have several potential sources of error. If the center of mass of wheelchair does not line up with the center of the bottom disk, error will be introduced. If the distance between two centers is a , the system error will be $+ma^2$ which would make the measured result larger than the actual value. During the entire experiment the

bottom plate must be kept level to avoid errant measurements. Another potential cause of error is swinging. Although the four-cable system reduces the amount of swinging versus a single wire, some swinging can still occur. Trials that swinging is observed should be considered invalid and should be repeated.

Simple measurement tools were used to collect data in this experiment and could have introduced error. However, other more accurate tools could be used to reduce this possibility. Counting time periods and measuring them with a stopwatch has limited accuracy and can be subjective. Analysis with uncertainty could eliminate error associated with human measurement.

A limitation of this study is that only one type of EPW was measured. Future work should aim to measure a variety of EPWs. Drawing comparisons in moment of inertia of categories of EPW, such front, mid, and rear wheel drive chairs, could lead to better control algorithms suited for a particular type. An anthropometric test dummy could also be included in the moment of inertia measurement to increase the real world applicability of these measurements. Another limitation of this study was that objects used for the testing of accuracy were dimensionally small and relatively light when compared to a typical EPW. A larger and heavier test object with a calculated moment of inertia could be calculated should be tested.

3.2.5 Summary

In this section, an experimental method used to evaluate the moment of inertia of the EPWs was presented. From the measurement results, the system could measure the moment of inertia with errors of less than 10%. The results suggested the method also could be used to measure inertia of manual wheelchair or other heavy irregular objects. The advantage of this method was that it

was convenient and could be performed inexpensive with a high degree of accuracy. With future improvement data could be collected that would lead to more accurate mathematical models of EPWs and better designed controllers.

3.3 SIMULATION OF MODEL BASED FEEDBACK CONTROL OF AN ELECTRIC POWERED WHEELCHAIR

3.3.1 Kinematic Model of an EPW

The kinematic model of a typical rear-wheel drive EPW (**Figure 3-6**) is described in this section. **Table 3-10** shows the definitions of the variables used in the kinematic and dynamic models. Due to the nonholonomic feature, the EPW could not move in the lateral direction. It was assumed that the driving wheels did not slip, and the kinematic model is shown in eq. (44).

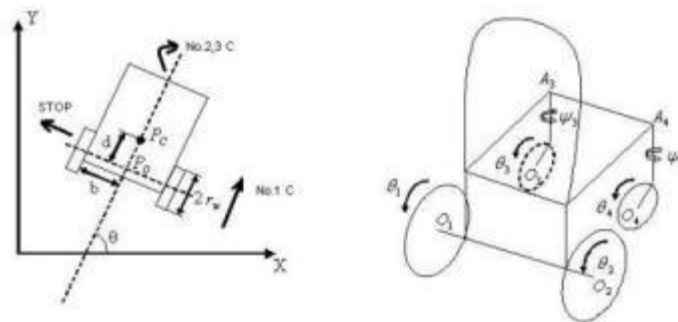


Figure 3-6: Free body diagram of an EPW

Table 3-10: Parameters of the mathematical model of an EPW

C : Center of Mass of the Wheelchair/Rider system
m : Total mass of the wheelchair = $m_c + 2 m_w + 2 m_f$
m_c : Mass of wheelchair without the driving wheels and the rotors of DC motors and the front casters
m_w : Mass of driving wheel with the rotor
m_f : Mass of front caster
I_c : Moment of Inertia of the wheelchair body
I_{w1} : Moment of Inertia of the driving wheel
I_{f1} : Moment of Inertia of the front caster
I_{w2} : Moment of Inertia of the driving wheel about the wheel diameter
I_{f2} : Moment of Inertia of the front caster about the wheel diameter
b : The distance between the driving wheels and the axes of symmetry
r_w : The radius of each driving wheel
r_f : The radius of each front caster
d : The distance from P_c to P_o
θ : The heading angle of the wheelchair
$\theta_1, \theta_2, \theta_3, \theta_4$: rolling angles of the wheels
φ_1, φ_2 : Yaw angles of the front casters
l : Distance from the rear axle to the front axle
W : Caster trail
τ_1, τ_2 : Input torques to the left and right rear wheels

$$A(q)\dot{q}=0 \quad (44)$$

Where

$$A(q) = \begin{bmatrix} -\sin \theta & \cos \theta & -d & 0 & 0 \\ -\cos \theta & -\sin \theta & -b & r_w & 0 \\ -\cos \theta & -\sin \theta & b & 0 & r_w \end{bmatrix}, \quad q = (x_c, y_c, \theta, \theta_1, \theta_2) \quad (45)$$

3.3.2 Dynamic Model

Lagrange formulation was used to establish equations of an EPW motion. The total energy of the wheelchair system was as follows:

$$K = 1/2(m_c + 2m_w + 2m_f)(x_c^2 + y_c^2) + 1/2(I_c + 2m_w(b^2 + d^2) + 2I_{w2})\dot{\theta}^2 + 1/2I_{w1}(\dot{\theta}_1^2 + \dot{\theta}_2^2) - 2m_w d\theta(\dot{y}_c \cos\theta - \dot{x}_c \sin\theta) + 1/2I_{f1}(\dot{\theta}_3^2 + \dot{\theta}_4^2) + 1/2I_{f2}(\dot{\psi}_1^2 + \dot{\psi}_2^2) \quad (46)$$

The EPW motion could be described below

$$d/dt(\partial K / \partial \dot{q}_i) - \partial K / \partial q_i = Q_i - a_{1i}\lambda_1 - a_{2i}\lambda_2 - a_{3i}\lambda_3 \quad (47)$$

Where $q = (x_c, y_c, \theta, \theta_1, \theta_2)$ with (x_c, y_c) defining the position of the center of gravity and θ being the heading angle. The Lagrange equations of motion of the EPW with the Lagrange multipliers λ_1, λ_2 and λ_3 are given by

$$m\ddot{x}_c + 2m_w d(\ddot{\theta} \sin\theta + \dot{\theta}^2 \cos\theta) - \lambda_1 \sin\theta - (\lambda_2 + \lambda_3) \cos\theta = 0 \quad (48)$$

$$m\ddot{y}_c - 2m_w d(\ddot{\theta} \cos\theta - \dot{\theta}^2 \sin\theta) + \lambda_1 \cos\theta - (\lambda_2 + \lambda_3) \sin\theta = 0 \quad (49)$$

$$2m_w d(\ddot{x}_c \sin\theta - \ddot{y}_c \cos\theta) + I\ddot{\theta} - d\lambda_1 + b(\lambda_2 + \lambda_3) = 0 \quad (50)$$

$$\underbrace{(I_{w1} + I_{f1}(g_1^2 + h_1^2) + I_{f2}(g_3^2 + h_3^2))}_{I_1} \ddot{\theta}_1 + \underbrace{(I_{f1}(g_1 g_2 + h_1 h_2) + I_{f2}(g_3 g_4 + h_3 h_4))}_{I_2} \ddot{\theta}_2 + \lambda_2 r_w = \tau_1 \quad (51)$$

$$\underbrace{(I_{f1}(g_1g_2+h_1h_2)+I_{f2}(g_3g_4+h_3h_4))\ddot{\theta}_1}_{I_2} + \underbrace{(I_{w2}+I_{f1}(g_2^2+h_2^2)+I_{f2}(g_4^2+h_4^2))\ddot{\theta}_2}_{I_3} + \lambda_3 r_w = \tau_2 \quad (52)$$

These five equations can be rewritten in the vector form as

$$M(q)\ddot{q} + V(q, \dot{q})\dot{q} + \tau_d = E(q)\tau - A^T(q)\lambda \quad (53)$$

where $q = (x_c, y_c, \theta, \theta_1, \theta_2)$ with (x_c, y_c) defining the position of the center of gravity and θ being the heading angle; $M(q) \in \mathbb{R}^{5 \times 5}$ is the symmetric positive definite inertia matrix; $V(q, \dot{q}) \in \mathbb{R}^{5 \times 5}$ is the centripetal and Coriolis matrix; $\tau_d \in \mathbb{R}^{5 \times 1}$ is the bounded unknown disturbances including unstructured un-modeled dynamics; $E(q) \in \mathbb{R}^{5 \times 2}$ is the input transformation matrix; $\tau \in \mathbb{R}^{2 \times 1}$ is the input torque vector; $A(q)$ means the wheelchair cannot slide in the lateral direction; and $\lambda \in \mathbb{R}^{1 \times 1}$ is the Lagrange multiplier vector of constraint force.

$$M(q) = \begin{bmatrix} m & 0 & 2m_w d \sin \theta & 0 & 0 \\ 0 & m & -2m_w d \cos \theta & 0 & 0 \\ 2m_w d \sin \theta & -2m_w d \cos \theta & I & 0 & 0 \\ 0 & 0 & 0 & I_1 & I_2 \\ 0 & 0 & 0 & I_2 & I_3 \end{bmatrix}$$

$$V(q, \dot{q}) = \begin{bmatrix} 2m_w d \dot{\theta}^2 \cos \theta \\ 2m_w d \dot{\theta}^2 \sin \theta \\ 0 \\ 0 \\ 0 \end{bmatrix}, \quad E(q) = \begin{bmatrix} 0 & 0 \\ 0 & 0 \\ 0 & 0 \\ 1 & 0 \\ 0 & 1 \end{bmatrix}, \quad \tau = \begin{bmatrix} \tau_1 \\ \tau_2 \end{bmatrix}$$

We then defined a 5 X 2 dimensional matrix $S(q)$ such that $A(q)S(q) = 0$. It is straightforward to verify that the following matrix had the required property

$$S(q) = [s_1(q) \quad s_2(q)] = \begin{bmatrix} c(b \cos \theta - d \sin \theta) & c(b \cos \theta + d \sin \theta) \\ c(b \sin \theta + d \cos \theta) & c(b \sin \theta - d \cos \theta) \\ c & -c \\ 1 & 0 \\ 0 & 1 \end{bmatrix}$$

Where the constant $c = (r_w / 2b)$. From the constraint equation (44), \dot{q} is in the null space of $A(q)$. Because the two columns of $S(q)$ are in the null space of $A(q)$ and are linearly independent, it is possible to express \dot{q} as a linear combination of the two columns of $S(q)$, that is, $\dot{q} = S(q)v$ (54)

The rationale behind (54) is to introduce a set of independent velocity variables v .

Owing to the choice of $S(q)$ matrix, we have
$$v = \begin{bmatrix} v_1 \\ v_2 \end{bmatrix} = \begin{bmatrix} \dot{\theta}_1 \\ \dot{\theta}_2 \end{bmatrix}$$

Differentiating equation (54) and substituting the expression for \ddot{q} into (44) and pre-multiplying it by S^T , we have $S^T(MS\dot{v}(t) + M\dot{S}v(t) + V) = \tau$ (55)

Using the state-space vector $x = [q^T \quad v^T]^T = [x_c, y_c, \theta, \theta_1, \theta_2, \dot{\theta}_1, \dot{\theta}_2]^T$ the dynamic model of an EPW in a state space can be represented as follows:

$$\dot{x} = \begin{bmatrix} Sv \\ f_2 \end{bmatrix} + \begin{bmatrix} 0 \\ (S^T MS)^{-1} \end{bmatrix} \tau \quad (56)$$

Where $f_2 = (S^T MS)^{-1}(-S^T M\dot{S}v - S^T V)$

This state equation can be further simplified as below

$$\dot{x} = \begin{bmatrix} Sv \\ 0 \end{bmatrix} + \begin{bmatrix} 0 \\ I \end{bmatrix} u \quad (57)$$

By applying the following nonlinear feedback

$$\tau = S^T MS (u - f_2) \quad (58)$$

3.3.3 Control Algorithm

As Equation (57) is not input-state linearizable, we could assume a new input u to linearize it.

Differentiating the output and substituting Equation (44), we obtain

$$\dot{y} = (\partial h(q) / \partial q) \dot{q} = J_h(Sv) = (J_h S)v = \Phi v \quad (59)$$

where Φ is the decoupling matrix represented in the following form:

$$\Phi = J_h(q)S(q) = \begin{bmatrix} \Phi_{11} & \Phi_{12} \\ \Phi_{21} & \Phi_{22} \end{bmatrix} \quad (60)$$

$$\Phi_{11} = c((b - y_r^c) \cos \theta - (d + x_r^c) \sin \theta) \quad \Phi_{12} = c((b + y_r^c) \cos \theta + (d + x_r^c) \sin \theta)$$

$$\Phi_{21} = c((b - y_r^c) \sin \theta + (d + x_r^c) \cos \theta) \quad \Phi_{22} = c((b + y_r^c) \sin \theta - (d + x_r^c) \cos \theta)$$

Differentiating Equation (59) again, we obtain

$$\ddot{y} = \dot{\Phi}v + \Phi\dot{v} \quad (61)$$

Substituting \ddot{y} with the linearized feedback v

$$v = \dot{\Phi}v + \Phi\dot{v} = \dot{\Phi}v + \Phi u \Rightarrow u = \Phi^{-1}(v - \dot{\Phi}v) \quad (62)$$

So we could use the desired path y^d to feedback the error $e = y^d - y$

$$\ddot{y} = v = \ddot{y}^d + K_d(\dot{y}^d - \dot{y}) + K_p(y^d - y) \quad (63)$$

From (63) we knew v and then we found u then \dot{x} , and integrated \dot{x} we solved this problem.

The control diagram is shown in **Figure 3-7**.

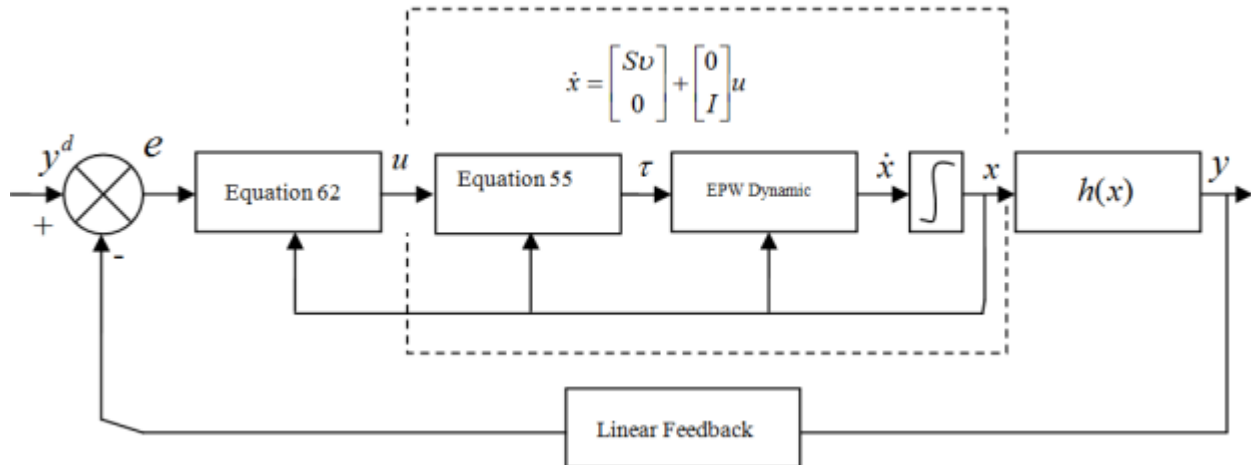


Figure 3-7: Output Feedback Control Diagram of the System

3.3.4 Simulation results

Simulation results were presented in this section. An EPW was initially directed toward positive X axes at rest. The three different paths used in the simulation are shown in **Figure 3-8**.

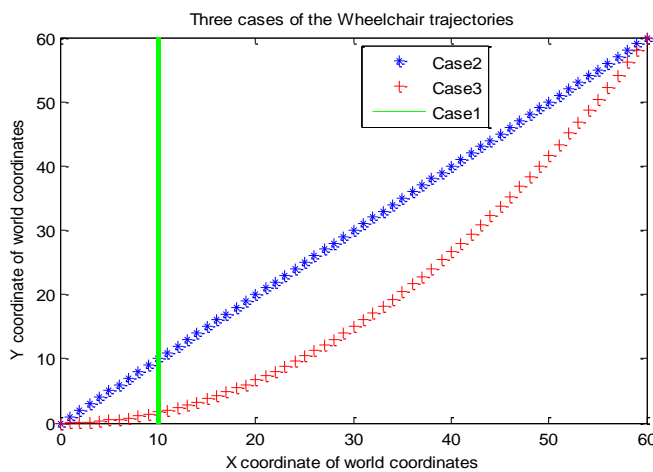


Figure 3-8: Three desired paths for the simulation: Case i: $Y=10$, Case ii: $Y=X$ and Case iii: $Y=X^2/60$

1) Case i) Straight line perpendicular to the X axes or the initial forward direction of the Wheelchair.

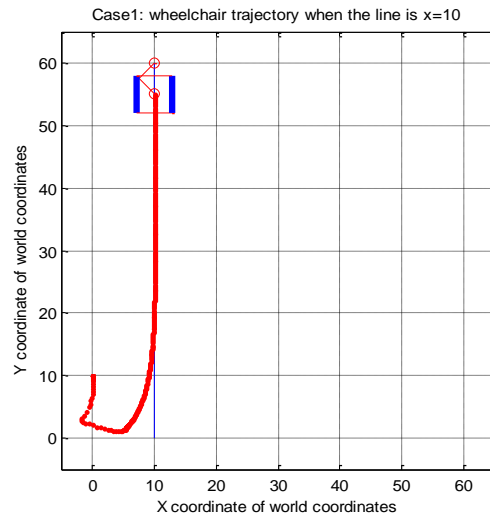


Figure 3-9: Trajectory of wheelchair for Case i

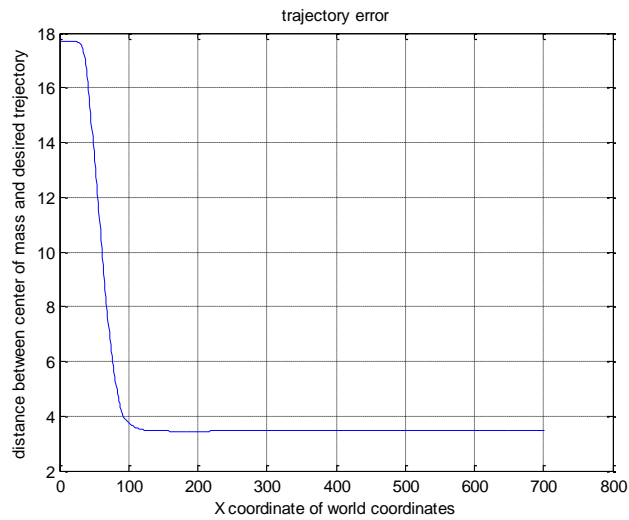


Figure 3-10: Trajectory errors between center of mass and desired path for case i

2) Case ii) Forward slanting line 45 degrees from X axes.

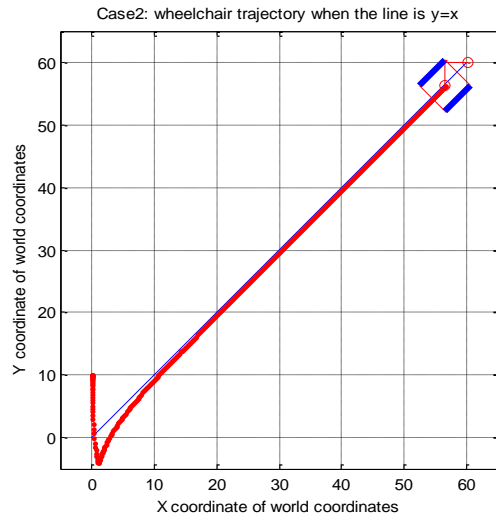


Figure 3-11: Trajectory of wheelchair for Case ii

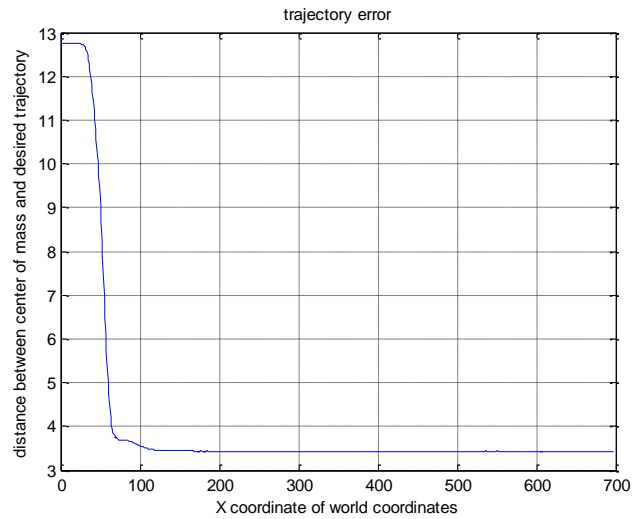


Figure 3-12: Trajectory errors between center of mass and desired path for case ii

3) Case iii) Forward curve Y coordination value equal to the square of the X coordination value divided by 60 ($Y=X^2/60$).

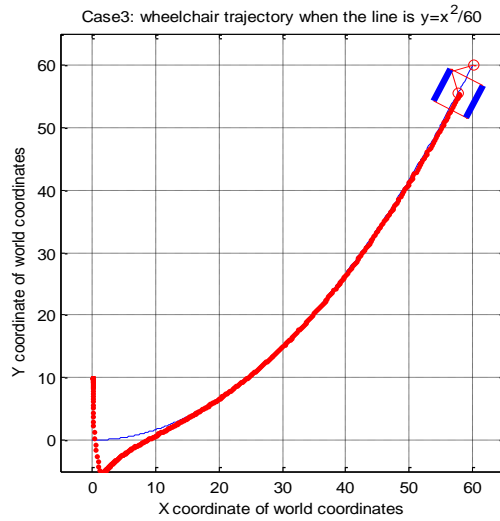


Figure 3-13: Trajectory of wheelchair for Case iii

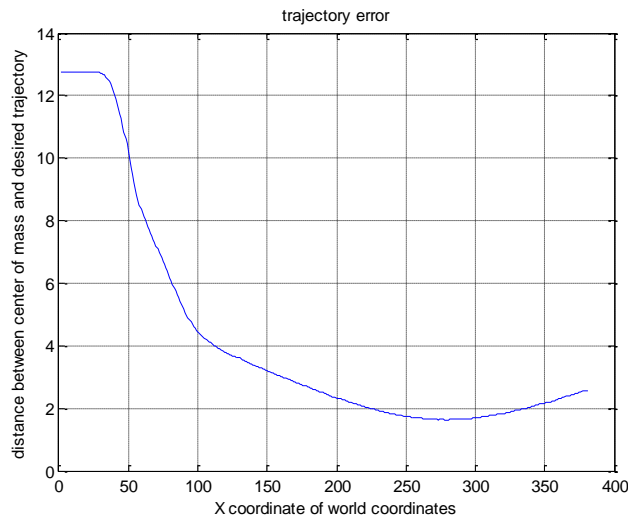


Figure 3-14: Trajectory errors between center of mass and desired path for case iii

The wheelchair dimensions in the simulation is 2.45cm (width between two rear wheel) by 1.74cm (length from axes between rear wheels and caster wheels) according to ratio of the real measurement in the above section for wheelchair model. The actual trajectories of the wheelchair for the three trajectories were shown in **Figure 3-9, 3-11, and 3-13**. From those figures it can be seen that the EPW moved backward for a short period of time at the very beginning to achieve the needed heading angle and then followed the desired trajectories very well. The backward motion was not explicitly planned, but a consequence of the control algorithm. The presence of such backward motion depended on the direction of a desired trajectory and the desired velocity.

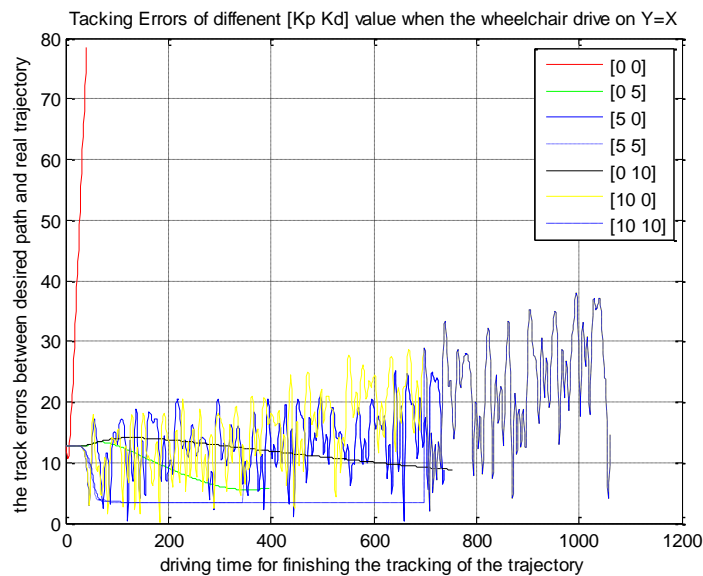


Figure 3-15: Trajectory errors between center of mass and desired path for case ii with different [Kp Kd] values

Figure 3-10, 3-12 and 3-14 plot the trajectory errors between the trajectory of the center

of mass and the desired path. The mean square error (MSE) was 0.8618 cm (35.2% of wheelchair width) for case i, 0.8588 cm (35.1% of wheelchair width) for case ii and 1.0568 cm (43.1% of wheelchair wide) for case iii.

We also examined the effect of control parameters K_p and K_d on the performances of the control algorithm. **Figure 3-15** shows the trajectory errors with different K_p and K_d for case ii trajectory ([0 0] represents $K_p=0$, and $K_d=0$).

3.3.5 Summary

We developed an output feedback controller for an EPW based on its kinematic and dynamic model, and demonstrated its effectiveness with simulation results. The results showed a good compliance with the study by Yamamoto et al. [60] that was controlling a mobile robot. The simulation results showed that our mathematical model was valid and a linearization feedback control algorithm based on the model could provide adequate control if appropriate control parameters were chosen.

3.4 DEVELOPMENT OF AN ADVANCED REAL-TIME EPW CONTROLLER

From the above sections, we successfully built a 3-D mathematical model of an EPW, measured the required the parameters for the mathematical model, and validated the model via simulation. In order to apply the model based control to real EPW driving, we needed a EPW platform to test the control algorithm. The commercial EPW controllers were not able to execute the control

algorithm due to the lack of computation power and feedback sensor package. Therefore, in this section, an advanced real-time wheelchair control platform is developed. The design goals for the controller were to be able to accept input from multiple sensors and produce various computed outputs to the driving wheels; with sufficient processing power and real-time capability to handle computation of complex control algorithms and possess ample storage for data logging; with no limits on the type or number of sensors; with ruggedized enclosure to be durable when subjected to tip over and crashes, as well as splashes from wet or icy conditions; with realistic dimensions and weight to not add significant length, width and weight to the EPW.

3.4.1 Electronic Design

The electronics design consisted of a core components group and a peripheral components group. The core group contained components that were required for the wheelchair to operate as a typical EPW and the infrastructure to interface with a variety of peripheral components. The peripheral group consisted of a variety of sensors and output devices that can be substituted depending on the application.

Core Components

The core components group was divided into high current components and low current electronic components. The high current components consisted of two 12 volt batteries, two 420 watt motors with brakes, two industrial amplifiers, a brake release circuit, a DC-DC converter, and fuses. The motors and batteries were original equipment retained from the Golden Alante power wheelchair that was chosen as the base. The Alante base was chosen for its simplicity and ability to operate as a front wheel or rear wheel drive EPW. The industrial amplifiers were made

by Advance Motion Control and were power rated for 25 amps continuous and 50 amps for 2 seconds and accepted a 20-28 volt input. The output for the amplifier was controlled by a pulse width modulated (PWM) signal and a digital direction and inhibition pin.

Also included in the high current components was the brake release circuit. The purpose of the brake release circuit was to disengage the brakes when a voltage was applied to the motors. The brakes were applied to the motors unless a 24 volt potential was present across the brake terminals. The brake circuit received an input from a digital input-output (IO) pin, conditioned with a Schmitt-Trigger Inverter, and passed it to the gate of a power metal-oxide-semiconductor field-effect transistor (MOSFET). The MOSFET was the high current switch that disengaged the brakes. The transition from the high current components to the electronics is performed by a DC-DC converter. The converter is required to reduce the batteries from 24 volts to 5 volts, 12 volts, and -12 volts, as required for the single board computer and peripherals. The triple output DC-DC converter was chosen for its compact size, 60 watt output and 18-40 volt input range.

The electronics components in the core group included a single board computer (SBC), data acquisition board (DAQ), counter board, controller area network (CAN) controller, and connector support board. The SBC contained a 1.6 GHz Pentium M processor and maximum 2 GB of DDR RAM. The SBC had numerous external interfaces in addition to the standard items. These included 8 channels of 12 bit A/D, 32 channels of digital IO, three 16 bit counters, a PC104 bus, and a PC104plus (PCI) bus. The SBC required a supply voltage of 5 volts at 4.6 amps during typical operation. This particular SBC configuration was chosen for its processing power and number of external interface options.

The SBC was programmed to receive inputs from various sensors, process these inputs and produce appropriate outputs as required by the application. One key output, which was used for all applications, was the two PWM signals, produced using the counters, for controlling the amplifiers. In addition to being a processor for control algorithms, the SBC in combination with a non-volatile storage device was used as a data logger for large number of driving variables. Initially, the non-volatile storage was a 2 GB Compact Flash card, which provides room for the firmware and many data logging applications. Larger capacity solid state hard drives could be connected for data logging applications that required large amounts of memory, such as continuous video capture.

The DAQ board was a PC104 analog and digital IO module. It had 16 channels of 16 bit resolution A/D and could acquire data at a rate of 200k samples/second. It also had 2 channels of 10 bit analog output and 16 lines of digital IO. The purpose of the DAQ board was to serve as a general data input/output peripheral interface.

Peripheral Components

The peripheral components were made up of a variety of sensors, which could be added or removed as required for a particular application. The following is the list of sensors.

Drive Wheel Encoder- Optical encoders were chosen to measure the true speed of the drive wheels. The encoders had 500 counts per revolution resolution, quadrature output, and require a 5 volt supply voltage.

Caster Spindle Encoder- Absolute encoders were chosen for measuring the orientation of the casters. The encoders featured both digital and analog outputs and have a supply voltage range of 5.5-16 volts.

- Core components housed in aluminum chassis
- Heat dissipation
 - Mechanically robust enclosure
- Multiple interfaces: USB, Serial, PS-2, COM etc.

- EBX-12 based VxWorks 6.3
- Sensor data processing
- PC104 and counter board
- Understand user's intention
- CAN network

- US digital drive wheel encoders
- US digital caster spindle encoders
- O-Navi 3 Axis Gyro/3Axis Accelerometer
- PC104plus (PCI) bus

- 50A8DDE amplifiers for motor
- Data acquisition board (DAQ)
- Current/ over-current sensing
- Brake control
- PC104plus (PCI) bus

Figure 3-16: Components of the wheelchair control platform

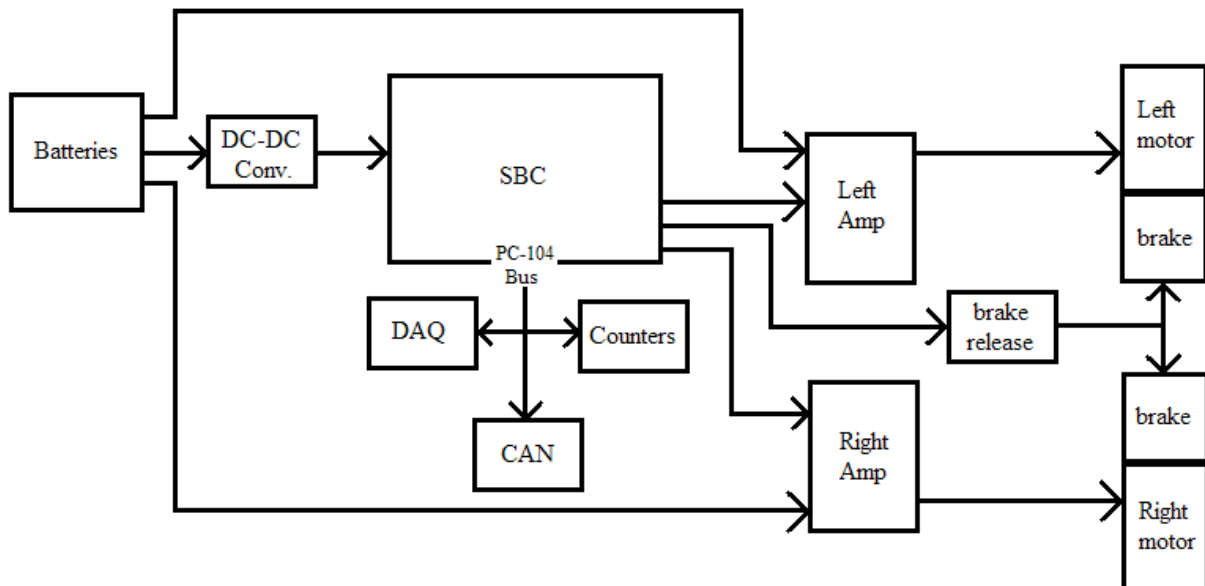


Figure 3-17: Layout schematic of electrical components

3 Axes Gyro / 3 Axes Accelerometer- The inertia sensing module included a 3 axes gyro, a 3 axes accelerometer, and a temperature sensor. All outputs were analog and require a 5 volt supply voltage. This sensor was used to detect tipping, terrain type, and vibration data.

Current Sensing Circuit- The amplifier featured a built in current sensing circuit. The motor current could be externally accessed via a scaled analog output.

Infrared Range Finder (Optional) - The infrared range finder had a 20-150 centimeter range. It had analog output and requires a 5 volt supply voltage.

Sonar Range Finder (Optional) - The sonar range finder has a 0.3-6 meter range and features a scaled digital output. It requires a 5 volt supply voltage.

Figure 3-16 shows the overall components used for the controller platform and **Figure 3-17** shows the layout schematic of the electrical components.

3.4.2 Mechanical Design

The core components were housed in a 5”x 17”x 10” aluminum chassis (**Figure 3-18**), which was secured to the frame of the EPW under the seat (**Figure 3-16**). The two industrial amplifiers were mounted vertically on the inside, front face of the chassis. A layer of thermal joint compound was applied between the amplifiers and the chassis to improve heat dissipation. The SBC was mounted to the left side of the floor of the chassis. The PC104 expansion boards stacked on top of the SBC. The DC-DC converter was secured to the inside of the right face with screws and thermal joint compound.

The original wiring harness and the controller connectors were retained from the EPW which included connectors for the battery terminals, left and right motor, and the joystick. A

breakout board connected to the SBC via a ribbon cable and provided an interface with several of the computers ports. These ports included a parallel port, 2 RS-232 ports, 2 USB ports, a PS2 keyboard port, a PS2 mouse port, 2 LED indicators, and a reset button. The breakout board was mounted in a cut out directly above the controller connector. A custom made plastic face plate was used to securely fasten the breakout board to the chassis (**Figure 3-19**).

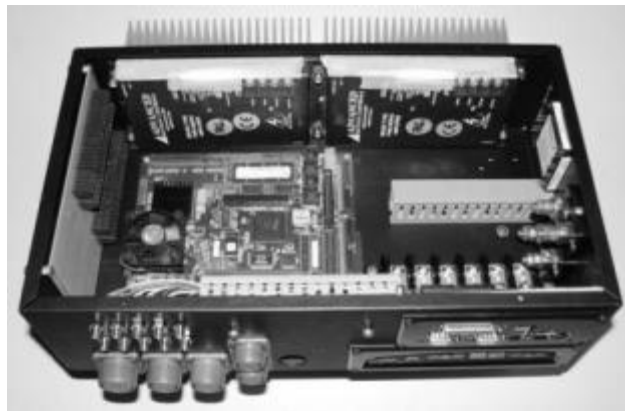


Figure 3-18: Core components installed in chassis

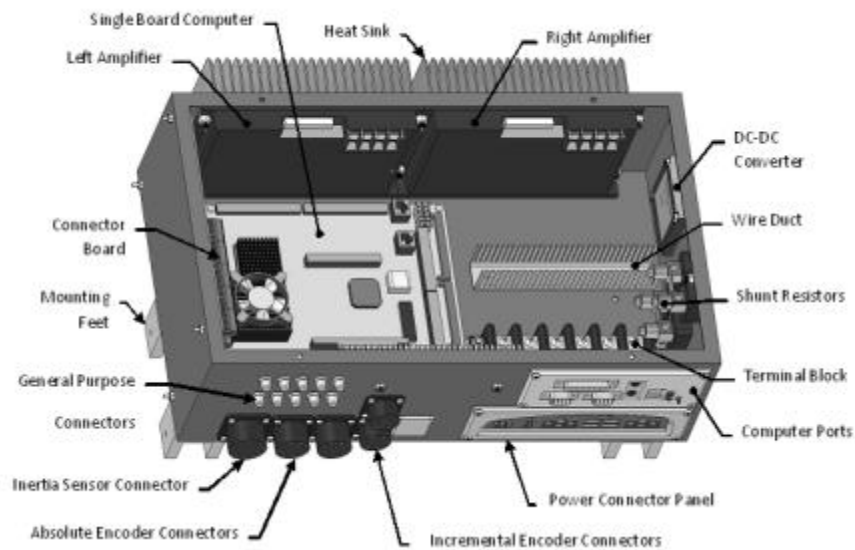


Figure 3-19: Layout of components in chassis

In addition to the breakout board, additional connectors were required to interface with the various sensors. For a general purpose connector, 4 position single ended molded cables and matching receptacles were chosen. These cables were designed for industrial environments and feature 24 AWG wire covered with yellow PVC. The 4 positions allowed for a power, ground, and two signal lines, providing enough infrastructures for I2C, USB, CAN, and other serial transmission modes, as well 2 channel analog sensors. Ten receptacles of this type were mounted on the rear face of the chassis with potential for additional ports in the future. The inertia sensor was mounted in a separate enclosure that was located near the center of mass of the wheelchair.

3.4.3 Software Design

The advanced real-time controller must complete various tasks such as motor control, tracking control, sensing, decision making, rules implementing and emergency commands in order to adapt to different kinds of users. Each task had different periodicity, priority, and computational load. For example, motor control which was a highly periodic task with a low computational load was a hard real time task. Rules implementing was also a periodic task but has a higher computational load than the motor control task. An emergency command was a sporadic task only activated when the user lost control of the wheelchair or created an error response. Since there were several different tasks and hard real time requirements regarding sensors and actuators, Wind River's General Purpose Platform, VxWorks Edition operating system was selected for use.

Vxworks was a C/C++ tool kit for the development of scaleable, hard, real-time operating systems (RTOS) for embedded systems. An RTOS allowed for precise scheduling of CPU tasks

to ensure that time critical portions of control algorithms were executed on a desired schedule. In addition, VxWorks is used in many safety-critical applications, so it includes features to prevent complete operating system failure.

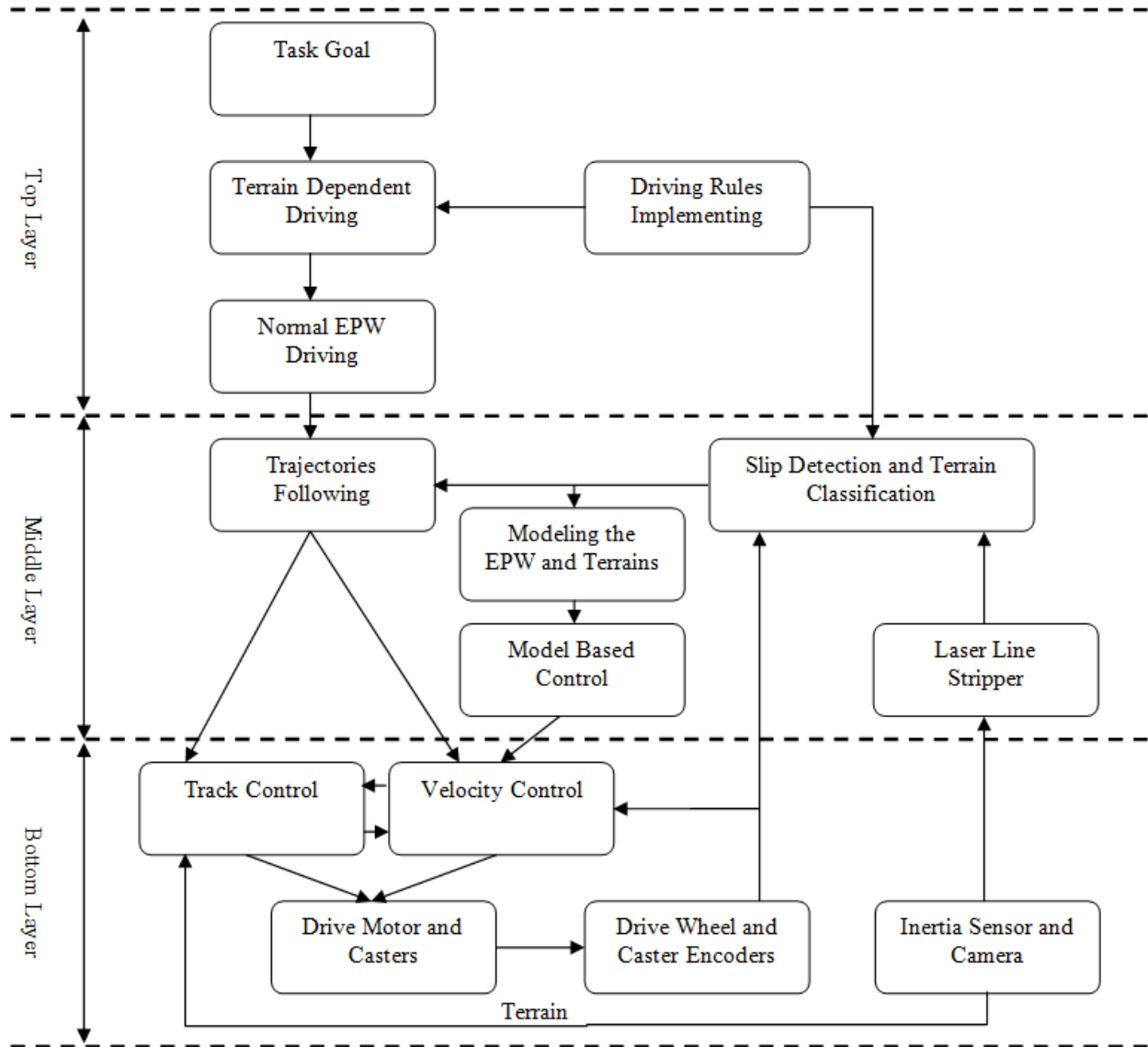


Figure 3-20: Control architecture of the advanced real-time controller platform

The control architecture had a hierarchical structure as shown in **Figure 3-20**. The controller had three layers. The bottom layer performed low level motor control and position feedback from the encoders and tracking control based on different terrain surfaces. The middle layer solved tasks related with environment sensing, slip detection, terrain classification, and trajectory following. The top layer dealt with tasks such as selection of movement strategy and driving rule implementing that are executed sporadically. However, the tasks that the top layer solved require much higher computational resources than those of the middle and bottom layer. Also, the middle layer tasks required higher computational resources than the bottom layer. The safety of the wheelchair system depended on the timely response of each task.

3.4.4 How the smart controller could be used?

The advantages of the smart controller design over conventional controllers were fourfold. Firstly, the real-time feature of the operating system and computational power of the SBC guaranteed that the wheelchair should not require any offline processing, nor should it halt to evaluate information whilst operationally engaged. Secondly, the feedback to the computer provided by the various sensors allowed the EPW to react to its environment dynamically by modifying the output signal sent to the drive wheel motors. This made the EPW much safer by allowing the wheelchair to sense and react to its environment with minimal user input. Features such as anti-slip, anti-tip, obstacle detection and avoidance were reactions the EPW could take based on the sensors input. Thirdly, the programmability of the controller computer allowed a high degree of customization possibilities for the joystick such as different axes, a larger center dead zone, and damping of user hand tremors. Lastly, the memory storage capability of the

computer allowed for extensive data logging of a wide variety of parameters which would allow researchers and clinicians to learn more about how people used their EPW.

The limitations of the smart controller design over conventional controllers were threefold. Firstly, the system required more power to run. With a full single board computer and peripheral sensors to run, there was definitely more of a drain on the battery than from a standard controller. However, during selection of the components, we tried to pick components with lower power consumption. Secondly, the current prototype controller enclosure was rather large and might not fit well on some wheelchairs. In addition, space must be found to fit all the sensors onto the EPW. Eventually though, the system would become smaller as the design and parts evolve. Lastly, the advanced real-time controller was more expensive owing to its much higher level of complexity. But, as electronic parts continued to get cheaper and the market demand improved, the cost of the controller would become more affordable.

With the advanced real-time controller developed, we were able to develop and test a real-time model based control, robust velocity control, real-time slip and tip-over control etc. In the following sections, the applications of the controller platform are presented in detail.

4.0 REAL-TIME MODEL BASED ELECTRIC POWERED WHEELCHAIR VELOCITY, TRACTION AND TIP-OVER CONTROL

This chapter evaluated the effects of three different control methods on driving speed variation and wheel-slip of an electric-powered wheelchair (EPW). A kinematic model as well as 3-D dynamic model was developed to control the velocity and traction of the wheelchair. A smart wheelchair platform was designed and built with a computerized controller and encoders to record wheel speeds and to detect the slip. A model based, a proportional-integral-derivative (PID) and an open-loop controller were applied with the EPW driving on four different surfaces at three specified speeds. The speed errors, variation, rise time, settling time and slip coefficient were calculated and compared for a speed step-response input. Experimental results showed that model based control performed best on all surfaces across the speeds.

4.1 CONTROLLER FOR EPWS

A 3D mathematical model for an EPW had been created and validated by simulation result. In the mathematical model we have the assumption that the EPW wheels would not slip. Similar assumptions had been made by other wheelchair modeling research [61]. However, this was not

true since EPW wheel slip frequently occurred when driving over low-traction terrain, deformable terrain, steep hills, or during collisions with obstacles, and could frequently result in wheelchair immobilization. Ding and Cooper reviewed the current technology and insight into future direction of the EPWs, in which the traction control of the EPWs was important as the increasing outdoors uses of the EPWs [62].

Several methods could be considered to estimate the wheel slip for automobiles. For most of them, wheel slip could be accurately estimated through the use of encoders by comparing the speed of driven wheels to that of un-driven wheels [63]. Ojeda and Borenstein compared redundant wheel encoders against each other and against yaw gyros as a fuzzy indicator of wheel slip, even when all wheels were driven [64], and had also proposed a motor current-based slip estimator [65]; however this technique required accurate current measurement and terrain-specific parameter tuning. A body of work existed in the automotive community related to traction control and anti-lock braking systems (ABS); however, this work generally applied at significantly higher speeds than was typical for autonomous robots and EPWs [66, 67].

A potential approach to detecting EPW driving terrain, slip and immobilization was to add and analyze GPS measurements. However, nearby trees and buildings could cause signal loss and multi-path errors and changing satellites could cause position and velocity jumps [68, 69]. Additionally, GPS provided low frequency updates (e.g. typically near 1 Hz [70]) making GPS alone undesirable.

Another potentially simple approach could rely on comparison of wheel velocities to a robot body velocity estimate derived from integration of a linear acceleration measurement in the direction of travel. However, such an approach was not robust at low speeds during travel on rough, outdoor terrain. Ward and Iagnemma presented a method for detecting robot

immobilization using a signal-recognition approach. Offline, a support vector machine (SVM) classifier was trained to recognize immobilized conditions within a feature space formed using inertial measurement unit (IMU) and optional wheel speed measurements. The trained SVM could then be used to quickly detect immobilization with little computation. Experimental results showed the algorithm to quickly and accurately detect immobilization in various scenarios [71, 72].

Based on above literature review, considering the advantages and disadvantages of different methods and the capabilities of our controller platform, a slip measurement method based on differential the driving wheels speeds and caster wheel speeds was developed and evaluated for later sections.

The purpose of this chapter was to evaluate the effects of three different control methods on driving speed variation and wheel-slip of an EPW. A controller based on the kinematic model as well as 3-D dynamic model, a proportional-integral-derivative (PID) and an open-loop controller were applied with the EPW driving on five different surfaces at three specified speeds.

4.2 DEVELOPMENT OF A 3-D HYBRID ADVANCED CONTROL SYSTEM

Our initial findings using a robust-velocity control (RVC) algorithm based on a 2D EPW model were described in [73, 74]. The simulation results showed that the RVC suppressed disturbances better than a PI controller. In this study, we further refined the previous EPW dynamic model by considering EPW motion in 3D on inclined surfaces with cross-slopes, **Figure 3-1**. We had

incorporated a tri-axial gyroscope for providing real time feedback of the incline and cross-slope angles.

4.2.1 Robust Velocity Control

(A). Modeling the EPW

We had built the mathematical model of the EPW in section 3.1, decided all the parameters for the model in section 3.2 and validated the model by simulation in section 3.3. Here focus was on control algorithm development.

(B). Model based robust velocity control system

The models described above were essential parts of simulation models to control the motion of the wheelchair. However, no matter how detailed the analysis, these models had uncertain parameters, such as the coefficient of rolling resistance, coefficient of friction and surface of the terrains.

The models of open-loop and closed-loop control systems that could be utilized to control the velocity are shown in **Figure 4-1** for each driving wheel of the wheelchair. The open-loop system was highly sensitive to these uncertainties and hence could yield poor velocity control, while the feedback system could dramatically reduce the effects of the model uncertainty. In the experimental test described in the following session, the closed-loop model based control system was employed as the RVC algorithm. The whole dynamic models of the chair and wheelchair-terrain interactions were described as above. In our study, a modified PID controller was adopted from [75] where the input to the derivative term of the PID was the reference signal instead of error signal.

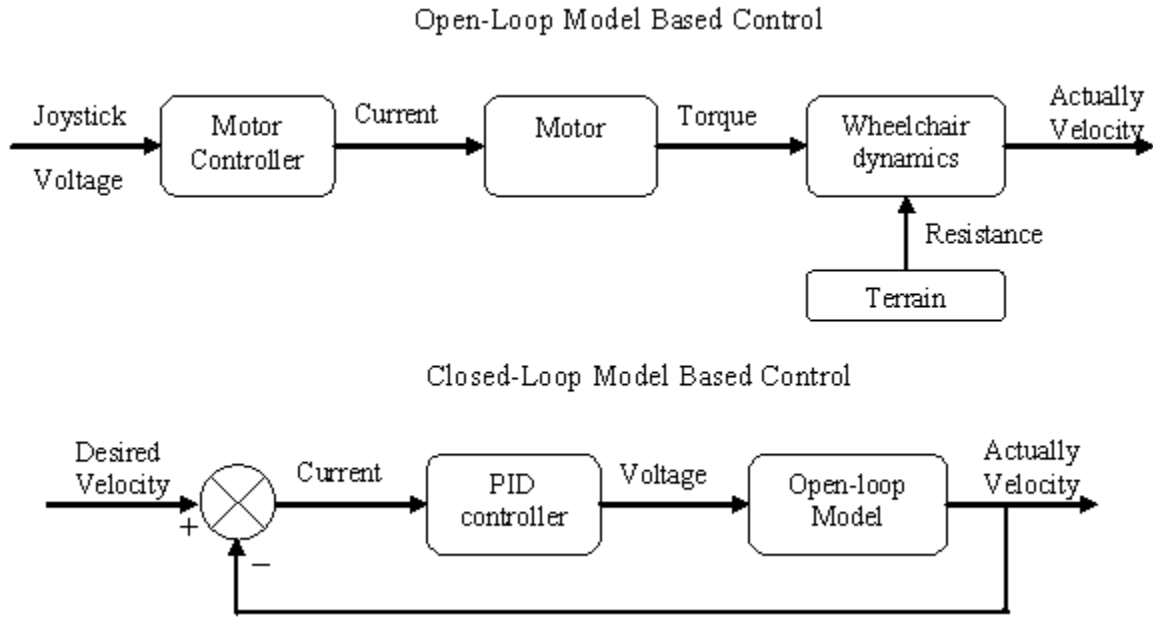


Figure 4-1: Open-loop and closed-loop control systems for the model based control of a wheelchair

For motor, the moment of inertia and viscous friction of the motor were assumed small enough compared with inertia and friction associated with the wheelchair thus could be ignored. The speed and current curve for the DC motor [76], which was of the form $\omega_w = -\eta I_m + b(V_m)$, where ω_w and I_m are respectively the angular velocity and current of the motor, when $\eta > 0$ such that the slope was negative, and $b(V_m)$ changed monotonically with the motor voltage V_m . The motor must be constrained such that $I < I_m$, where represented the maximum current allowable before the motor was in danger of overheating and burning out. The motor control could be treated as an electrical drive system for the motor. In this study the Advance Motion Control 50A8DDE motor controller had been utilized.

4.2.2 Traction Control

Traction control worked to ensure minimum slip between the surface and the tires, even under less-than-ideal conditions. For example, a wet or icy sidewalk surface significantly reduced the friction (traction) between the tires and the pavement. Since the tires were the only part of the wheelchair intended to touch the ground, any resulting loss of friction could have serious consequences. Traction control reduced wheel slip, and thus improved mobility and safety over various terrains. Due to tire friction characteristics, the control problem was highly uncertain and nonlinear, so we developed a robust traction controller (RTC), where the torque T applied to the wheel was the input, the wheel slip $^{3/4}$ was the output; the wheel velocity ω_w and the wheelchair velocity V were state variables.

The dynamic equation for the angular motion of the wheel was given as

$$\dot{\omega}_w = \frac{T - r_w F_t - T_f}{J_w} \quad \text{--- (64)}$$

where T_f was the wheel disturbance torque and F_t is the traction force which directly depended on the friction coefficient between the surface and tire, and in turn depended on the wheel slip as well as surface conditions.

$$F_t = \mu(\zeta) \cdot N \quad (65)$$

where N was the normal tire reaction force and μ was the adhesion coefficient.

The simplified wheelchair dynamics could be written as follows:

$$\dot{V} = \frac{F_t}{M} \quad \text{---(66)}$$

The wheel slip ζ was usually defined by a nonlinear function of the wheel velocity ω_w , wheel radius r_w , and the wheelchair velocity V as follows:

$$\zeta = \frac{\omega_w r_w - V}{\omega_w r_w} \quad \text{--- (67)}$$

The wheel slip ζ could be monitored via the above equation 64, which also functioned as a switch between the RTC algorithm and RVC algorithm, i.e.

$$\begin{aligned} \text{RTC, } & \zeta \geq \zeta_{limit} \\ \text{Controller=} & \\ \text{RVC, } & \zeta < \zeta_{limit} \end{aligned}$$

Defined the state variables as

$$x_1 = V, x_2 = \omega_w$$

We could write

$$\zeta = \frac{x_2 - x_1}{x_2}$$

$$\dot{\zeta} = \frac{-\dot{x}_1 + (1 - \zeta)\dot{x}_2}{x_2} \quad \text{---- (68)}$$

Substituting equation (64) and (66) into the above equation (68), we got the slip state equation as

$$\dot{\zeta} = f + bu$$

where f and b are known matrices and u is the torque input.

These algorithms served as the basis for our hybrid robust controller that was compared to open-loop and PID classical methods. In our research, the data from the caster encoder which was the caster velocity represents the velocity of the wheelchair, and from encoder data of the driving wheel we collected the wheel velocity. If a wheel slip was detected, there would be a

difference between wheelchair velocity and wheel velocity. The threshold of slip coefficient ζ_{lim} for whether the traction controller would be chosen based on the experimental results.

If a slip was detected, while the driving wheel velocity was bigger than wheelchair velocity, in order to get enough traction, the controller slowed down the driving wheel velocity until the wheelchair began moving. In case that the wheelchair did not move before it completely stopped, user input might be required to either turn the wheelchair or backup the wheelchair to exit from the slippery situation.

4.3 EXPERIMENTAL TESTS

4.3.1 Test Wheelchair

The advanced real-time controller platform described in section 3.3 was used for the experimental test. The driving wheel encoders, caster wheel encoder and the inclinometer data collected were recorded at 200 HZ on an onboard 32 Gig bytes solid state hard drive. Control algorithms were written in C language implemented on a VxWorks Operating System.

4.3.2 Software Algorithms

All control algorithms were embedded within the VxWorks real-time operating system. For open-loop control, no feedback was applied to the controller and the EPW actual speed was

directly proportional to the joystick output. The control output frequency and sample frequency for data collection were set at 200HZ.

For PID control, the instantaneous wheels speeds were used as feedback to the controller which adjusted the error signal between the desired speed (set by the joystick) and the actual wheel speed to track the desired speed.

The model based controller was based on our 3-D EPW model. The physical parameters for the model were measured within the laboratory with the inertia of the EPW was measured using the method stated in section 3.2. The traction forces provided by the motor F_R, F_L were measured using the SMART^{HUB} [52]. The anti-slip control algorithm compared the speeds of the driving wheels and the caster. The caster wheels were not powered, and therefore caster speed provided an estimate of the EPW velocity. Loss of traction, wheel slip, was defined as a difference in the angular velocity of the each drive wheel with respect to the caster of greater than 20%.

4.3.3 Experimental Protocol

The experimental protocol consisted of driving the EPW with each of the control algorithms in-turn on five different surfaces which incorporated both indoor and outdoor environments (**Figure 4-2**) and collecting data about the wheelchair speeds. A 2.44m Teflon sheet attached to an adjustable slope ramp with maximum 50 was used to simulate a slippery surface (e.g., ice, snow, wet grass). The initial set-up of the slope ramp was 30. For each of the surfaces, in order to decrease the experimental error, the EPW was driven in the same manner for each trial. The control parameters were measured and recorded during each trial. The driving test was carried

out using a step-response at three different desired speeds, fast 2 m/s, medium 1.5 m/s, and slow 1 m/s. All tests were conducted driving straight forwards, turns and reverse driving tests would require further development and were left for future studies. The order of testing the driving surfaces was randomly chosen; however, for each surface, the EPW was always driven with the fastest speed first, then medium and then slow speed. Also tests on the next surface were initiated after all the tests on the former surface were completed. The actual speeds of the two driving wheels and the caster were collected by encoders incorporated on the EPW. For PID and model based control, driving wheel encoder data were used as feedback to the controller. The caster encoder data were compared with the average of the driving wheel encoder data in the controller to detect the slip then initiate traction control if slip was detected. Data for each trial were analyzed using Matlab 7 (R14) and normalized to 10 seconds for comparison purposes.

In order to evaluate the performance of each control algorithm, the following variables were calculated and compared: rise time, settling time, speed error, speed variance and slip coefficient. Control algorithm performance was defined by lower errors and variances as well as faster response and shorter rise times. The rise-time was measured as the time it took for the wheelchair output speed to rise beyond 90% of the desired speed for the first time. The settling-time was recorded as the time from beginning to the time it took for the system to converge to its steady-state. The steady state here was the desired speed for PID and model based control and the stable speed for open loop control since with open loop control, the wheelchair could not be able to reach the desired speed. The system was considered to be steady state while changing of the velocity within 95% of the desired speed. This variable shows how fast the wheelchair could settle down to the desired speed. The 10 second normalized root mean square error (NRMSE) between the desired speed and real speed recorded by the encoders was used as the speed-error.

Variance of the error between desired speed and actual speed at steady-state was used for representing the speed-variance to examine “bucking” of the control on different surfaces at different speeds. EPW drivers are sensitive the “bucking” and will reject controllers with intolerable speed-variance. The difference between driving wheel speed and wheelchair speed (caster speed) normalized to the driving wheel speed was used to define the slip-coefficient to evaluate traction control.



Figure 4-2: Five different surfaces on which the experiment was conducted

4.3.4 Experimental results

The parameters for the PID controller were chosen based on computer simulation results. During the experimental tests the PID parameters were: $K_i=0.8$, $K_p=1.5$ and $K_d=1.25$. Before the process of applying the model based control, physical parameters for the test EPW system were measured (see **Table 4-1**). The mass parameter in the table includes the EPW and the test-pilot (146 lb).

Table 4-1: Physical parameters for the test EPW and test surface

Constant Variables	Result				
H (height of COM)	23.23(cm)				
l (distance between COM and rear axle)	7.63(cm)				
L (chair length between rear and front axle)	17.05 (cm)				
W (width of wheelchair between two rear footprints)	21.22(cm)				
M (weight of wheelchair)	123.75(kg)				
I_z (inertia of wheelchair to Z axes)	5.00(kg·m ²)				
Surface Variables	Teflon	Tile	Asphalt	Slope	Grass
μ (friction coefficient) ^{*1}	0.04	0.55	0.72	1.02	0.35
α (Up/downhill slope of road)	5 ⁰	3 ⁰	1 ⁰	11 ⁰	0 ⁰
β (Side slope of road)	0 ⁰	1.2 ⁰	0.7 ⁰	8 ⁰	0 ⁰
θ (Chair direction)	0 ⁰	0 ⁰	0 ⁰	0 ⁰	0 ⁰

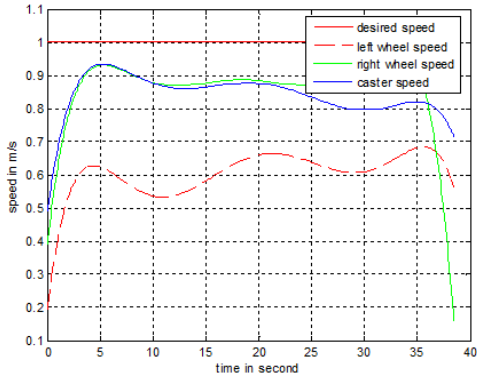
Table 4-2 shows the overall mean, standard deviation of speed errors, speed variance, rise time, settling time and slip coefficient. For both left and right wheels, speed errors of PID (left wheel: 1.46 ± 1.47 m/s; right wheel: 0.93 ± 1.03 m/s) and model based control (left wheel: 1.47 ± 1.38 m/s; right wheel: 0.69 ± 0.44 m/s) were much smaller than open loop control (left wheel: $2.56 + 1.99$ m/s; right wheel: $1.91 + 1.58$ m/s). As for the speed variance, model based control (left wheel: 1.35 ± 1.07 m/s; right wheel: 0.44 ± 0.28 m/s) was less than PID (left wheel: 1.47 ± 1.49 m/s; right wheel: 1.03 ± 0.93 m/s) control while PID control was less than open loop

¹ * means the parameters were found from other resources
[\[http://www.roymech.co.uk/Useful_Tables/Tribology/co_of_friect.htm\]](http://www.roymech.co.uk/Useful_Tables/Tribology/co_of_friect.htm)

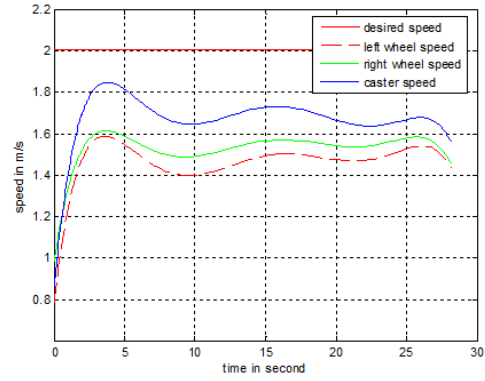
control (left wheel: 1.99 ± 1.77 m/s; right wheel: 1.58 ± 1.39 m/s). For the rise time, both PID (3.08 ± 2.09 second) and model based (2.92 ± 1.69 second) control were slightly longer than open loop control (2.15 ± 0.66 second), but the difference was less than 1 second. The settling time of PID (8.59 ± 5.91 second) and model based control (8.59 ± 5.26 second) were similar and less than half second longer than open loop control (8.08 ± 5.09 second).

Table 4-2: Test results of the mean, standard deviation and variance of the wheels speed NRMSE of all the three control methods

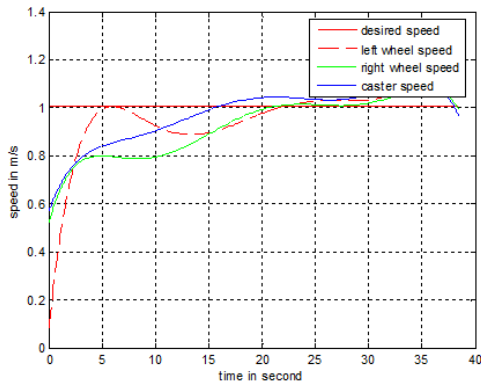
Method	Speed Error (Mean (Std)) (m/s)	Variance (m/s)	Settling Time (s)	Rise Time (s)	Slip Coefficient
Open Loop	Left: 2.56 (1.99)	1.99 (1.77)	8.08 (5.09)	2.15 (0.66)	0.11 (0.04)
	Right: 1.91 (1.58)	1.58 (1.39)			
PID	Left: 1.46 (1.47)	1.47 (1.49)	8.59 (5.91)	3.08 (2.69)	0.06 (0.04)
	Right: 0.93 (1.03)	1.03 (0.93)			
Model Based	Left: 1.47 (1.38)	1.35 (1.07)	8.59 (5.26)	2.92 (1.69)	0.04 (0.02)
	Right: 0.69 (0.44)	0.44 (0.28)			



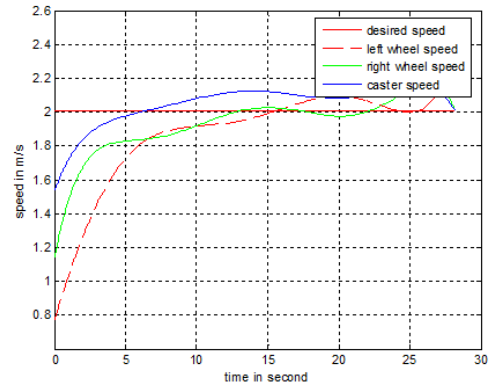
a. Open loop control with slow speed



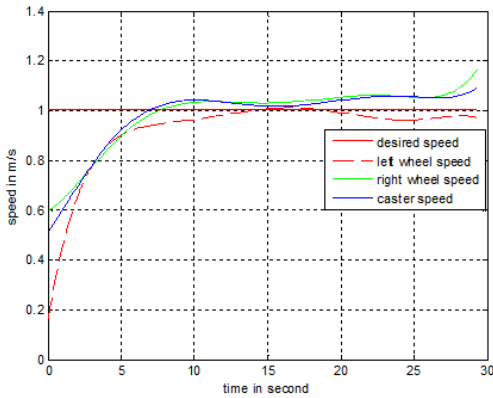
b. Open loop control with high speed



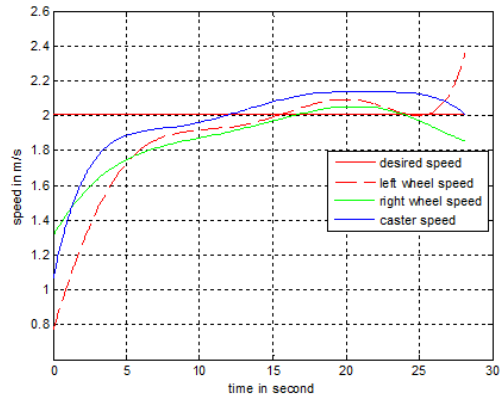
c. PID control with low speed



d. PID control with low speed



e. Model based control with low speed



f. Model based control with high speed

Figure 4-3: Example figures of two driving wheels and caster speeds with different controllers applied at low and high speeds on a grass surface.

The slip coefficient of the wheelchair driving on 2m/s on grass surface is shown in

Figure 4-4.

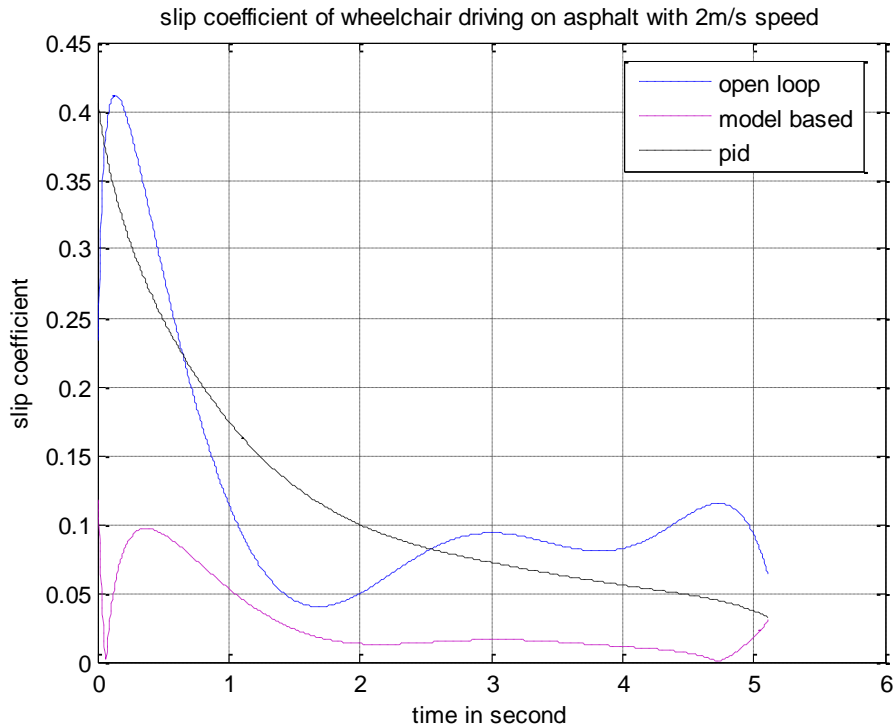
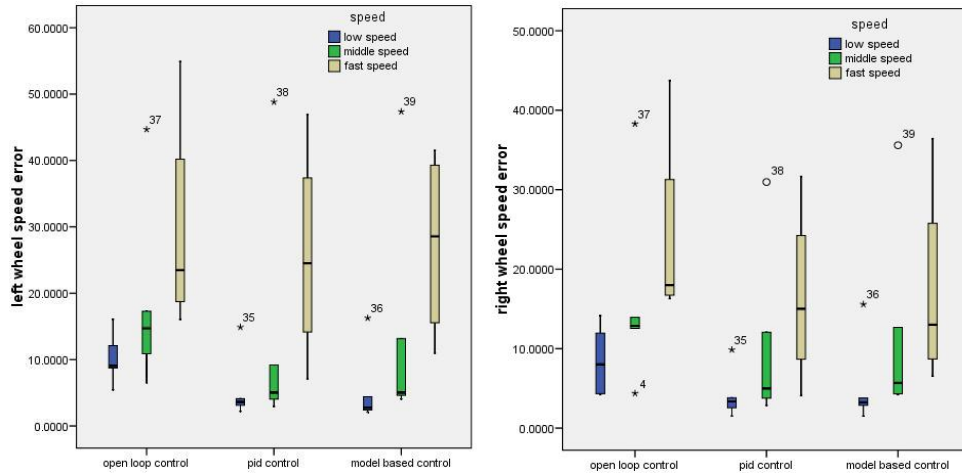


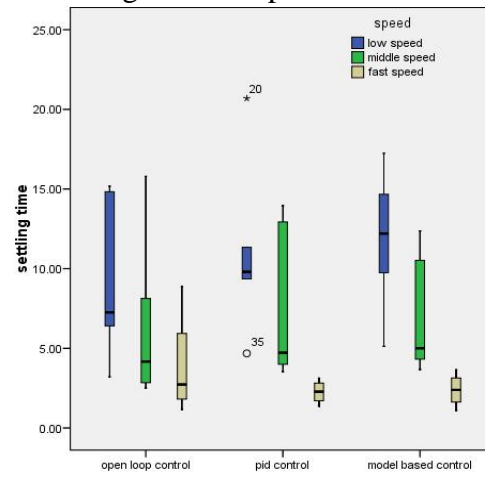
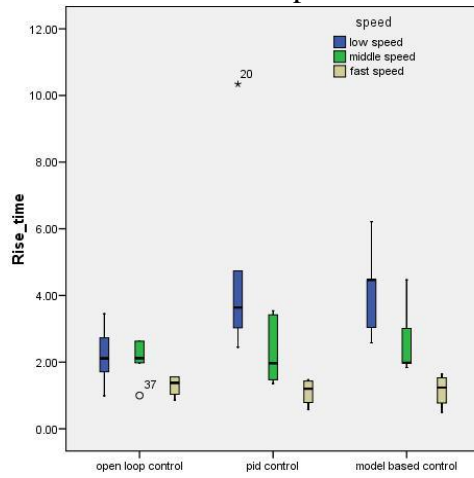
Figure 4-4: Slip coefficients of three controllers with the wheelchair driving on grass at 2 m/s

Figure 4-5 (a-e) shows box plots of the different variables between the three control methods categorized by speed. From Figure 4-5 (a) and (b) it may be seen that for the same method, higher speeds induced larger errors and variances than the low speed. For the rise time and settling time, the faster the speed, less time was needed. The slip-coefficient, with open-loop and PID control, the faster the speed, the bigger the slip coefficient.



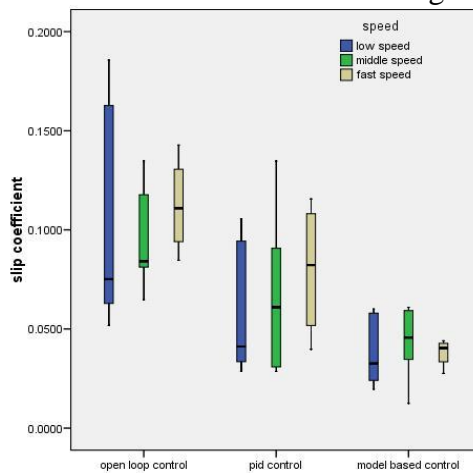
a. Left wheel speed error

b. Right wheel speed error



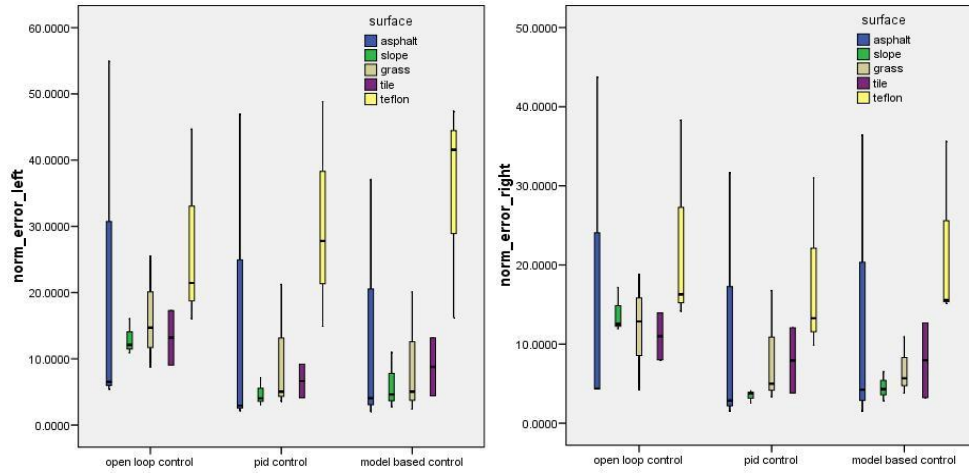
c. Rise time

d. Settling time



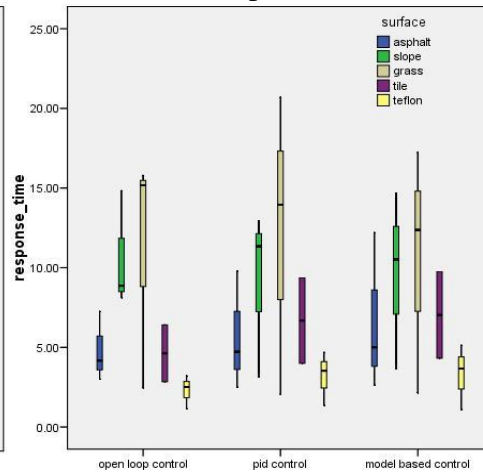
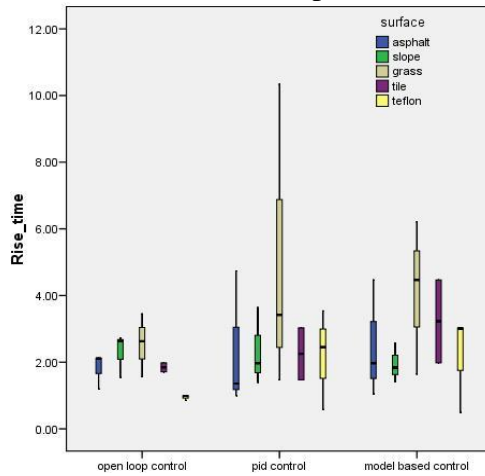
e. Slip coefficients

Figure 4-5: Wheelchair performances with three controllers at three different speeds



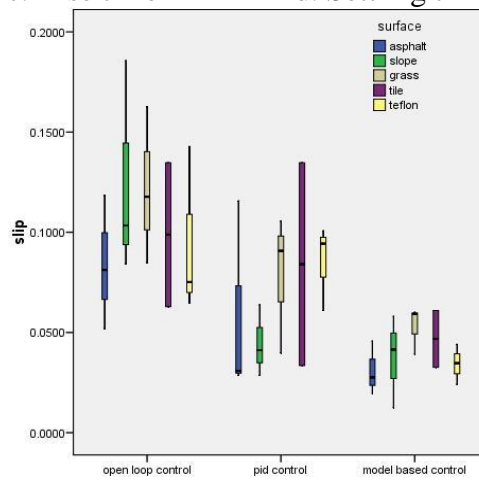
a. Left wheel speed error

b. Left wheel speed error



c. Rise time

d. Settling time

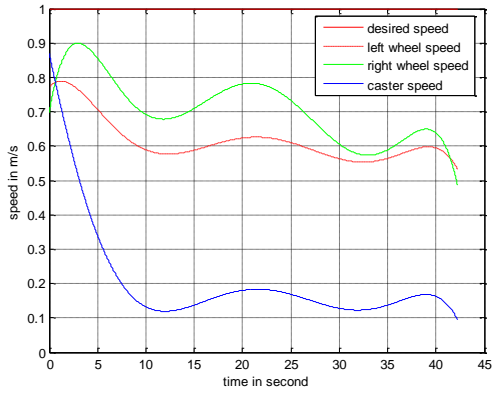


e. Slip coefficients

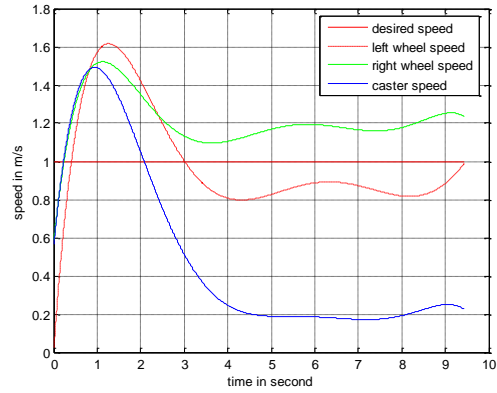
Figure 4-6: Wheelchair performances with three controllers on five different surfaces

Figure 4-6 (a-e) shows box plots of the different variables between three methods categorized by surface. From **Figure 4-6** (e) one can see that greater slip occurred for open-loop and PID control then model based control. When examining the model based controller, there was more slip on grass than any other surfaces. For the left and right wheel speed error (**Figure 4-6** a, and b), there was larger error on the Teflon surface than any other surface. For the rise time and settling time (**Figure 4-6** c, and d), the tougher the surface (grass and slope), the more time was needed to obtain the desired speed and to reach a stable speed.

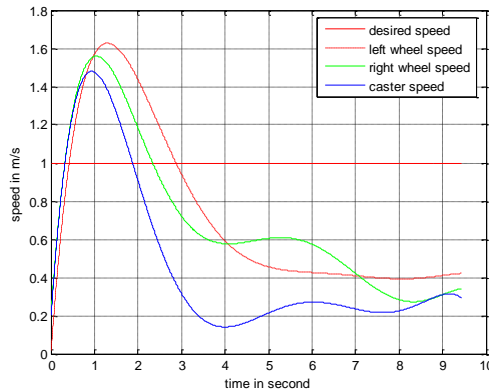
During the experimental tests, no slip could be seen by the investigators while observing the tests. However, our focus group participants reported having seen their wheels slip. Therefore, future studies should examine other surfaces or conditions. In order to test whether the anti-slip control method was effective, we put the Teflon on a ramp with 5⁰ degrees slope on which the wheelchair was driven. The following **Figure 4-7** a-c shows how the wheelchair performed during this scenario. From **Figure 4-7** (a) and (b) we observed that with open-loop and PID control, when slip happened, the two driving wheels kept spinning while the speed of the EPW was almost zero. In **Figure 4-7** (c), we could observe and recorded that the controller decreased the driving wheel speed in order to gain traction. However, Teflon surface length was insufficient to have the EPW fully reject slip, and regain the desired speed. Anti-slip control is an area where further work is needed to overcome slip more rapidly and effectively.



a. Slip measurement with Open loop



b. Slip measurement with PID control



c. Slip could not recover when the driving wheels lost traction completely

Figure 4-7: Slip measurements with three different controllers: open loop, PID and model based control

4.3.5 Effectiveness of the controller

The data collected indicated that both the PID controller and model based controller decreased the error between the desired speed and actual speed of the wheelchair as compared to open-loop control over all test conditions (terrain and speeds). The results also showed that the model based control had smaller variances of error than PID control and open-loop control (**Table 4-2** and **Figure 4-3**) showing that the speed performance of the model based control is most consistent

over different surfaces and speeds. The rise time and settling time for the model based control were close to PID and open-loop which indicates that the additional complexity of the model based control did not significantly sacrifice response time to decrease speed error and variance. Furthermore, the slip coefficient for model based control was smaller than PID and open-loop control demonstrating that model based control has greater sensitivity and better control when loss of traction may occur (**Table 4-2** and **Figure 4-4**). Overall, model based control provided superior performance than PID and open-loop control.

Examining the performance of the wheelchair while driving at different speeds (**Figure 4-5** a-e and **Figure 4-3** (a) and (b)), it was observed that for each control algorithm higher speed had larger errors and variances than the low speed. This is understandable since under higher speed conditions, the distance traveled is longer between sampling periods for a fixed sampling rate. A more detailed model may improve the model based control at the fastest speed. Rise time and settling time were lower at the faster speeds. The slip coefficient, with open loop and PID control, the faster the speed the larger the slip coefficient indicating greater reduction in traction. However, with model based control, the slip coefficient was similar at different speeds because when slip exceeded the pre-defined threshold the algorithm decreased the driving wheel speed to increasing the traction. Further investigation is needed to develop more effective and rapid means of implementing anti-slip control. However, one challenge is to avoid introducing unnecessary complexity and maintaining low-cost. Fortunately, sensor, computing, and memory costs continue to decline.

Focusing on the performance of the wheelchair while driving over different surfaces (**Figure 4-6** a-e) there was greater speed error on the low-friction surface (Teflon) than with the other surfaces for model based control. This was due to our anti-slip controller decreasing the

driving wheel speed when slip was detected (**Figure 4-7**), essentially trading-off speed for traction. The results of this study showed that our anti-slip control was ineffective if the wheelchair lost too much traction which requires further study. Future work on anti-slip control should examine control of wheel torque as well as speed to reduce slip. This may have the desired effect of reducing speed error and increase effectiveness over a wider variety of terrain (e.g., sand and gravel). From **Figure 4-6 (e)**, it can be seen that the slip coefficient is larger for open-loop and PID control than model based control as a result of the anti-slip algorithm. For the model based controller, the slip coefficient was between the thresholds set in the algorithm resulting in higher values than for the other surfaces. A rapid method for detecting terrain may be helpful for setting terrain-specific slip coefficient control thresholds or even entirely different control approaches.

The tougher surfaces (grass and slope) required more time to get the desired speed and stabilize at the desired speed. These surfaces induced more involuntary jostling of the test-pilot, which may have caused deviation from the model based control parameters. Incorporation of a more accurate human model within the algorithm may improve control. Further study should have both the human pilot and wheelchair in the 3-D model.

From Table 4-2 and Figure 4-3, 4-5 and 4-6, it may be observed that the left and right drive wheels did not perform the same during the experiments despite no tasks requiring turns. The EPW model assumed for simplicity that the two drive wheel motors of the EPW were symmetric. In practice, EPWs do not use matched motors, and their parameters might vary notably resulting in differences between the speeds of the driving wheels, especially with open-loop control. Future studies might benefit from using matched motors or a model that did not assume symmetry during the further development and testing.

These control system experiments could be expanded to incorporate more driving scenarios. The results of this study might be dependent on the test EPW setup and test-pilot so further experimentation might be necessary to generalize the results to other EPW types. A wider variety of terrains should be tested such as different types of carpets, slippery surfaces and ramps. As more is learned about the challenges of driving an EPW, the information will be used to develop and refine our driving control algorithms with the goal of creating a higher level of safety and usability for all EPW users.

In future studies, models based on front- and middle- wheel drive wheelchairs including caster dynamics will be tested; the dynamics and performances of users will be included in the model to provide better feedback from the wheelchair users; the stability and safety of the users and wheelchairs should be considered during deciding the thresholds of control parameters; more sensors will be added and more effective control algorithms will be developed to improve the performance of EPWs. At the same time, we are working on to design a more compact, durable and economic affordable controller box which could be marketed and served as future controller.

4.4 Real-time Slip Detection and Traction Control of Electrical Powered Wheelchairs

In the above session a real-time model based velocity and traction controller was developed and tested. In this session, the control algorithm to detect and compensate for wheel-slip in real-time is further developed and evaluated. To evaluate the controller, the EPW was driven over five different surfaces at three speeds. Paired t-tests showed that with anti-slip control, there was significant ($p < 0.001$) lower slip coefficient than without anti-slip control. Experimental results showed that the performance of anti-slip control was consistent on the varying surfaces at different speeds.

4.4.1 Traction control of EPWs

Wheelchair control methods are important to safety and performance. However, wheelchair users usually have difficulty on ice, slippery surfaces and soft ground [77]. Wheelchair tires, even though provided with special tread patterns, might slip on slippery or icy surfaces. It is not unusual during cold weather for a wheelchair to become immobilized due to spinning of the drive wheels. The user might thereby be subjected to unnecessary exposure to cold as a result of the inability of the wheelchair to move. By implementing traction control on an EPW, the driving environment might be expanded and driving safety improved. However, little research has addressed enhancing traction of an EPW under sub-optimal surface conditions. Work related to traction control was usually found in the literature on automobiles [78, 79].

Research Questions:

1: To determine whether the developed controller could be able to detect wheel slip consistently.

2: To determine whether the proposed controller could provide improved control of traction consistently.

4.4.2 Set-up for the slip detection

The slip detection method and control was the same as the previous session. The experimental protocol consisted of driving the EPW with and without the control algorithm in turn on five different surfaces which incorporated both indoor and outdoor environments (**Figure 4-2**) and collecting data about the wheelchair speeds. A 2.44m Teflon sheet attached to an adjustable slope ramp with maximum 5° was used to simulate a slippery surface (e.g., ice, snow, wet grass). For each of the surfaces, in order to decrease the experimental error, the EPW was driven in the same manner for each trial. The control parameters were measured and recorded during each trial. The driving test was carried out using a step-response at three different desired speeds, fast 2 m/s, medium 1.5 m/s, and slow 1 m/s. The order of testing the driving surfaces was randomly chosen; however, for each surface, the EPW was always driven with the fastest speed first, then medium and then slow speed. Also tests on the next surface were initiated after all the tests on the former surface were completed. The actual speeds of the two driving wheels and the caster were collected by encoders incorporated on the EPW. The caster encoder data were compared with the average of the driving wheel encoder data in the controller to detect the slip then initiate traction control if slip was detected.

In order to evaluate the performance of the control algorithm, slip coefficient, defined as difference between driving wheel speed and wheelchair speed (caster speed) normalized to the driving wheel speed, was used to evaluate traction control. Data for each trial were analyzed using Matlab 7 (R14) and normalized to 10 seconds for comparison purposes. The difference of slip coefficient for the two methods was compared using the paired t-test. The alpha level was set at 0.05 *a priori*.

4.4.3 Experimental results

The physical parameters for the test EPW system were measured (see **Table 4-1**). The mass parameter in the table includes the EPW and the test-pilot (146 lb). **Table 4-3** shows that overall the traction control (0.04 ± 0.02) had significantly decreased the slip-coefficient compared with open loop control (0.11 ± 0.04). The slip-coefficient, with open-loop, the faster the speed, the bigger the slip coefficient indicating greater slip was detected. However, with traction control, the slip coefficient was visibly lower at all desired speeds (**Figure 4-8**). Similarly, with the traction control, lower slip coefficient was observed on all the five tested surfaces (**Figure 4-9**).

Table 4-3: Slip coefficient of all the tests with and without traction control

method	Slip Coefficient (Mean \pm Std)	P
with traction control	0.04 \pm 0.02	P<0.001
without traction control	0.11 \pm 0.04	

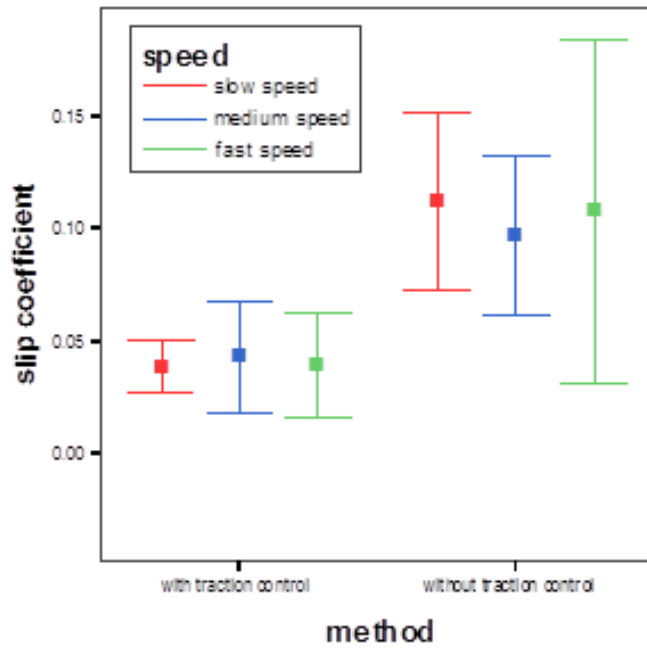


Figure 4-8: Slip coefficients with and without traction control during the tests across three speeds

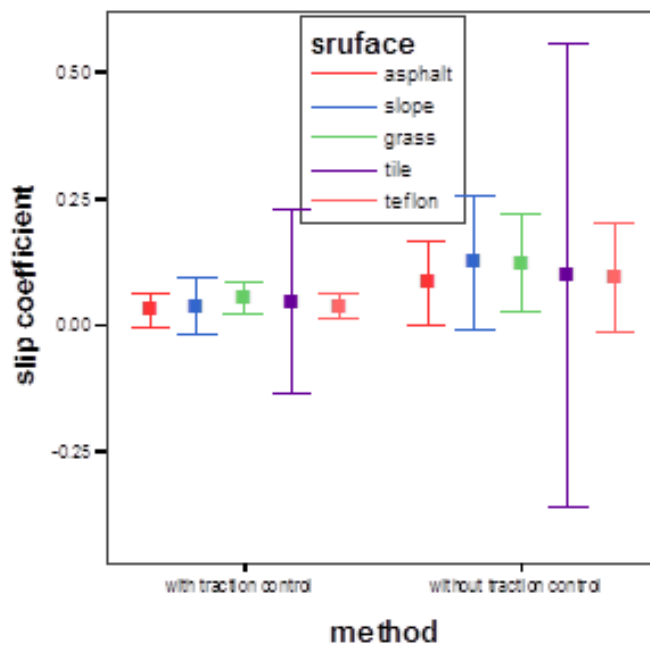


Figure 4-9: Slip coefficients with and without traction control during the test on five surfaces

During the experimental tests, no slip could be seen by the investigators while observing the tests. In order to test whether the anti-slip control method was effective, we put the Teflon on a ramp with 5° degrees slope on which the wheelchair was driven. The **Figure 4-10** and **Figure 4-11** showed how the wheelchair performed during this scenario. From **Figure 4-10** we observed that with open-loop, when slip happened, the two driving wheels kept spinning while the speed of the EPW was almost zero. In **Figure 4-11**, we could observe and recorded that the controller decreased the driving wheel speed in order to gain traction. However, Teflon surface length was insufficient to have the EPW fully reject the slip and regain the desired speed. Anti-slip control was an area where further work was needed to overcome slip more rapidly and effectively.

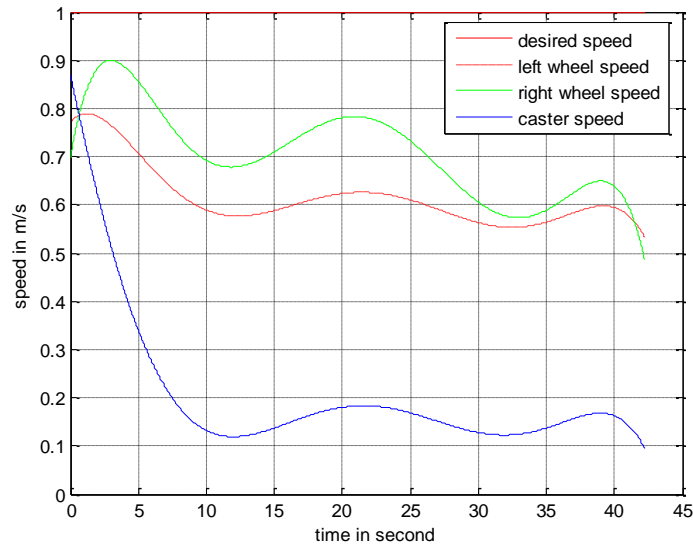


Figure 4-10: The desired speed, left and right driving wheel speed and caster speed for the wheelchair driving at 1 meter per second on a Teflon surface without traction control when slip happened

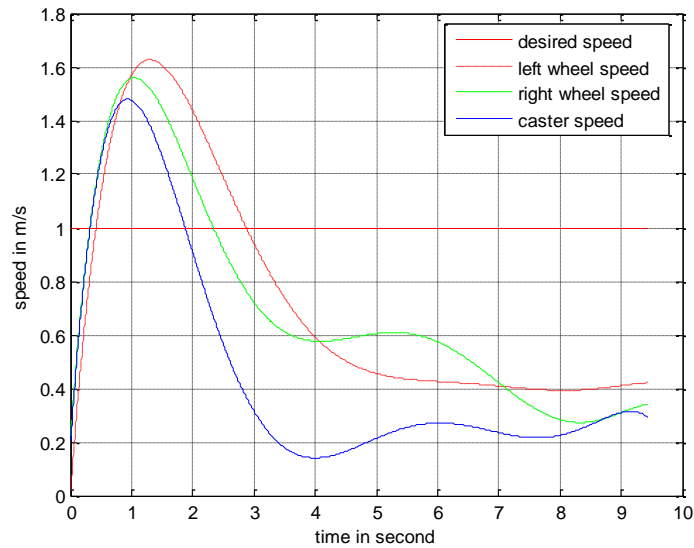


Figure 4-11: The desired speed, left and right driving wheel speed and caster speed for the wheelchair driving at 1 meter per second on Teflon surface with traction control when slip happened

4.4.4 Summary

The data collected indicated that the anti-slip controller successfully detected slip and significantly decreased the slip coefficient over all test conditions (terrain and speeds). The results also showed that the performance of slip-detection and traction control was consistent over different surfaces and speeds. With open loop control, the faster the speed, the larger the slip coefficient indicated greater reduction in traction. However, with anti-slip control, the slip coefficient was similar at different speeds because when slip exceeded the pre-defined threshold the algorithm decreased the driving wheel speed to increasing the traction. There was no obvious change of slip coefficient on the five surfaces as there was with different speeds. The possible reason for this was that we did not visibly see the slip of the wheelchair.

This control system test experiment could be improved in several ways. The driving program needed to incorporate feedback from the inertia sensor on the wheelchair base to more accurately detect the slip and in act control of traction. The results obtained might be only valid for the current EPW setup and user so further tests are necessary to generalize the results. More terrain types should be tested such as different types of carpets, wet surfaces, cross-slopes, and additional ramps. Further investigation is needed to develop more effective and rapid means of implementing anti-slip control.

4.5 Real-Time Forwarding Tipping Detection and Prevention of a Front Wheel Drive Electric Powered Wheelchair

4.5.1 What is the problem of EPW tipping?

Engaging in an active lifestyle is beneficial for maintaining quality of life [80] and EPW could help towards providing that lifestyle for an estimated 300,000 EPW users in the US [81]. A recent focus group study identified two situations where EPW users were most concerned: (1) slipping (loss of traction on the drive wheels) and getting stuck (immobilized), and (2) tipping (loss of stability) [82]. The participants stated that tipping was a concern on cross slopes, at transitions from a slope to horizontal such as curb cuts, and when stopping suddenly on a hill. The participants agreed that generally these problems affected front and rear wheel drive EPWs more than mid wheel drive EPWs due to their six wheel configuration. A previous study showed that the roll rate followed a very similar and predictable pattern when the front wheel drive EPW

was subjected to a rapid deceleration on a downward sloping ramp and that the faster the speed the bigger the roll rate [83]. However in that study, only one slope was tested and there was no control algorithm to decrease the roll rate. Thus in this study, we proposed a controller that detected tipping in real time and compensated to decrease the roll rate of the FWD- EPW to prevent forwarding tipping.

The purpose of this study was to develop a front wheelchair drive electrical powered wheelchair (FWD-EPW) control system with the ability to detect and compensate for forward tipping in real-time. The advanced real-time EPW controller platform was used to develop and evaluate the control algorithm. The tipping rate was defined by the pitch direction angular velocity of the wheelchair. To evaluate a simple wheelchair tipping control strategy, the EPW was driven over a ramp at different speeds. Experimental results showed that the tipping could be accurately detected as it was happening and the performance of the tipping prevention strategy was consistent on the slope across different speeds.

Research Questions:

- 1: To determine whether the controller was able to detect forwarding tipping as it happens.
- 2: To determine whether with the anti-tip controller, the wheelchair could traverse the slope without tipping across different speeds.

4.5.2 Experimental approach

Forward tipping tendency is a problem for FWD- EPW because if the chair decelerates too fast, the inertia of the chair and the user continues to move forward faster than the drive wheels so that the drive wheels become pivot axes around which the faster-moving chair and user rotate.

The problem becomes worse on a downward slope (**Figure 4-12**) because the center of gravity (CG) is shifted forward of the drive wheel axes, thereby providing less resistance to keep the inertia from rotating the chair and user forward.

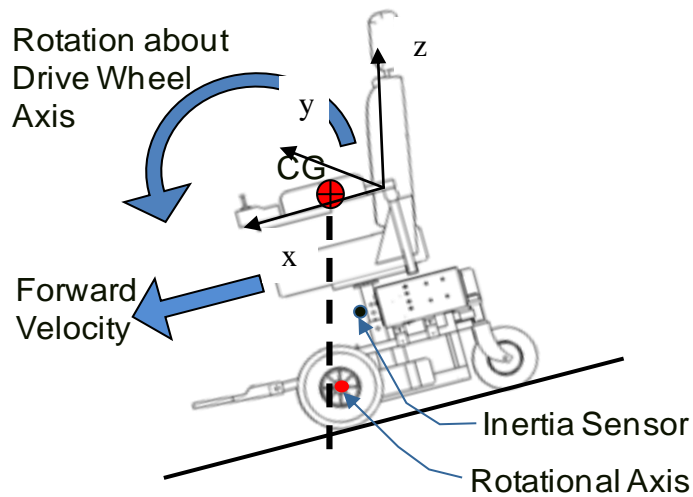


Figure 4-12: Diagram of EPW on Slope

We had developed and demonstrated the advanced real-time EPW controller platform was able to successfully detect and apply a real-time slip controller in above sessions. Here the same platform was used to measure angular velocity (ω_y) about the lateral (Y) axes of a FWD-EPW (**Figure 4-12**) using an inertia sensor and the speed of the EPW (V) determined through optical encoders on the casters. Previous studies [83] showed that with an inertia sensor, the angular velocity while driving on a slope transition could be detected. According to our definition, there were two driving phases: 1) EPW was transitioning from a level surface to slope and then continuing down the slope; 2) EPW was driving from a slope to a level surface. From

the change of the accelerations and angular velocities, the phase transition of the wheelchair could be estimated.

The control rule was determined based on the pre-test results. In this preliminary study, we developed the control rule based on the performance of the wheelchair:

- 1) The threshold speed at which the system tips on a slope when stopped suddenly was defined as $SPEED_{max}$;
- 2) The speed threshold for the system to safely drive from a slope to level ground was defined as $SPEED_{min}$;
- 3) When the controller detected a slope, it would slow down the wheelchair to less than $SPEED_{max} - \Delta_{max}$. In our study, the threshold speed was set to $(SPEED_{max} - 0.2)$ m/s. When the controller detected a transition from a slope to a level surface, and the speed was smaller than $SPEED_{min} + \Delta_{min}$, it would accelerate the wheelchair. In our study, the speed threshold speed in this case was set to $(SPEED_{min} + 0.3)$ m/s;
- 4) We used the z-axes acceleration to determine which transition phase the wheelchair was being driven through. When a wheelchair transitions from a level surface to a slope, there is a positive change in the z-axes acceleration, and the reverse is true when driving from a slope onto a level surface.

The wheelchair was loaded with the 100kg RESNA test dummy which while conducting the tests (**Figure 4-13**). The dummy was secured on the EPW with straps and ropes at different locations (**Figure 4-13**).



Figure 4-13: Experimental setup of the EPW

The experimental protocol consisted of driving the FWD-EPW with and without the control algorithm activated and collecting data from the inertia sensor. An emergency stop braking condition was used to stop the EPW. The control parameters were measured and recorded during each trial. The driving test was carried out using a KVM switch to remotely control the wheelchair at three different speeds: 1.5 m/s (3.6 mph), 1 m/s (2.2 mph), and 0.5 m/s (1.1 mph). All tests were conducted at the same starting point and following the same trajectory (one meter level ground, followed by the slope and then one meter level ground after the slope). The order of speeds of the EPW for each trial was randomly chosen. For each speed, there were three trials conducted and the system was brought to a stop twice each time: once when the EPW was on the test slope; and again when the EPW was driven from the slope to the level surface. The performance of the control system was visual observed for each trial and the data from the inertia sensor were recorded for later analysis.

Data were recorded at 200 HZ via an onboard 2 Gb Compact Flash drive. Data were analyzed using Matlab 7 (R14). The Matlab CurveFit tool box was used to filter the data (a cubic

polynomial fitting model was used). All data were normalized to equal trial length for comparison and the inertia sensor data were normalized to 100% of maximum.

4.5.3 What we got

The physical parameters of the EPW and the test slope were measured. The mass of the EPW and the dummy together weigh 396 lb. The slope was 140 cm long and 19 cm high. **Figure 4-14** showed how the results of inertia data for an upward transition at 0.5 m/s and **Figure 4-15** showed the results of inertia data for a downward transition at 0.5 m/s. The residuals of the model were also shown. **Figure 4-16** shows the results of the angular velocities of the wheelchair about the wheel axes which indicated the tipping angle at three different speeds.

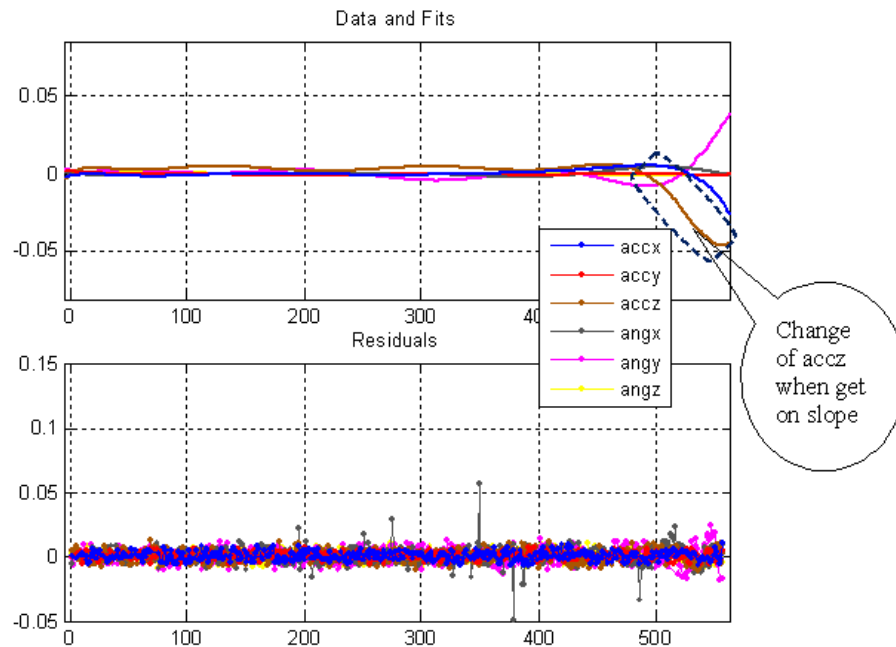


Figure 4-14: Inertial data and residuals after filtering at slow speed when the wheelchair transitioned from level ground to the downward slope

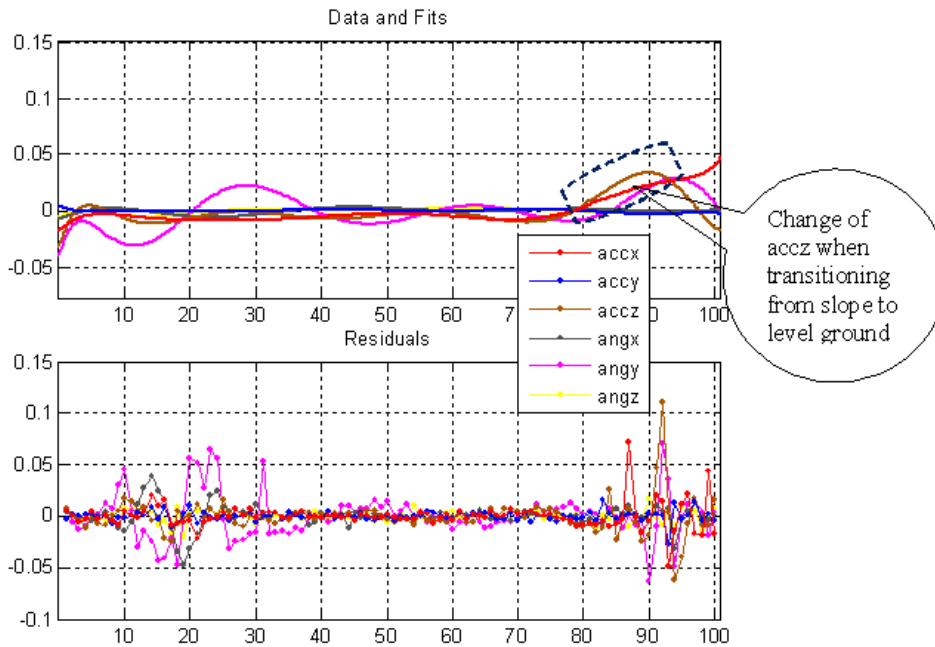


Figure 4-15: Inertial data and residuals after filtering at the slow speed when the wheelchair transitioned from the slope to level ground

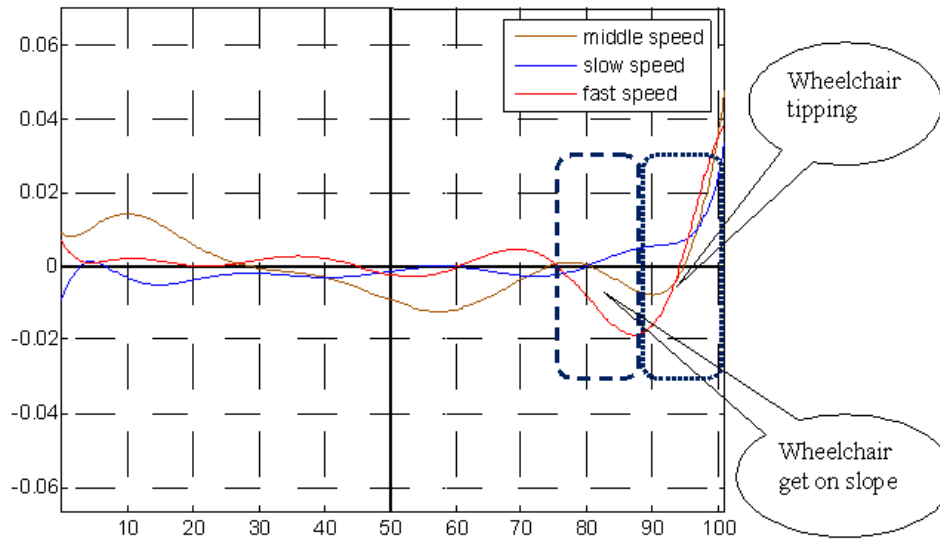


Figure 4-16: Angular velocities about the wheel axes at the three test speeds when the wheelchair transitioning from level ground to the slope

Table 4-4: Performance of the wheelchair for all the experiment tests with and without tip-prevention control applied

System status Tests	Without controller		With controller	
	Level ground to slope and stop	Slope to level ground	Level ground to slope and stop	Slope to level ground
Trial1 (slow speed)	No tipping	stopped	No tipping	Went through
Trial2 (fast speed)	Tipping	Went trough	Tipping*	Went through
Trial3 (slow speed)	No tipping	stopped	No tipping	Went through
Trial4 (middle speed)	Tipping	Went trough	No tipping	Went through
Trial5 (middle speed)	Tipping	Went trough	No tipping	Went through
Trial6 (fast speed)	Tipping	Went trough	No tipping	Went through
Trial7 (middle speed)	Tipping	Went trough	No tipping	Went through
Trial8 (slow speed)	No tipping	stopped	No tipping	Went through
Trial9 (fast speed)	Tipping	Went trough	No tipping	Went through

In our experiment, $SPEED_{max}$ was set as 1.4 m/s and the $SPEED_{min}$ was set as 0.5 m/s. These were based on our experimental results. The results of wheelchair tipping with and without control system applied were listed at **Table 4-4**. After the controller was applied, for a nominal speed of 0.5 m/s, the controller did not intervene when the wheelchair transitioned from a flat surface to a slope; however, it did activate to increase the speed of the wheelchair when transitioning from a downward slope to a level surface. At 1.0 m/s the controller did not

intervene at either transition. At 1.5 m/s the controller only intervened when the chair transitioned from the level surface to a downward slope.

4.5.4 Summary

The data collected indicated that the system successfully detected tipping to prevent a possible rollover. Our findings were consistent with our previous work where we discovered that the roll rate followed a consistent and predictable pattern when the EPW was subjected to a rapid deceleration on a downward sloping ramp [83]. The controller that we implemented successfully changed the speed of the wheelchair in real-time to ensure that excessive tipping did not occur.

There were some limitations to this study and this forward tipping controller could be improved in several ways. The thresholds were decided experimentally; however, there should be a relationship between tip angle, the degree of slope, the material surface, the dimensions of the wheelchair and user, and the speed. Future studies should model the entire system to predict pre-defined thresholds. In this study, there was only one slope tested, and the slope is slightly steeper than the ADA standard (maximum slope is 1/12 but our slope is about 1/8); more tests on different slopes and in varying environment are needed to demonstrate robustness of both tipping detection and prevention. The data obtained may not apply to other EPW designs; therefore further experimentation and mathematical modeling will be necessary to generalize the results. The proposed controller was simple and for some situations the wheelchair might tip even the speed was low, thus a more complex controller might need to be developed to control for tipping. This was a dummy based experiment with the wheelchair driven with fixed speeds, thus the safe range might vary based for real users.

5.0 DEVELOPMENT AND EVALUATION OF ELECTRICAL POWERED WHEELCHAIR DRIVING RULES ON DIFFERENT TERRAINS

The purpose of this study is to investigate electrical powered wheelchair (EPW) users' driving parameter preferences about EPW driving performance on different terrains. This study was conducted in two phases. In Phase I, the researchers analyzed EPW performance when using different driving parameters on three different surfaces through analysis of the critical slip ratio, calculated via encoders mounted on the EPW. The key finding of the phase one study was that the driving parameters that cause a critical slip ratio changes on different surfaces. Therefore, different driving rules for different surfaces should be implemented to maximize EPW performance. For example, on a wet tile surface, users should drive at the same speed as dry tile with but with a recommended acceleration and deceleration rate of 1.08m/s^2 . On gravel surfaces, users should drive at a speed of 1.97 m/s and utilize acceleration and deceleration rates of 1.89m/s^2 . In Phase II, ten subjects without physical disabilities were recruited and tested with the same protocol, and user feedback regarding the comfort, safety, and ease or difficulty of operating the EPW was collected. The time to complete each test, the number of direction changes, and the critical slip ratio were calculated and compared. The maximum angular velocities along the longitudinal, lateral and vertical axes were collected for all the slope surfaces. The results showed that the driving rules developed in phase I were in agreement with

the phase II study: Using the optimal parameters from phase I, all of the users could successfully complete the driving trials without hindrance. The time to complete the trials, number of direction changes, critical slip ratio and maximum angular velocities results agreed with user ratings. In addition, the driving rules developed for wet tile and gravel also worked well with grass and slopes. Finally, a table of driving rules for the surfaces tested was generated. In a future study, EPW users with and without experience will be further tested in order to develop further rules. Furthermore, a terrain-dependent electric powered wheelchair add-on system will be developed to increase the quality of life of EPW users.

5.1 EPW PERFORMANCES ON DIFFERENT TERRIANS

As of 2002, approximately 155,000 individuals in the United States were electrical powered wheelchair (EPW) users, of which approximately 55,000 were older adults (age>65 years) [84]. EPW use is at an all time high and growing in the United States with an estimated 400,000 EPW users in 2010 [85]. A variety of studies have been conducted to demonstrate the effectiveness of EPW use to improve functional independence, community participation, emotional well-being, and quality of life in older adults [86]. However, EPW users are inadequately prepared for outdoor driving situations [87] and a limited number of EPW users show an ability to adjust to hazardous surfaces [88]. As a result incidents of user control loss, device failure, and control failure occur more frequently outdoors than indoors [89] and account for about 60% of injuries each year [90]. In 2003, more than 100,000 wheelchair related injuries were treated in emergency departments in the US, and tips and falls accounted for 65-80% of injuries [91]. As

control systems research has achieved broad application in other areas, such as telecommunications, robotics, automation, and medicine, some research studies are working on the development of better EPW controls with functions like obstacle avoidance, path planning, trajectory generation and manipulation [92]. However, few researchers have considered EPW driving performance related control problems such as robust motion control, traction control, and tip-over control. Previous research found that with a model-based controller, traction performances of an EPW on different terrains could be improved by changing the driving speed and acceleration [93]. Further studies found that by controlling driving speed, acceleration and deceleration, slips and potential tips could be controlled [94, 95]. These findings also indicated that EPW performance is terrain-dependent - i.e. driving performance is affected by the underlying terrain in addition to the choice of driving speed and acceleration/deceleration rate. Recent focus group studies revealed that three of the more challenging driving scenarios active EPW users encounter are getting stuck due to loss of traction, slipping, and tipping over [32]. Additionally, users in these focus groups had developed driving strategies based on experiences such as driving fast in the absence of obstacles, not taking quick turns on sidewalks, maintaining momentum and not turning on sand and gravel, driving slowly or avoiding wet grass or slippery surfaces, and driving straight up and down hills slowly [32]. It is believed that these strategies and adjustments are adequate to meet the needs of highly skilled operators of EPWs in most circumstances. However, many users still have difficulty operating an EPW in environments they regularly encounter (e.g., grassy surface and snow/ice) [96].

Current EPWs typically allow the creation of several driving profiles (e.g., indoor driving, outdoor driving) with different driving parameters (forward speed, acceleration, deceleration, etc). Rehabilitation engineers and clinicians have previously been unable to account

for different surfaces such as slopes, slippery surfaces, and uneven terrain when creating the driving profiles [97]. Instead, rehabilitation engineers and clinicians reported that these driving parameters are adjusted based on a short (around 1 hour) driving test when users come to a clinic to pick up a new EPW [32]. Terrain-dependent control systems are currently in commercial use in motor vehicles such as the “Terrain Response” system used on the 2010 Land Rover LR3, 2011 Ford Explorer commercial vehicles, and the 2012 Jeep Grand Cherokee [98-100]. In this study, a methodology for quantifying terrain-dependent driving rules for EPWs is sought for the purpose of developing a rule-based, terrain-dependent EPW driving system.

Specific Aim 1: Determine how the EPWs perform on different terrains under various conditions, including selected speeds, and accelerations/decelerations.

Hypotheses 1.1: With different driving speeds and accelerations/decelerations, the driving time, the number of direction changes, the amount and frequency of critical wheel slips, and maximum angular velocities will be different on different terrains.

Hypotheses 1.2: With different driving speeds, and accelerations/decelerations, user driving performance on different terrains will vary.

Specific Aim 2: Use the data collected to quantify and validate driving rules for different terrains.

Hypotheses 2.1: With the data about users’ feelings and EPW performances, driving rules can be quantified.

5.2 DEVELOPMENT OF THR DRIVING RULES

The study was designed in two phases. In phase I, the driving rules were developed and evaluated; in phase II, user subject tests were conducted to refine and validate the driving rules.

5.2.1 Phase I

A Pride Q6400Z mid-wheel drive EPW was chosen for the driving rules development. Two driving wheel encoders and one caster encoder were installed to measure the driving wheel speed and caster speed for calculating the slip ratio – the same as the methodologies used in previous studies. The slip ratio was calculated in this equation: $slip\ ratio\ r = abs(\frac{v_{caster}}{v_{drive\ wheel} - v_{caster}})$. An inclinometer was installed on the base of the EPW to measure the slope of the driving surface. A laptop was used to record the data from the sensors and a standard control programmer for the Pride Q6400Z EPW was used to adjust the driving speeds, acceleration and deceleration. . The EPW and encoders are shown in **Figure 5-1**.

To determine the driving rules, the main outcome variable was the slip ratio. Using a slip ratio of greater than 80% as critical slip was considered unacceptable as previous experiments showed that when the EPW drove on a Teflon surface with a greater than 80% slip ratio, the EPW could not re-gain traction to complete the test [93].

- Laptop
 - Recording all the data
- Inclinometer
 - Measuring the angle of the slopes the EPW driving on
- Wheel Encoder
 - Measuring driving wheels speed
- Caster Encoder
 - Measuring caster speed which represent EPW speed

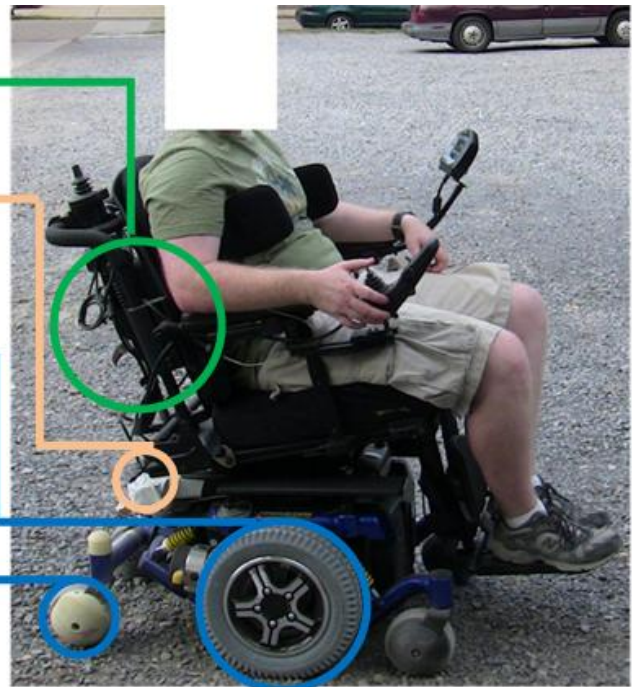


Figure 5-1: The EPW with encoders and inclinometer for data collection

The independent variables were forward driving speed, acceleration/deceleration, and surface type. The driving speeds and accelerations/decelerations that were considered are listed in **Table 5-1**. These numerical values were represented in the controller as values of 20%, 35%, 50% and 65% of maximum speed, and 5%, 20%, 35% and 50% of maximum acceleration/deceleration. These levels were selected because they reflect the 15%-20% common difference between program settings used by clinicians. Three common but potentially hazardous driving surfaces were selected for the initial study: wet tile floors, gravel, and slopes of different inclinations (**Figure 5-2**).

Table 5-1: Driving parameters used in Phase I testing

Speed(m/s)	Acceleration/Deceleration(m/s ²)
0.76	0.27
1.34	1.08
1.97	1.89
2.56	2.71



Figure 5-2: Three surfaces selected for Phase I test

The test protocol: In this study only straight driving was considered. Fifteen meter long sections of all three surfaces were selected for testing purposes. For the wet floor, the wheelchair was driven from a start line with maximum speed for at least 3 seconds, and then fully stopped, and repeated for three trials while data was recorded (**Figure 5-3** left). The slopes and gravel terrains were limited by the length of the surfaces, so all three trials could not be completed in one driving test. Therefore the EPW was driven from the start line to end location for one trial, then the process was repeated to complete three total trials (**Figure 5-3** right).

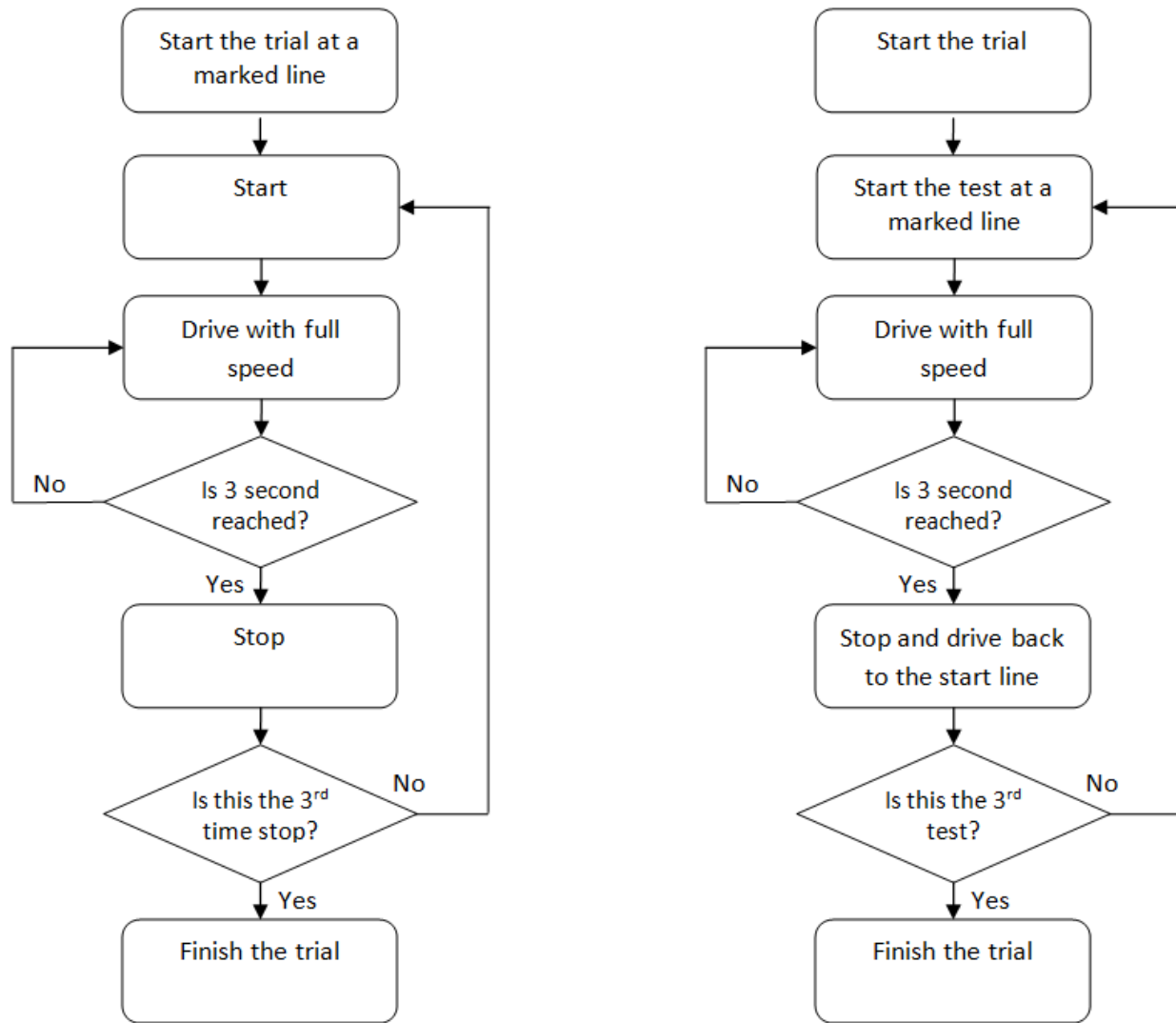


Figure 5-3: Driving protocol for dry and wet tile (left) slopes and gravel (right)

Data was recorded at 70 Hz and the slip ratio was calculated using the same method as in previous studies [94]. The distributions of critical slip values for different driving parameters were calculated and compared using SPSS 15.0. One way Analysis of variance (ANOVA) was used. If there was a significant difference found, post-hoc analysis with Bonferroni adjustment was applied. The level of significance was set at $\alpha=0.05$ *a priori*.

5.2.2 Phase II

The same Pride Q6400Z mid-wheel drive EPW system used in Phase I studies was used for Phase II. A six degree of freedom inertia sensor was mounted to the system and used to record the angular velocities about longitudinal, lateral, and vertical axes. To give the researchers better access to the data recording while other individuals operated the EPW, the laptop computer was replaced with a HP Slate tablet. Additionally, as an added safety measure, an emergency stop button was mounted on the EPW to shut down the whole system.

Ten participants were recruited to provide feedback on the device equipped with different driving settings in Phase II. The inclusion criteria were between the ages 18 and 65 without physical disabilities, able to operate the power wheelchair after some training, and weighing less than 300 lbs (the weight capacity of the EPW is 300lbs). The study was approved by the University of Pittsburgh Institutional Review Board.

The four driving settings used in the Phase II study are listed in **Table 5-2**. These settings represent a large percentage of the range of allowable driving settings deemed safe on various terrains in the Phase I study. It should be noted it was found in Phase I that control loss through wheel slip is unlikely at speeds higher and lower than that of **Table 5-1**. Though this proved the EPW was capable of safe navigation at these settings, clinicians recommended a smaller range to comply with driver cognitive abilities. This is why the speed, acceleration, and deceleration rate for each of the driving settings does not exceed 60% of the maximum speed and acceleration/deceleration settings of the EPW.

Table 5-2: The four driving settings used in Phase II studies

Driving Settings	Speed(m/s)	Acceleration/Deceleration(m/s ²)
1	1.34	1.08
2	1.97	1.08
3	1.34	1.89
4	1.97	1.89

All research activities were performed at the University of Pittsburgh Department of Rehabilitation Science and Technology Bakery Square location by the study investigators, accompanied by a rehabilitation scientist, research engineer, physical therapist, occupational therapist, or assistive technology professional (ATP). For each participant, the session required one or two visits, approximately 3 hours long. The ten able-body subjects who had no prior or limited experience driving an EPW were provided with basic training on EPW driving. All subjects were given ample time to get familiar with the EPW and the course before testing; during the training session, a study investigator explained the study procedures and the operation of the device to each participant. The subjects were also introduced to the indoor and outdoor drive settings on the test wheelchair and informed that they could adjust the setting at their own discretion. To ensure safety, subjects were required to wear a seat belt, and also one investigator followed each participant throughout the course to bring the wheelchair to an immediate halt if a risk or danger to the participant was perceived (as well as provide assistance when requested by the participant). During this free driving session, participants were asked to become familiar with how the EPW operated and to assess whether changes in driving parameters (e.g. speed, turning speed, acceleration) were needed.

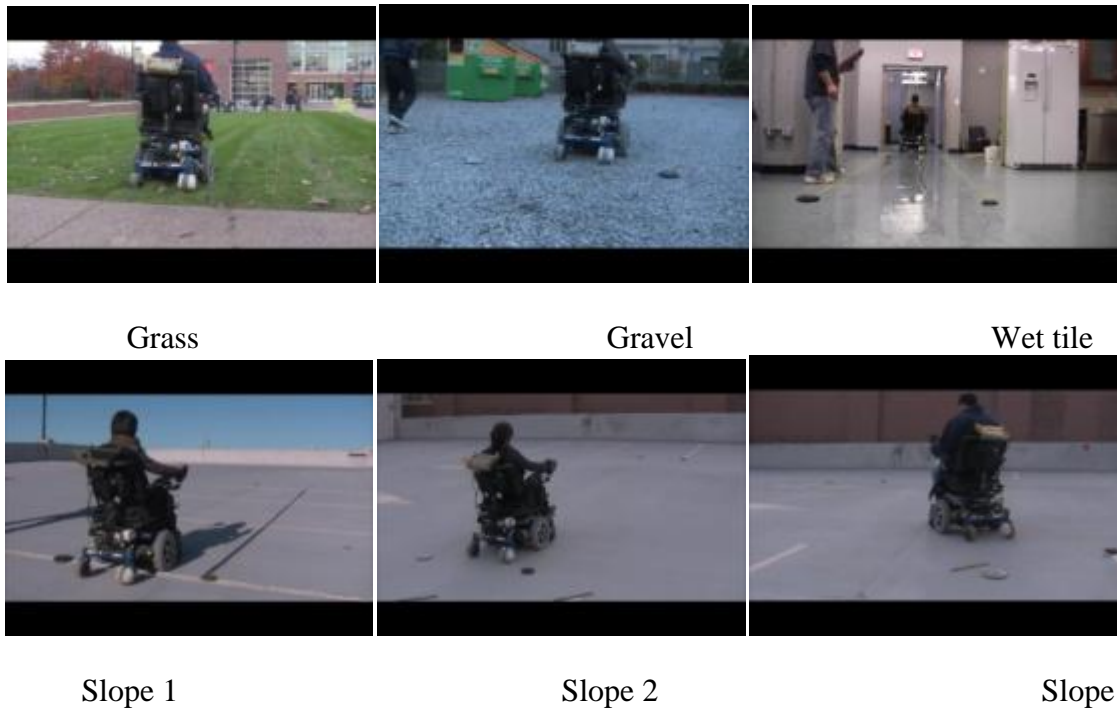


Figure 5-4: Driving surfaces for the Phase II study

The driving courses included four driving surfaces (shown in **Figure 5-4**): 1) an 8 meter-long grass surface; 2) an 8 meter-long gravel surface; 3) an 8 meter-long wet tile surface; 4) three up and down 8 meter-long by 2 meter-wide sloped surfaces of different inclinations. The first slope had a grade of 5 degrees, the second slope was 3 degrees cross-sloped and the third slope was a combination of a 3 degree grade and a 2 degree cross-slope. It should be noted that these angles are within the ADA standards for accessible slopes [101]. Colored tape was used to mark the direction of the driving course.

Each subject was asked to drive straight with the maximum velocity allowed by the driving profile (commanded through full forward joystick positioning) on each of the surfaces. The participant completed this task with each of the four driving settings given in **Table 5-2**. During testing, the speed, acceleration and angular velocity of the EPW were recorded. The

order in which the driving profiles were presented was randomized and subjects were blinded to which driving profile was being used. Users were asked about their impressions after finishing three trials of each drive setting for each surface. The study investigators who analyzed the data were also blinded to which driving profile was being used.

The user feedback was collected using a self-developed rating questionnaire based on a Likert Scale (listed in the appendix). User feedback about how comfortable they were, how safe they felt, and how easy or difficult the trial seemed to be was collected and analyzed. The driving data was recorded at 70 Hz and stored on the tablet attached to the EPW. Data was analyzed using Matlab 7 (R14). The data was filtered with local regression using weighted linear least squares and a 2nd degree polynomial model. Zero weight was assigned to data outside six mean absolute deviations in the regression to increase the robustness. The time to complete each trial and the number of direction changes were normalized to the distance traveled in each trial. The critical slip ratio was calculated in the same way as in Phase I. The maximum angular velocity about the longitudinal, lateral, and vertical axes were collected by the inertia sensor. The distributions of slip ratio and velocity for the different driving parameters and surfaces were calculated and compared using SPSS 15.0. The assumption of normal distribution and homogeneity of variance of the data were checked before running the statistical analysis. One way analysis of variance (ANOVA) was used if the normality assumptions were met and Kruskal-Wallis non-parametric test was used if the assumptions were not met. If there was a significant difference found, post-hoc analysis (T-test or Mann-Whitney test) with Bonferroni adjustment was applied. The level of significance was set at $\alpha=0.05$ *a priori*.

5.3 RESULTS

5.3.1 Phase I results

Wet Tile Surface: The distribution of the critical slip was normal and the homogeneity of variance assumption was also satisfied. ANOVA test results showed that on the wet tile surface there was a significant difference ($F=17.380$, degree of freedom =3, $\alpha=0.004$) on the distribution of critical slip values among different driving speeds (**Figure 5-5**). Post-hoc comparison with Bonferroni adjustment showed that with the highest speed of 2.56 m/s, there was significantly more critical slip ($6.2\% \pm 0.6\%$) than at other speeds ($0.8\% \pm 0.7\%$ for speed 1.97 m/s, $1.0\% \pm 0.7\%$ for speed 1.34 m/s, and $0.5\% \pm 0.7\%$ for speed 0.76 m/s). There were no significant differences among the other three speeds. No significant differences were found on distributions of critical slip values among the acceleration/deceleration combinations but it is obvious from **Figure 5-6** that 1.08 m/s^2 yields the least likelihood of experiencing critical slip.

Gravel surface: There was a significantly ($F=10.975$, $\alpha=0.003$) higher occurrence of critical slip with EPW acceleration (7.3%) than deceleration (5.4%). This is likely due to the buildup of loose rocks around the wheels which can help the EPW decelerate but is preventative to acceleration. No significant differences were found for distributions of critical slip values among different acceleration/deceleration combinations and speeds (**Figure 5-7** and **5-8**). **Figure 5-7** shows that at an acceleration/deceleration rate of 1.89 m/s^2 , though not significant, less critical slip occurs compared to the other tested rates. Therefore, 1.89 m/s^2 was considered to be the most desirable acceleration/deceleration based on wheel slip.

Distribution of critical slip ratio for different driving speeds on wet tile surface

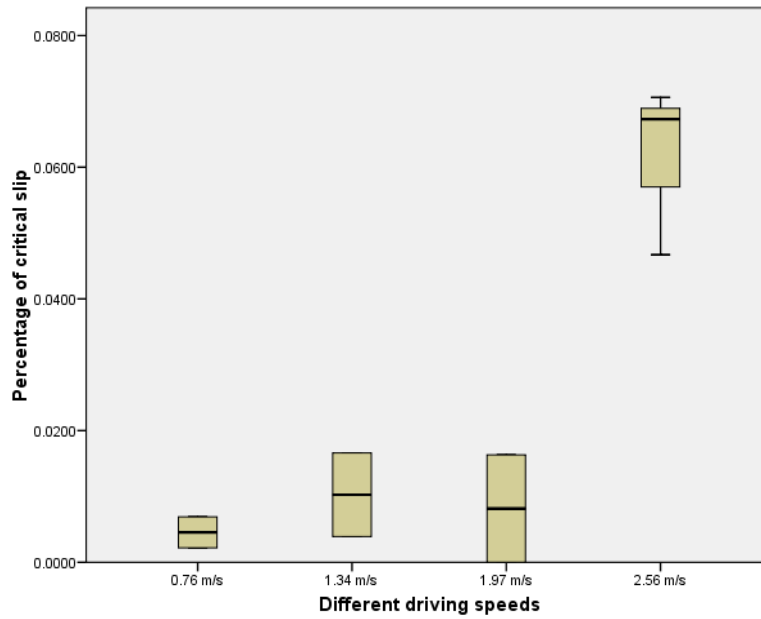


Figure 5-5: Distributions of critical slip values for different driving speeds over wet tile surface

Distribution of critical slip ratio among different acceleration and deceleration combinations on wet tile surface

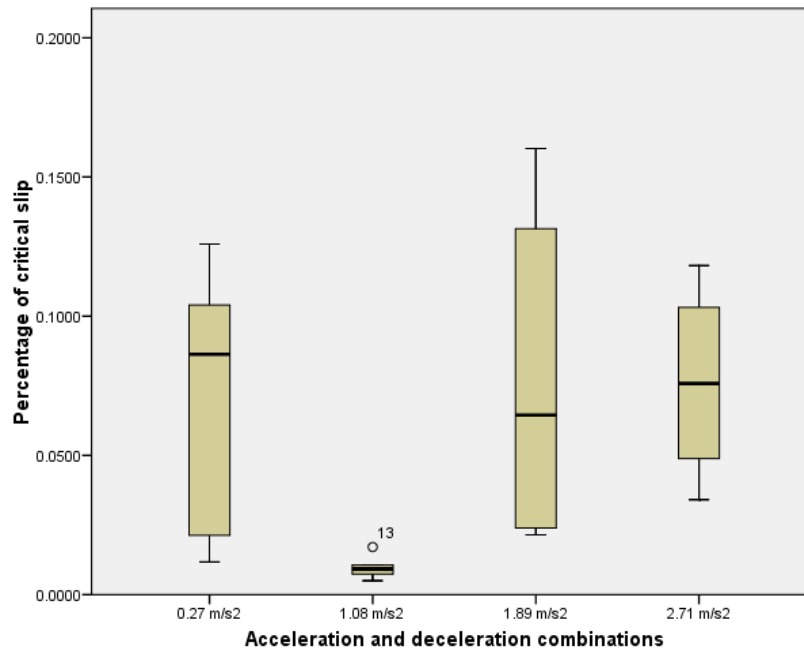


Figure 5-6: Distributions of critical slip values for different acceleration/deceleration combinations over wet tile surface

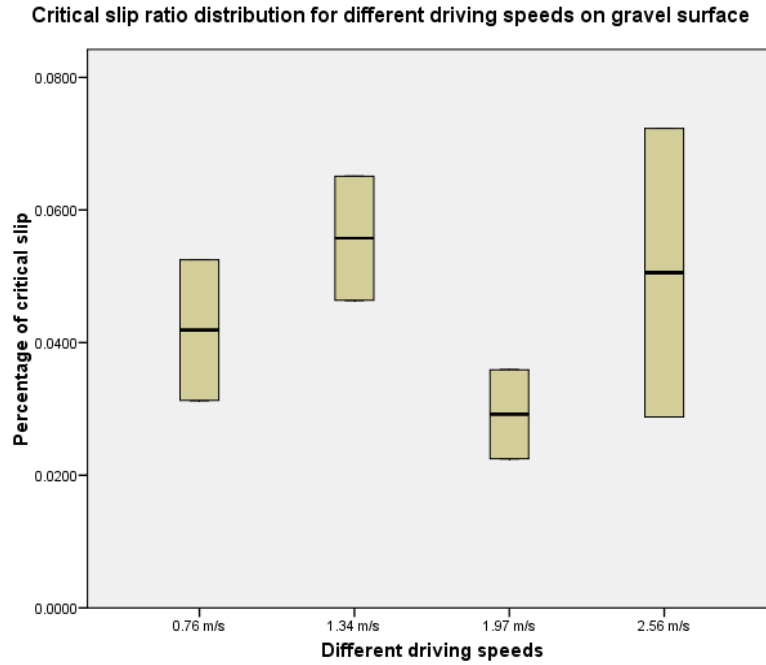


Figure 5-7: Distributions of critical slip values for different driving speeds over gravel surface

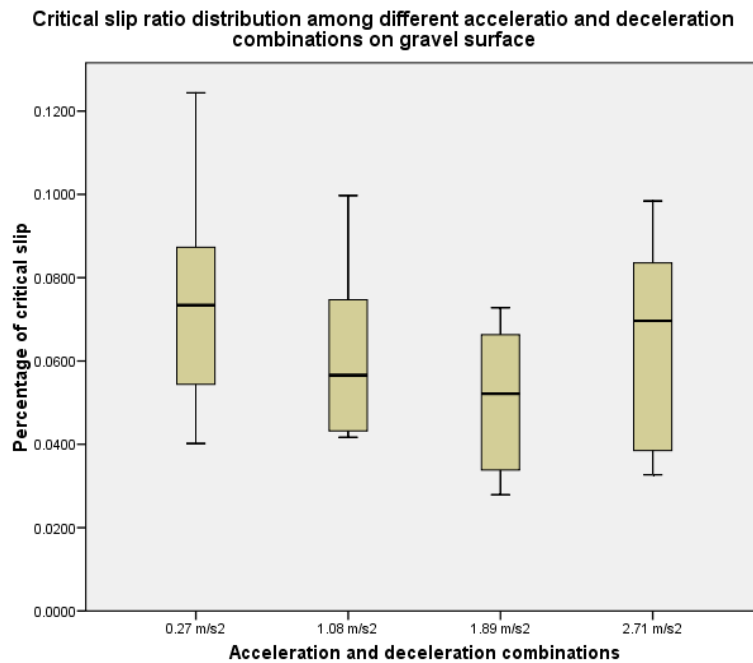


Figure 5-8: Distribution of critical slip for different acceleration and deceleration combinations over gravel surface

Slopes: There was no significant difference in critical slip values among speeds and acceleration/deceleration over different slopes. This was as expected, as it is believed that tipping and rider comfort are more important considerations on slopes and cross-slopes than wheel slip. **Figure 5-9** showed the measured angles from the inclinometer, the real angle measured from an angle meter, and an angle measurement correction that uses a least squares fit of the raw measurement and acceleration/deceleration measurement from the wheel encoder. Although the correction seems accurate, it has a fairly high amount of noise due to the differentiation of the encoder measurements. It is expected that an accurate, less noisy measurement of slope can be achieved by replacing the encoder acceleration/deceleration measurement with an accelerometer estimate. This could lead to control approaches for automated seat adjustments for slopes.

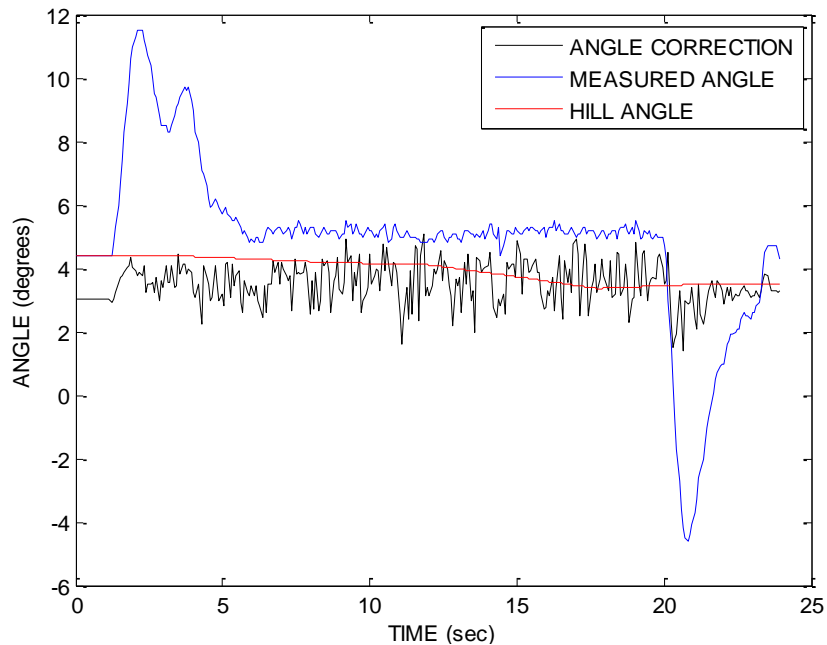


Figure 5-9: Measured angles of the EPW from inclinometer; correction angles with encoder values and real slope angle

5.3.2 Phase II Results

Eleven subjects consented to the Phase II Study, but one subject quit the study because of unavailability. The other ten subjects successfully completed all the drive tests and provided feedback about their driving experiences. The demographic information of the subjects is listed in **Table 5-3**.

The results of user ratings regarding comfort, safety, and difficulty operating the EPW were not normally distributed and the homogeneity assumption was not met, therefore the Kruskal-Wallis test was used to analyze user responses. When examining user ratings for the four settings, there were significant differences among the four driving settings regarding comfort ($\chi^2=8.164$, $df=3$, $\alpha=0.043$), safety ($\chi^2=41.102$, $df=3$, $\alpha<0.001$), and operation ($\chi^2=29.020$, $df=3$, $\alpha<0.001$). Mann-Whitney tests with adjusted $\alpha=0.008$ were used to compare between the drive settings. Users reported significantly higher safety scores with setting 1 than setting 2 ($p<0.001$) and setting 4 ($p<0.001$). Users reported significantly higher ease scores in operating the EPW with setting 1 than with setting 2 ($p<0.001$) and setting 4 ($p<0.001$). Users reported significantly higher safety scores with setting 3 than with setting 2 ($p=0.001$) and setting 4 ($p<0.001$). Users reported significantly higher ease scores in operating with setting 3 than with setting 2 ($p=0.004$) and setting 4 ($p=0.001$). Users reported significantly higher comfort scores with setting 3 than with setting 4 ($p=0.008$), and significantly higher comfort scores with setting 1 than with setting 4 ($p=0.032$). This ultimately means that while users generally felt safer and more comfortable using more conservative settings (slowest speed, low deceleration/acceleration rates), the users felt the more aggressive of the settings to be easier to use. The mean rank for each drive setting regarding user comfort, safety, and operation is listed in **Table 5-4**.

For each individual surface, no significant difference was found among the four driving settings regarding comfort, safety, and operation on wet tile, gravel, grass, slope 1 up, and slope 3 up and down. There were significant differences among the four drive settings regarding operation on driving down slope 1 ($p=0.032$); there was a significant difference among the four drive settings regarding safety on slope 2 up ($p=0.043$) and down ($p=0.036$); there was a significant difference among the four drive setting regarding operation (0.039) and comfort (0.049) on driving down slope 2; there was a trend toward significant differences among four drive settings regarding safety on driving up ($p=0.060$) and down ($p=0.071$) slope 1 and up ($p=0.072$) and down ($p=0.053$) slope 3. The mean rank for comfort, safety and operation ratings is listed in **Table 5-5**.

Table 5-3: Demographic information of the participants

Gender	Age (years)	Education	Marital status	Racial Group	Primary Language	Occupation
Male: 7; female: 3	27.7±5.1; range:21-37	master degree: 6; bachelor degree: 1; currently in college: 2	Single: 8; married:2	Asian: 6; White Caucasian: 2; Hispanic: 2	Chinese: 6 English: 2 Spanish: 2	Students: 10

Table 5-4: Mean rank of users' overall rating on the four driving settings

Ratings Drive Settings	Comfort (Mean Rank)	Safety (Mean Rank)	Operation (Mean Rank)
1	190.53	218.86	143.50
2	174.44	156.42	206.19
3	198.97	210.72	159.73
4	158.06	136.01	212.58

Table 5-5: Mean rank of user ratings on the four drive settings at each testing surface

Ratings Surface	Drive Settings	Comfort (Mean Rank)	Safety (Mean Rank)	Operation (Mean Rank)
Wet tile	1	22.50	24.50	16.10
	2	20.05	18.80	24.85
	3	22.50	24.35	19.65
	4	16.95	14.35	21.40
gravel	1	19.05	22.75	17.00
	2	17.35	14.80	27.50
	3	23.25	25.35	15.90
	4	22.35	19.10	21.60
grass	1	19.95	22.85	17.60
	2	19.30	18.95	20.80
	3	22.45	24.00	20.35
	4	20.30	16.20	23.25
Slope 1 up	1	21.70	26.60	18.60
	2	18.45	14.80	23.90
	3	22.60	24.25	18.10
	4	19.25	16.35	21.40

Slope 1 down	1	26.50	27.05	11.45
	2	17.10	15.00	26.05
	3	21.20	23.30	21.60
	4	17.20	16.65	22.90
Slope 2 up	1	24.35	26.40	16.20
	2	20.10	20.35	23.00
	3	22.50	23.10	16.80
	4	15.05	12.15	26.00
Slope 2 down	1	19.25	22.85	17.30
	2	21.05	16.90	22.80
	3	28.10	28.10	13.95
	4	13.60	14.15	27.95
Slope 3 up	1	21.05	27.05	16.70
	2	21.10	17.45	23.95
	3	22.70	23.05	15.30
	4	17.15	14.45	26.05
Slope 3 down	1	20.40	25.85	14.30
	2	21.60	18.60	21.10
	3	22.55	24.55	20.40
	4	17.45	13.00	26.20

After checking the assumptions, time to complete, number of direction changes, and critical slip ratio, it was decided that the best means of comparison for these quantities was a one way ANOVA test. When the overall time to complete, number of direction changes, and critical slip ratio were examined, there were no significant differences among the four drive settings on number of direction changes and critical slip ratio. There was a significant difference for time to complete the trial among the four drive settings ($F=15.179$, $df=3$, $\alpha<0.001$). A post-hoc test with

Bonferroni adjustment showed that as expected, at faster speeds (settings 2 and 4), users finished the trial significantly faster than at slower speeds (settings 1 and 3). The average time used to complete each test, average number of direction changes, and average critical slip ratio for each drive setting are listed in **Table 5-6**.

Table 5-6: Means and standard deviation of time to complete the trials, number of direction changes and critical slip ratio for the four drive settings

Parameters Drive Settings	Time to complete	Number of direction change	Critical slip ratio
	Mean±Std (second / meter)	Mean±Std (counts / meter)	Mean±Std (%)
1	0.94±0.14	1.65±0.99	4.14±4.01
2	0.83±0.20*	1.69±0.83	4.09±4.01
3	0.93±0.18	1.79±0.93	4.29±4.05
4	0.87±0.18*	1.73±0.79	4.09±4.02

For each individual surface, the Kruskal-Wallis test was used since the assumptions for ANOVA tests were not met. There were significant differences among the four drive settings for completing the trials on grass ($p=0.006$), slope 1 up ($p=0.041$), slope 1 down ($p=0.004$), slope 2 up ($p<0.001$); there were trends towards significant differences among the drive settings for completing the trials on slope 2 down ($p=0.065$), slope 3 up ($p=0.063$), slope 3 down ($p=0.054$). There were no significant differences among the four drive settings for completing the trials on wet tile and gravel.

There was no significant difference among the four driving settings for number of direction changes on all surfaces, but there were trends toward significance on slope 2 up ($p=0.071$) and down ($p=0.065$).

There was no significant difference among the four driving settings for critical slip ratio on all surfaces. The mean rank of time for completing the trials, number of direction changes, and critical slip ratio for each driving settings on all surfaces is listed in **Table 5-7**.

Table 5-7: Mean rank of time to complete each trial, number of direction changes and critical slip ratio for the four driving settings

Measures Surface	Drive Settings	Time	Direction changes	Slip ratio
Wet tile	1	26.30	14.90	19.10
	2	15.50	18.50	21.20
	3	24.30	25.90	21.10
	4	15.90	22.70	20.60
gravel	1	28.60	22.80	20.20
	2	15.00	18.70	21.40
	3	25.40	21.90	21.50
	4	13.00	18.60	18.90
grass	1	25.60	19.00	19.90
	2	16.00	15.80	18.80
	3	28.90	24.70	22.80
	4	11.50	22.50	20.50
Slope 1 up	1	32.40	15.60	19.20
	2	12.60	23.10	18.10
	3	24.40	24.00	23.00
	4	12.60	19.30	21.70

Slope 1 down	1	27.90	19.20	21.40
	2	15.70	23.50	19.70
	3	25.40	20.50	19.80
	4	13.00	18.80	21.10
Slope 2 up	1	31.90	21.70	18.70
	2	12.10	16.90	21.30
	3	27.90	23.30	19.60
	4	10.10	20.10	22.40
Slope 2 down	1	27.50	19.20	21.60
	2	16.20	25.90	17.50
	3	25.10	13.40	21.30
	4	13.20	23.50	21.60
Slope 3 up	1	27.60	21.50	21.50
	2	17.15	22.05	16.85
	3	23.50	16.20	25.80
	4	13.75	22.25	17.85
Slope 3 down	1	22.70	17.10	21.00
	2	26.90	19.40	22.10
	3	18.20	22.40	18.10
	4	14.20	23.10	20.80

As mentioned in the method section and results showed from Phase I, the critical slip ratio did not provide much information about driving performances on slopes. Therefore, in Phase II, we collected the maximum angular velocities along longitudinal, lateral, and vertical axes of the EPW when driving on slopes in order to evaluate the driving performance on slopes in terms of driving smoothness. The assumptions for ANOVA tests were checked, and were not met. The Kruskal-Wallis non-parametric test was then used. Overall, there were significant

differences among the four driving settings for maximum angular velocities in the lateral ($\chi^2=14.149$, $df=3$, $\alpha=0.03$) and vertical ($\chi^2=18.801$, $df=3$, $\alpha<0.001$) axes. The Mann-Whitney test with adjusted $\alpha=0.008$ was used to compare among driving settings. The maximum angular velocity in the lateral axes for driving setting 4 was significantly higher than for driving setting 1 ($p<0.001$). The maximum angular velocity about the vertical axes for driving setting 4 was significantly higher than for driving setting 1 ($p=0.004$). The maximum angular velocity about the vertical axes for driving setting 4 was significantly higher than for driving setting 3 ($p<0.001$). The maximum angular velocity about the vertical axes for driving setting 2 was significantly higher than for driving setting 3 ($p=0.002$). There was a trend towards significance that the maximum angular velocity about the lateral axes for driving setting 4 was higher than for driving setting 3 ($p=0.02$). There was a trend towards significance that the maximum angular velocity about the vertical axes for driving setting 2 was higher than for driving setting 1 ($p=0.026$). There was a trend towards significance that the maximum angular velocity about the lateral axes for driving setting 4 was higher than for driving setting 2 ($p=0.018$). The mean rank of maximum angular velocity about the three axes for the four driving settings is listed in **Table 5-8**.

When each individual surface was examined, there were significant differences among the four driving settings for maximum angular velocities regarding lateral movement when driving down from slope 2 ($\chi^2=8.978$, $df=3$, $\alpha=0.03$), and driving up from slope 3 ($\chi^2=7.910$, $df=3$, $\alpha=0.048$). There was a trend towards significance of maximum angular velocity about vertical axes when driving up slope 1 ($\chi^2=6.622$, $df=3$, $\alpha=0.085$) and slope 3 ($\chi^2=6.827$, $df=3$, $\alpha=0.078$). Mann-Whitney tests with adjusted $\alpha=0.008$ were used to compare between driving settings. Maximum angular velocities about the lateral axes for driving down from slope 2 was

significantly higher for drive setting 4 than for drive setting 1 ($p=0.007$). The mean rank of maximum angular velocities is listed in **Table 5-9**.

Table 5-8: Mean rank of maximum angular velocity about the longitudinal, lateral and vertical axes for the four driving settings

Maximum Angular Velocity Ranking Driving Settings	Longitudinal (Mean Rank)	Lateral (Mean Rank)	Vertical (Mean Rank)
1	106.22	100.23	107.92
2	117.83	116.73	135.01
3	123.42	117.98	95.67
4	134.54	147.06	143.41

Table 5-9: Mean rank of maximum angular velocity regarding to longitudinal, lateral and vertical axes for the four driving settings on all slopes

Maximum Angular Velocity Ranking Surface	Driving Settings	Longitudinal (Mean Rank)	Lateral (Mean Rank)	Vertical (Mean Rank)
Slope 1 up	1	13.80	14.90	17.80
	2	21.60	26.20	24.40
	3	26.30	17.70	14.10
	4	20.30	23.20	25.70
Slope 1 down	1	18.30	22.50	18.40
	2	21.00	19.30	23.10
	3	19.50	20.10	18.40
	4	23.20	20.10	22.10
Slope 2 up	1	18.30	16.40	21.00
	2	23.60	20.60	18.20

	3	16.00	20.00	15.90
	4	24.10	25.00	26.90
Slope 2 down	1	19.90	15.40	16.50
	2	20.20	19.80	25.30
	3	22.60	17.10	15.50
	4	19.30	29.70	24.70
Slope 3 up	1	18.30	14.90	16.80
	2	19.00	17.70	24.60
	3	19.50	20.60	14.70
	4	25.20	28.80	25.90
Slope 3 down	1	19.40	17.00	19.40
	2	16.00	17.80	22.70
	3	22.10	24.10	19.20
	4	24.50	23.10	20.70

5.4 THE DRIVING RULES

From Phase I, it was discovered that wheel slip values on wet tile were not affected by driving speed until the speed was higher than 2.56 m/s. Therefore users could drive at the same speed indoors on wet and dry tile. Extremely slow accelerations (0.27m/s^2 or less) on wet tile do not yield enough traction; this was particularly true if starting from rest. It was also found that accelerations and decelerations of magnitude greater than 2.71m/s^2 are highly likely to cause a wheel slip. As discussed later, the ideal level of acceleration and deceleration was found to be between $1.08\sim 1.89\text{ m/s}^2$ based on the Phase II user acceptance tests. On gravel surfaces, slip was more likely to occur when the wheelchair had low momentum (drove slower) than high moment (drove faster). Ultimately, highest performance on gravel was experienced between $1.34\sim 1.97$

m/s which eliminate the low momentum problems and the steering difficulties that result from violent vibrations at high speeds. It was also found that an acceleration/deceleration of 1.89 m/s^2 on gravel surfaces gave the least likelihood of wheel slip among the settings tested. On slopes, the slip ratio saw little variation based on driving speed, acceleration, or deceleration. Thus a different metric must be used to identify proper settings for these parameters. A method for determining the slope angle is also presented in Figure 47 which reduces error associated with raw inertial measurements. This could be used for future study to address a problem identified in a focus group study, which noted that seat positioning was critical to user comfort on slopes [32].

In Phase II, the system worked well through all the trials, with the exception of one drop-out when testing on a gravel surface. The connector for the battery came loose on this occasion due to the high vibration. The connector was then reconnected and secured. No other data loss occurred. This validated the effectiveness of the hardware and software. The driving parameters selected in Phase II were speeds of 1.34 m/s and 1.97 m/s , and acceleration and deceleration combinations of 1.08 m/s^2 and 1.89 m/s^2 , because these settings met the criteria of the Phase I study and clinician feedback. Speeds higher than 2.56 m/s were not picked due to the significantly increased critical slip ratios. This agreed with previous findings by Cooper et al. which found that EPW users drove their wheelchair considerably less than the wheelchair's maximum speed most of the time. The capacity for the wheelchair to drive at or near 2.7 m/s is typically used in only short spurts of a few meters for tasks such as crossing intersections, avoiding pedestrians, and other similar maneuvers [102].

Overall, setting 2 and setting 4 with fast speeds took a significantly shorter time to complete the trial than settings 1 and 3. This made sense that for the same travel distance, with a faster speed, less travel time was needed. However, when looking at individual surfaces, there

were no significant differences in time to complete the test among the four driving settings on wet tile and gravel. One possible reason was that even though there were no significant differences among the four driving settings on critical slip ratio over wet tile and gravel, the wheel slips happened more frequently when driving with faster speeds on these two surfaces than with slower speeds [97]. Another possible reason was that users might not have pushed the joystick to the maximum position out of safety concerns when driving on wet tile at a fast speed since it was a confined indoor surface, and they did not drive the speed they were asked to on gravel for comfort reasons [32].

There were no significant differences among the four driving settings on number of direction changes. This might relate to how we defined the direction change. In this study we counted the direction change when the left wheel and right wheel speeds had a difference larger than 0.05 m/s. This was empirically selected, and in a future study, we may need to find the relationship between the speed differences and EPW drive performance. There was a trend towards significance that with fast speeds, there were more direction changes than at slow speeds when driving on cross slopes. This was expected since on cross slopes; users had to push the joystick towards the uphill direction to compensate for gravity in order to keep driving straight. With higher speeds, it was easier to cause direction changes when adjusting the joystick position for straight driving [32].

No significant differences on critical slip ratio were found for all surfaces among the four driving settings. There were two possible reasons for this. First, consistent with the Phase I study, the speed, acceleration, and deceleration combinations we chose were already pre-selected with less critical ratio. Secondly, the threshold (more than 80%) we chose for the critical slip ratio might have limitations. We selected the threshold based on complete loss of traction on a

Teflon surface, though this might not be true for other surfaces [93]. Further study might need to look at whether varying the threshold of critical slip ratio for different surfaces would cause any significant differences among the four driving settings.

We found that on the slopes, overall, the maximum angular velocities about lateral axes were significantly higher for the fast speed high acceleration/deceleration than for the slow speed low acceleration/deceleration. This agreed with previous studies on forward tipping, and Salatin et al. showed that with higher speed, acceleration and deceleration, angular velocities about lateral axes were higher than slower speed acceleration and deceleration [95, 103]. A trend towards significance was found that with fast speed high acceleration/deceleration, there were higher maximum angular velocities about lateral axes than fast speed low acceleration/deceleration. This indicated that when driving on slopes, acceleration and deceleration might affect EPW tips more than speed (in previous studies, we already found EPW tips related with maximum angular velocities about lateral axes). We also found that with fast speed, there were higher maximum angular velocities about vertical axes than slow speed. This agreed with the findings from the number of direction changes that high speed on slopes leading to higher chances of veering. When looking at individual surfaces, significantly higher maximum angular velocities about lateral axes were found with fast speed and high acceleration or deceleration on slope 2 down and slope 3 up. We expected to see this result on slope 1 up and down as well as users reported in the focus group study [32]. Further study is needed to explain this. Trends toward significances were found that when driving up slope 1 and 3 with fast speed high acceleration and deceleration, there were higher maximum angular velocities about vertical axes than at other settings. One reason might be that the caster wheels might not line up, or the

EPW had a higher chance to veer when driving up slopes with fast speed acceleration and deceleration.

Users had significantly higher rating scores on comfort, safety, and ease of operation with slow speeds. This might be because they were not EPW users, and did not have much experience with EPW driving. The reason to start with able-bodied subjects was to test the validity of the system, but more importantly to ensure all the necessary safety measures had been implemented for EPW users. For individual surfaces, no significant differences were found regarding comfort, safety, and operation on wet tile, grass, gravel, grass, slope 1 up, slope 3 up and down. With fast speed high acceleration and deceleration, users reported the lowest safety, comfort, and ease to operate scores on cross slopes. This was consistent with the above quantitative results from the number of direction changes and maximum angular velocities about lateral and vertical axes.

Comparing findings from this study to the previous focus group and interviews [32] show that previous user-developed mobility strategies were similar to these results. For example, when driving on gravel it is important not to drive too slowly or make sudden starts/stops. However, driving fast over gravel is also a problem as the bouncing could set off very uncomfortable spasms in the user or cause their hand to be jostled off the joystick control. The best strategy is to drive as fast as one can tolerate over gravel to avoid bogging down. Wet tile or other slippery surfaces were identified as requiring similar strategies, such as not making sudden changes in speed and direction. Strategies for slopes were as follows: 1) when driving down a steep slope, slow down and avoid sudden stops; 2) drive straight up a steep slope; and 3) avoid sharp turns on steep slopes. Additionally, it was suggested that EPW users should drive along a steep cross slope with their joystick pointing somewhat towards the top of the slope in order to avoid causing the lighter uphill drive wheel to slip.

Table 5-10: Recommended driving rules for novice and experience EPW users

Driving rules Surface	Rules for novice users	Rules for experienced users
Wet tile	Setting 1	Setting 2
Gravel	Setting 3	Setting 4
Grass	Setting 1	Setting 2
Up/Down slope driving up	Setting 1	Setting 4
Up/Down slope driving down	Setting 3	Setting 2
Cross slope driving up	Setting 1	Setting 2
Cross slope driving down	Setting 3	Setting 2
Combined slope driving up	Setting 1	Setting 2
Combined slope driving down	Setting 1	Setting 2

In summary, by combining user ratings on safety, comfort, ease to operate, time to complete the trial, number of direction changes, critical slip ratio, and maximum angular velocities on slopes, we developed the driving rules for EPW users (listed in **Table 5-10**) for the nine surfaces: setting 1 represents slow speed, low acceleration and deceleration; setting 2 represents fast speed, low acceleration and deceleration; setting 3 represents slow speed, high acceleration and deceleration; setting 4 represents fast speed, high acceleration and deceleration;. Two sets of driving rules were recommended. For experienced EPW users, we had learned from the focus group study [32] that they would like to drive faster, and they had enough experience and skill to handle the faster speed. For new users, conservative rules were suggested to make sure they could go through different terrains with maximum safety guaranteed.

There were some limitations to this study. First, only a middle-wheel drive EPW was used to develop the driving rules. The rules may not work with front-wheel drive or rear-wheel drive EPWs, especially on slopes. Therefore, in a future study, different types of EPWs should be tested to validate the rules. Second, there were only 10 able-bodied participants. The sample size was small, and the results based on convenience samples might not generalize to EPW users. However, those subjects could drive the EPW with identified driving rules with acceptable comfort, safety and operation. In addition, 6 out of 10 of our subjects were not familiar with EPW driving which well-represented novice EPW users. In a future study, we plan to recruit EPW users with and without experience and a larger sample size. Third, there were only three surfaces tested in Phase I and a total of four surfaces (the three surfaces used in Phase I and 1 new surface) for Phase II. Although these surfaces were chosen based on focus group studies, more surfaces should be considered to validate the driving rules. The rules we developed based on wet tile and gravel in Phase I worked well for grass and slopes in the Phase II tests. We did not take user experience with EPW driving into consideration. There might be a relationship between user experience and which rules work best for them on certain surfaces. All of the experiments and driving rules were for straight driving. Turning driving rules have not been developed and validated yet. In the future, we will develop a terrain-dependent EPW driving assistance system with the capacity to implement the driving rules in real-time.

6.0 DEVELOPMENT OF AN ADVANCED MOBILE BASE FOR PERSONAL MOBILITY AND MANIPULATION APPLIANCE GENERATION II (PERMMA GEN II)

This section presents the development of the mobile base for Personal Mobility and Manipulation Appliance Generation II (PerMMA Gen II), a stair climbing wheelchair able to move in structured and unstructured environments, to climb over up to an 8” curb, and go to up and down stairs. The mechanical, electrical, and software systems of the mobile base are presented in detail. The mobile base of PerMMA Gen II has two operating modes: “advance driving mode” on flat and uneven terrain, and “automatic climbing mode” during stair climbing. The different operating modes are triggered either by local and dynamic conditions or by external commands from users. A step climbing sequence, up to 8”, is in development and to be evaluated via simulation. The mathematical model of the mobile base is introduced. A feedback feed-forward controller has been developed to maintain the posture of the passenger when driving over obstacles, uneven surfaces, or slopes. The effectiveness of the controller has been evaluated by simulation using the ODE tool. Future work for PerMMA Gen II mobile base is implementation of the simulation and control on a real system, and evaluation of the system via more experimental tests.

6.1 WHY PERMMA GENII

As of 2002, approximately 155,000 individuals in the United States were electrical powered wheelchair (EPW) users, of which approximately 55,000 were older adults age>65 years [84]. There were an estimated 400,000 EPW users by 2010 in the United States [85]. Previous research has showed enhanced activity and participation [104-106], satisfaction [107] and quality of life [108] among EPW users. These wheelchairs have also given the users independence [105, 107]. The EPW user population is growing, and manufacturers are offering an expanding range of wheelchair options [109-112]. Nevertheless, architectural barriers still exist in many cities and buildings, and it is expensive and time consuming, if not impossible, to eliminate all of them. Thus, there are physical environmental barriers preventing EPW users from visiting friends and family [105] and carrying out more activities [112, 113] – especially with regards to stairs, doorsteps, etc. Studies show user adapt their behavior [114, 115] by choosing routes without physical barriers or by going to accessible places rather than to places they really want to go [116]. In addition, research shows that EPW users are inadequately prepared for outdoor driving situations since new EPW users normally receive little to no outdoor driving training [117, 118]. The focus group studies also found that EPW users either have to bring someone with them or avoid certain surfaces such as ramps, cross slopes, snow etc. during their daily activities [32].

A few systems for climbing stairs or clearing obstacles have been developed over the last 15 years, such as the TopChair [119], the Explorer [120], and the iBOT [121, 122]. With these new devices, half the users were able to climb stairs independently and felt that this capability was helpful. The remaining users were able to climb stairs with some assistance. All users agreed that such devices should be made available to war veterans who use wheelchairs [121, 122].

The TopChair comprises combined wheels and a caterpillar track. The TopChair was tested in France among 25 persons with SCI, and results showed that all participants were able to successfully operate the power wheelchair indoors and outdoors. One drawback of the TopChair is that due to its electromechanic properties and caterpillar tracks, it is a little bulkier and heavier than other power wheelchairs with similar functions. In addition, the mechanism of TopChair may not provide assistance when users drive on cross slopes or become stuck on a gravel surface. Like the TopChair, the Explorer is a stair-climbing wheelchair with wheels for level surfaces and tracks for climbing. The seat automatically takes the right tilt when moving up stairs. This wheelchair has 2 rear wheels but a single front wheel, limiting outdoor use.

The iBOT Mobility System also can travel over uneven terrain and climb curbs and stairs. It contains gyroscopes that serve as motion sensors to maintain balance automatically. The gyroscopes respond to motion by sending signals to built-in computers, which use the information to control the motors in order to maintain stability. This system continuously realigns and adjusts the wheel position and seat orientation to keep the user upright and stable at all times, even when driving up and down steps. Stair-climbing is performed by rotating the 2 sets of powered wheels about each other; however, the user must either hold a handrail or receive help from an assistant to stabilize the wheelchair. The iBOT was developed in the 1990s but obtained U.S. Food and Drug Administration approval only in 2003 because of safety concerns. It was put on the market in 2005 in the United States and the United Kingdom. Even though the iBOT is a good mobility option for persons with ambulatory impairment, it is an expensive device with no Medicare funding unavailable; hence, it is no longer available on the market.

There is also some research on stair-climbing wheelchairs. The concept of a stair-climbing wheelchair called Wheelchair.q, with the ability to move in structured and unstructured

environments, to climb over obstacles, and to go up and down stairs, has been presented by Giuseppe and his colleague [123, 124]. More research on stair-climbing wheelchairs has also been done with regards to mechanical design [125, 126], kinematics [127], coordinated motion control [128], kinematic model and experimental validation [129], environment adaptation [130], and improved design [131]. Chen and Pham also presented a new stair-climbing robotic wheelchair and the stability analysis of the system was reported [132]. A company from Israel called Galileo Mobility has some drawings on an EPW with capabilities to climbing stairs, elevate seat or lower to ground, support stand-up position, and traverse sand, gravel or grass [133]. Researchers from Japan also worked on rough terrain mobile robot call RT-Mover with four drivable wheels and two leg-like axles [134].

All current and proposed EPWs have significant problems. The TopChair is bulkier and heavier than most EPWs and not able to provide assistance on cross slope; iBOT is too expensive and has been discontinued due to unavailable funding from Medicare; the related research, proposes wheelchairs whose mechanisms have good rolling efficiency and conceptual simplicity but present a high actuating cluster torque, a large number of wheels that have to be driven and braked, difficulty in adding a steering mechanism, and a dramatic increase in weight, size, and cost. In addition, the fact that these proposals could only climb stairs or were too difficult to use indoors resulted in a lack of user involvement to evaluate the performance of the system.

Series of focus group studies had been conducted to identify the problems of EPWs driving over different terrains, and developed some driving rules with different speeds, acceleration, and deceleration for different terrains [97]. However, during the user study, we found out that under certain circumstances, rule based driving failed due to the limitation of current EPWs. For example, when the driving wheel lost traction completely on a gravel surface

or a slippery surface, it was impossible for the user to re-gain traction and drive through [93]. Therefore, there is a need for EPWs with comparable dimensions to current EPWs for indoor use as well as capabilities to drive through tough terrains like gravel and cross slopes, and the ability to climb curbs and steps.

The focus of this study is to develop a mobile base for our Personal Mobility and Manipulation Appliance Generation II (PerMMA Gen II). The design, development, and evaluation of PerMMA Gen I has been reported previously [138]. The emphasis of PerMMA Gen II is enhanced mobility. The design object is to develop a PerMMA Gen II mobile base with

- 1) Comparable dimensions to current EPWs - therefore no modification of users' home will be needed;
- 2) A flexible base allowing for adjustments to the driving wheel and caster wheel
 - a. Allow a lap-to-floor distance smaller than 26" - therefore users can access their office desks;
 - b. Safely go through both indoor and outdoor terrains such as carpet, floor mats, wet tile, gravel, cross slopes, curbs, and steps.

The same hardware platform used for previous research on smart controllers and PerMMA Gen I has been adapted for the PerMMA Gen II mobile base, with the aim to propose a valid alternative to a wide range of existing solutions developed to improve disabled mobility. In section 2 the wheelchair system design and operating modes are presented, and in section 3 an inside description of the control design and development is shown. In section 4, simulation results are shown for the verification of the control, and finally the conclusion and future works are illustrated in section 5.

6.2 SYSTEM DESCRIPTION

PerMMA Gen II is a stair-climbing wheelchair able to move in both structured and unstructured environments, to climb over obstacles, and to go up and down stairs (see **Fig. 6-1**). The PerMMA Gen II mobile base uses a six-wheel design, similar to many current electric powered wheelchairs. The front and rear wheel casters are mounted to the main frame via 4-bar linkages. The position of the front and rear casters is controlled via four independent pneumatic actuators.

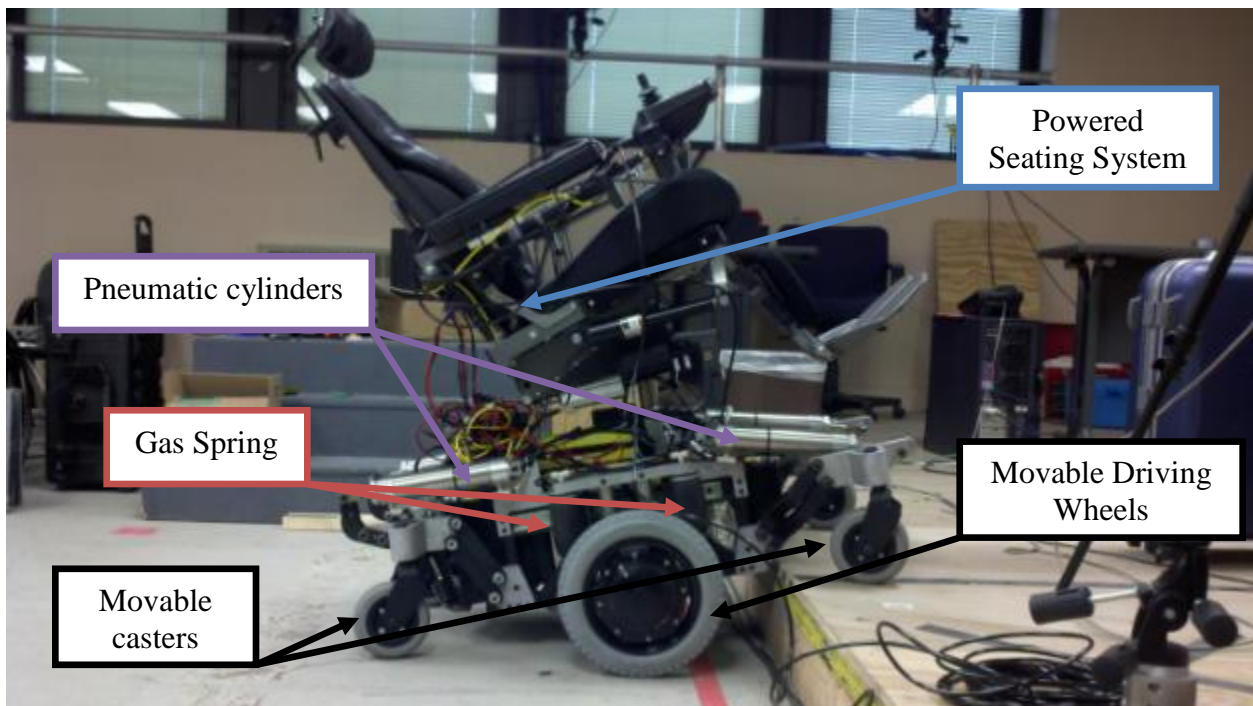


Figure 6-1: PerMMA Gen II system overview

The actuators permit leveling of the seat with roll and pitch of the driving surface, as well as curb/step climbing. The drive wheels use hub-motors and are mounted to the frame via an x-y

sliding platform, which allows the drive wheels to be moved up/down independently with pneumatic actuators, and fore-aft to alter the center of mass and driving dynamics with a carriage and an electric linear actuator. This helps in obstacle negotiation, allows for optimization of the drive dynamics for indoor and outdoor driving, and expands options for negotiating challenging terrain (e.g., gravel, grass, side-slopes, and ice). The movable caster wheels and driving wheels make the wheelchair capable of performing a lateral tilt for pressure relief. The seat, as shown in Fig. 1, is a standard EPW seating system with power seating functions of tilt, recline, seat elevator, and elevated footrest.

The real-time EPW control platform developed [93] and evaluated in previous studies [94, 95] was used as a model to develop the PerMMA mobile controller because of its demonstrated capabilities of handling multiple tasks in real-time while providing rich interfaces. Control algorithms were also developed, such as real-time slip detection and prevention, real-time tip-over detection and prevention, and terrain-dependent driving to prevent slips and falls.

6.2.1 Electrical system

The PerMMA Gen II electrical design was expanded with more electrical components from the control platform as shown in **Figure 6-2**: a relay board to control the seating functions, a relay board to control the pneumatic cylinders for moving the four casters and driving wheel up and down, the electrical motor for moving the driving wheel forward and backward, a replay board to control the caster brakes during curb and stair climbing, a PWM generation board to generate a PWM signal to control the pneumatic system, a circuit board to control the caster brakes, and a digital I/O board for receiving feedback from the pneumatic cylinders. All the pneumatics,

electrical motors, caster brakes, and power seating functions can be controlled either by the on-board single board computer through digital I/Os or by a keypad through relay boards.

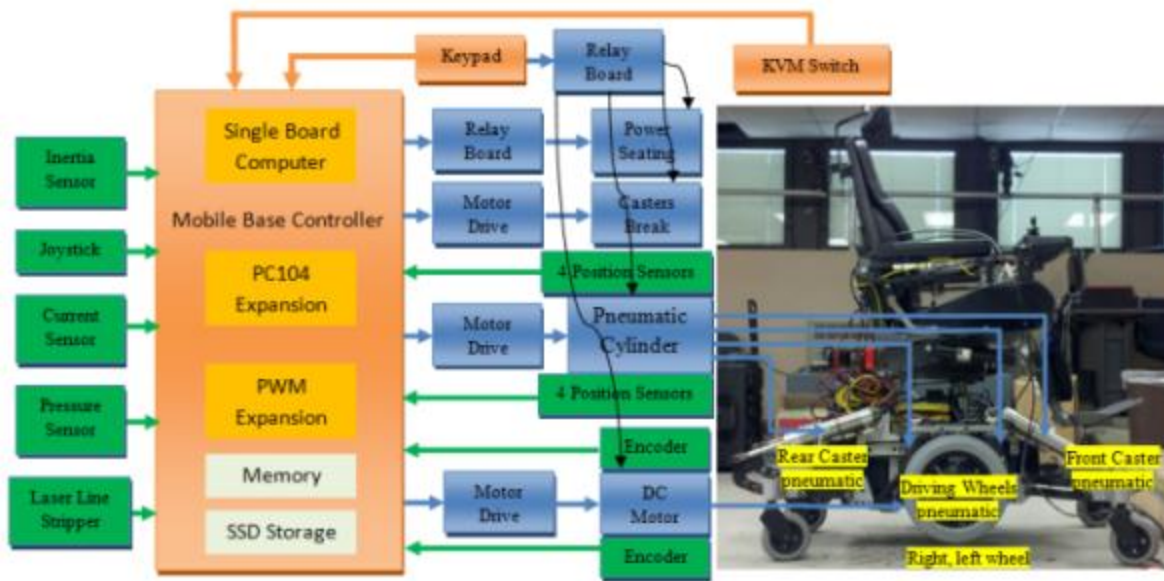


Figure 6-2: Electrical system diagram of PerMMA Gen II

6.2.2 Software system

PerMMA Gen II software inherits the multiple-layer software packages for the control platform. In order to increase wheelchair stability and at the same time to guarantee a comfortable horizontal seat to the passenger, a posture control module was added as shown in **Figure 6-3**. This module was to keep the passenger's posture in a predefined safety and comfort zone. The safety zone is determined by the maximum protection for each surface, and the comfort zone is defined depending on the speed and acceleration used for driving and the weight and height of

the user. The system calibrates itself when the user is sitting on the chair and detects the user's center of gravity (COG). Then the distribution of the user's COG is monitored by sensors.

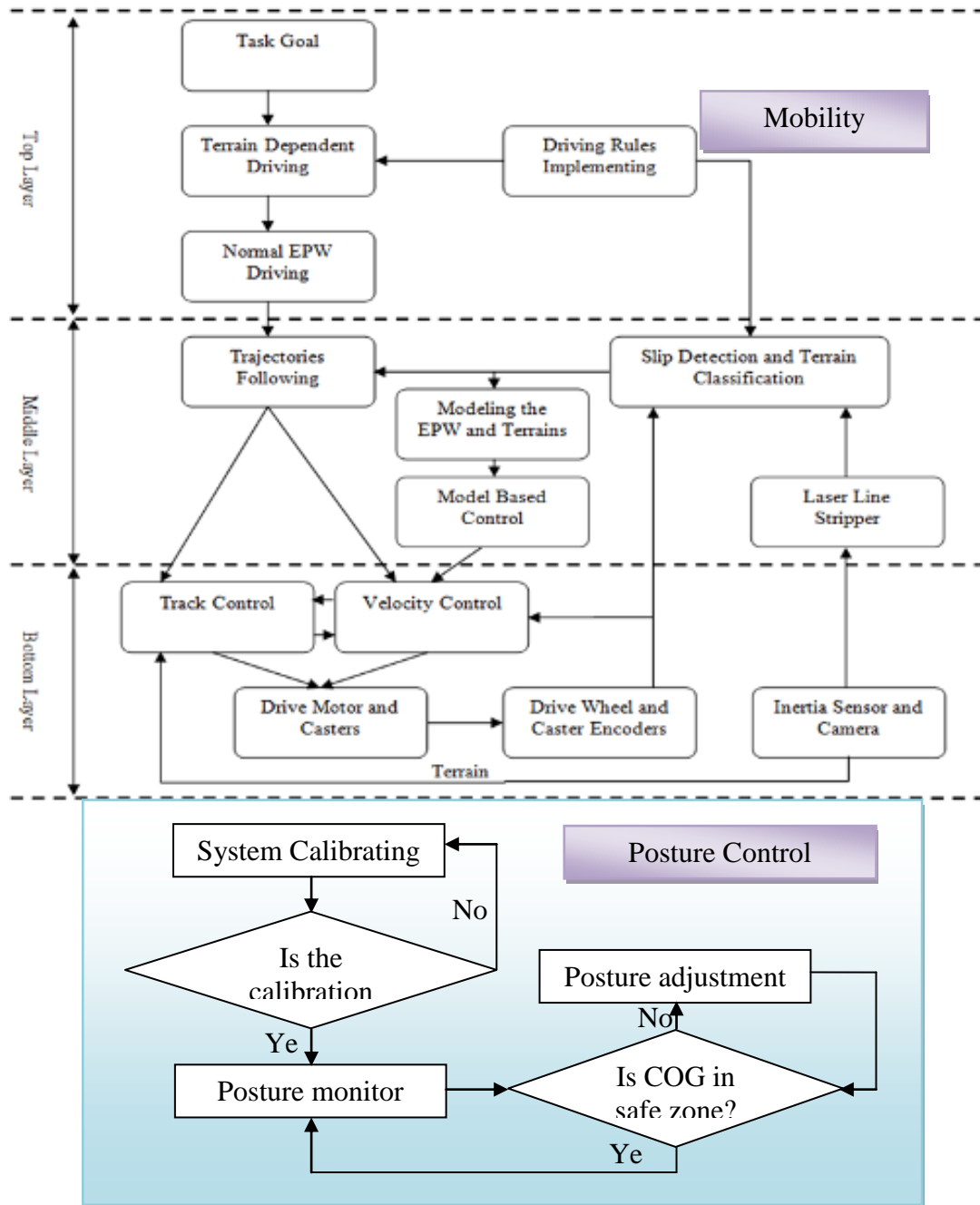


Figure 6-3: PerMMA Gen II software modules

6.2.3 Description of different kinds of motion

As will be explained in the next section, the system provides two options for users to change between “advanced driving mode” and “automatic climbing mode”: these modes can be switched by a user’s manual input, or triggered by automatic function.

1) Advanced Driving Mode (ADM): When the wheelchair moves on flat or uneven terrain, the two motorized driving wheels are always in contact with the terrain. The caster wheels can be configured for front-wheel drive (rear caster wheels in contact with the terrain), rear-wheel drive (front caster wheels in contact with the terrain), or middle-wheel drive (both front and rear caster wheels in contact with terrain). While the wheelchair would be stable with all the six wheels in contact with the ground (especially during off road travel), this configuration is not optimized for traversing obstacles such as curbs, grass, gravel, uneven terrain and snow compared with front-wheel drive configuration.



Figure 6-4: PerMMA Gen II in automatic climbing mode

2) Automatic Climbing Mode (ACM): During stair climbing operations, more importance is given to wheelchair stability and so all the four caster wheels are in contact with the ground when the driving wheels are lifting up for stair climbing (as shown in **Figure 6-4**). Caster brakes are engaged when the driving wheels are not in contact with the ground.

6.2.4 Climbing strategies

The goal of PerMMA Gen II is to climb stairs. The step climbing strategy (**Figure 6-5**) is the correct sequence of actions that allow the wheelchair to surmount a single step of height of 20.32 cm (8 inches) or less. The wheelchair is driven in ADM when the system is in front of a curb, and then switches to ACM. When ACM is triggered, the system will start the sequence by aligning the wheelchair perpendicular to the curb using the pressure sensors in the front casters (**Fig. 6-5-1**). The driving wheels will be moved forward to be in front-wheel drive. Next, the wheelchair will be moving at a slow constant speed (1m/s). This action, in combination with the elevation of the caster wheels, is used to measure the curb height. Then, the front casters will elevate to 8 inches in height (**Fig. 6-5-2**). If the height is not reached, the rear casters will rise as well to move to the desired height. Then, the front casters will move down once placed on the curb (**Fig. 6-5-3**). This action will suspend the driving wheels in the air. Next, the driving wheels will move back until they make contact with the ground and then drive forward (**Fig. 6-5-4**). The purpose of this action is to place the wheelchair base on the curb in order to move the driving wheels onto the curb as well. When the front casters are positioned on the curb, caster brakes are applied to prevent the wheelchair from rolling backwards. Next, the rear casters will be pushed down using the pneumatic system and the driving wheel will be raised up, leaving the driving

wheel suspended in the air (**Fig. 6-5-5**). The driving wheel carriage will be moved forward until the driving wheels are on top of the curb (**Fig. 6-5-6**). The driving wheels will then be pushed down until contact is made with the curb. Then, the driving wheel carriage will be moved back until the wheelchair base is completely on the curb (**Fig. 6-5-7**). Once the driving wheels and front casters are on the top of the curb, the driving wheels will be lowered down to move the rear casters onto the curb (**Fig. 6-5-8**). Finally, the wheelchair will drive automatically until all wheels are making contact with the new surface of the curb (**Fig. 6-5-9**).

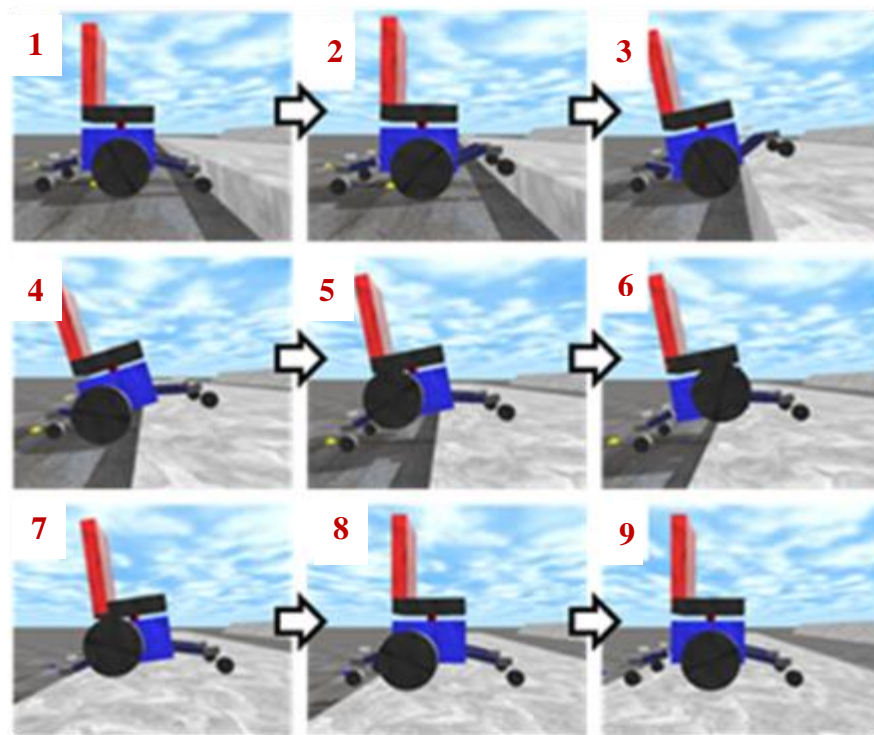


Figure 6-5: PerMMA Gen II step climbing sequences

6.3 MOBILE BASE CONTROL SYSTEM

6.3.1 Sensor system

Operating the PerMMA Gen II requires a fairly complex sensorial system. There are six pressure sensors: four in the front and back caster arm actuators to detect the instant at which the casters touch the step to either remind the user or to automatically switch the mode from ADM to ACM, and two in the gas springs of the driving wheels to detect whether the driving wheels are touching the ground. To measure the positions of the different actuated degrees of freedom, there are seven encoders - two in the front caster arms, two in the rear caster arms, two in the up-down racks of the driving wheels, and one in the fore-aft rack of the driving wheels. There is also an inertia sensor on the frame to measure the laterality and verticality of the chair and to detect the instant when the chair is driving on a cross slope for implementation of the auto posture compensation control. Finally, there are four switches (two per side) to indicate the maximum and minimum positions for the driving wheels horizontally along the rack.

6.3.2 Actuator system

The movement of the PerMMA Gen II mobile base is powered by two driving wheels with a built-in hub motor. The PW-12H wheelchair hub motor (brush/gear) is used for its low cost, compact size, linear power, and mechanic-electrical characteristics (24 V, 180w-300w, maximum torque 23.82 Nm, 7.2Kgs). The fore-aft movement of the two driving wheels is powered by a liner actuator taken from a Permobil seat elevator (Part number: 308730). The liner

actuator and the hub motor are powered by a 50A8DD Advance Motion Control PWM servo amplifier rated for 25 amps continuous and 50 amps for 2 seconds and accept a 20-28 volt input. The up-down movement of two driving wheels is powered by two Thin-Sleeve Style adjustable air-powered springs (usable stroke: 4.4", 8" extended height, 3.25" maximum outside diameter, maximum force when fully extended: 110lbs, maximum force when fully compressed: 360lbs). The movement of the four caster arm cylinders is powered by pneumatic cylinders (Clippard miniature Stainless Steel Universal Double Acting Rotating Rod pneumatic cylinder with 2" Bore, and 4" stroke). Finally, the 5 port solenoid valve and a single base manifold are used to pump the air for the cylinders and air springs.

6.3.3 Mathematical model of PerMMA Gen II

PerMMA Gen II is designed to face different situations within both structured and unstructured environments: driving on flat, inclined or undulating ground, driving on uneven terrain, climbing stairs, or driving over obstacles. The kinematic relations are necessary to identify each kind of motion. These equations take place from the description of the mechanical system and as shown

in **Figure 6-6**. Where, driving wheel position: $x_d = \begin{Bmatrix} x_d \\ y_d \end{Bmatrix}$, front caster position: $x_f =$

$$\begin{Bmatrix} l_1 + l_f \cos \theta_f \\ l_f \sin \theta_f \end{Bmatrix}$$

Rear caster position: $x_r = \begin{Bmatrix} -(l_2 + l_r \cos \theta_r) \\ l_r \sin \theta_r \end{Bmatrix}$, center of gravity position: $x_{cg} = \begin{Bmatrix} x_{cg} \\ y_{cg} \end{Bmatrix}$

Wheelchair base tilt angle: θ_0

$$\text{Total force: } R_d + R_r + R_f - \frac{W}{2} = 0$$

$$\text{Reaction forces: } R_d = \begin{Bmatrix} R_d \sin \theta_0 \\ R_d \cos \theta_0 \end{Bmatrix}, R_r = \begin{Bmatrix} R_r \sin \theta_0 \\ R_r \cos \theta_0 \end{Bmatrix}, R_f = \begin{Bmatrix} R_f \sin \theta_0 \\ R_f \cos \theta_0 \end{Bmatrix}$$

$$\text{Total torque: } R_d \cdot x_d + R_r \cdot x_r + R_f \cdot x_f - \frac{W}{2} \cdot x_{cg} + \tau_d + \tau_r + \tau_f = 0$$

Where τ_d , τ_f , and τ_r are the torques applied on the driving wheel and front and rear casters.

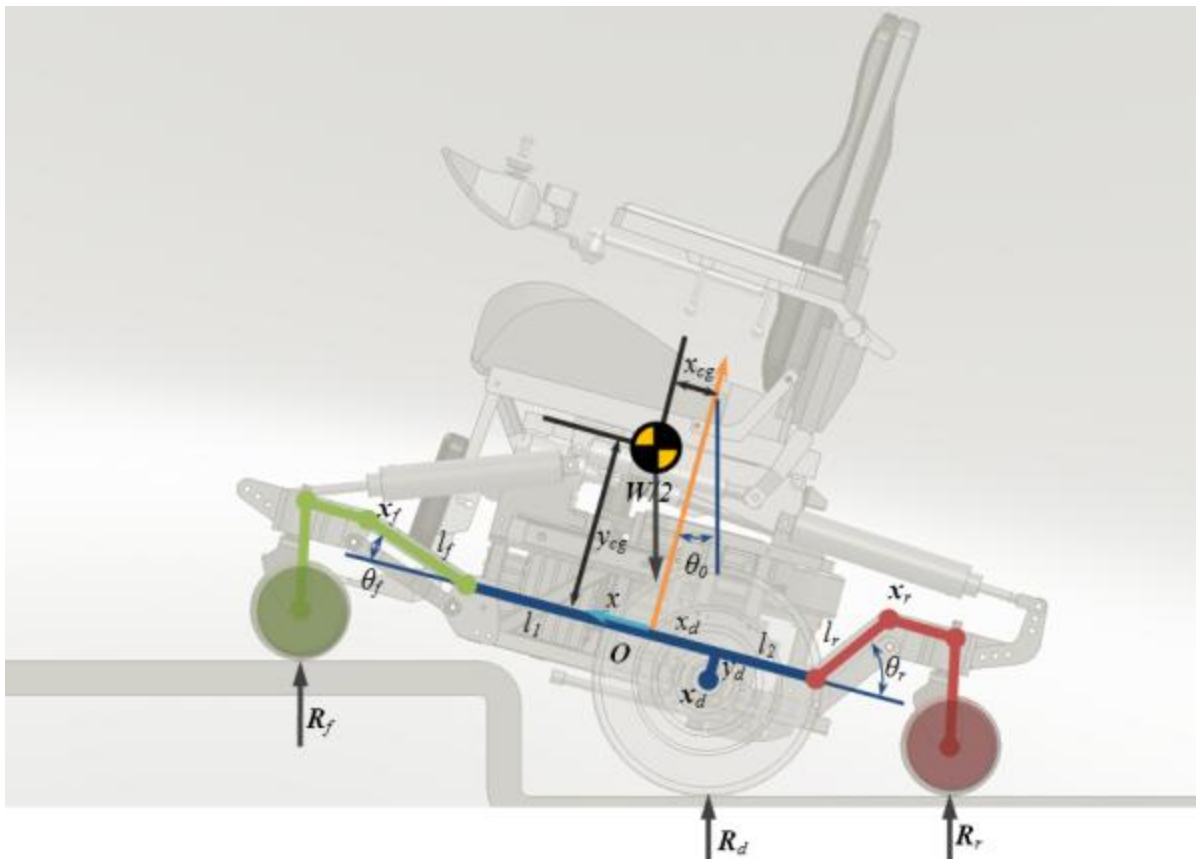


Figure 6-6 Mathematical model of PerMMA Gen II mobile base

Based on the mathematical model, Euler method is applied for dynamic of the system. Two assumptions are made before the dynamic function: first, assume relative small velocity of

the system, the centrifugal force and Coriolis Effect are ignored. Therefore the inverse dynamics model can be expressed as

$$\begin{aligned}
\tau_{dl} &= f_{11}\ddot{\theta}_{dl} + f_{12}\ddot{\theta}_{dr} + f_{13}\ddot{\theta}_{fl} + f_{14}\ddot{\theta}_{fr} + f_{15}\ddot{\theta}_{rl} + f_{16}\ddot{\theta}_{rr} + f_{17}\ddot{P}_h + f_{18}\ddot{P}_{vl} + f_{19}\ddot{P}_{vr} + f_{110}\ddot{\theta}_0 + g_1 \\
\tau_{dr} &= f_{21}\ddot{\theta}_{dl} + f_{22}\ddot{\theta}_{dr} + f_{23}\ddot{\theta}_{fl} + f_{24}\ddot{\theta}_{fr} + f_{25}\ddot{\theta}_{rl} + f_{26}\ddot{\theta}_{rr} + f_{27}\ddot{P}_h + f_{28}\ddot{P}_{vl} + f_{29}\ddot{P}_{vr} + f_{210}\ddot{\theta}_0 + g_2 \\
\tau_{fl} &= f_{31}\ddot{\theta}_{dl} + f_{32}\ddot{\theta}_{dr} + f_{33}\ddot{\theta}_{fl} + f_{34}\ddot{\theta}_{fr} + f_{35}\ddot{\theta}_{rl} + f_{36}\ddot{\theta}_{rr} + f_{37}\ddot{P}_h + f_{38}\ddot{P}_{vl} + f_{39}\ddot{P}_{vr} + f_{310}\ddot{\theta}_0 + g_3 \\
\tau_{fr} &= f_{41}\ddot{\theta}_{dl} + f_{42}\ddot{\theta}_{dr} + f_{43}\ddot{\theta}_{fl} + f_{44}\ddot{\theta}_{fr} + f_{45}\ddot{\theta}_{rl} + f_{46}\ddot{\theta}_{rr} + f_{47}\ddot{P}_h + f_{48}\ddot{P}_{vl} + f_{49}\ddot{P}_{vr} + f_{410}\ddot{\theta}_0 + g_4 \\
\tau_{rl} &= f_{51}\ddot{\theta}_{dl} + f_{52}\ddot{\theta}_{dr} + f_{53}\ddot{\theta}_{fl} + f_{54}\ddot{\theta}_{fr} + f_{55}\ddot{\theta}_{rl} + f_{56}\ddot{\theta}_{rr} + f_{57}\ddot{P}_h + f_{58}\ddot{P}_{vl} + f_{59}\ddot{P}_{vr} + f_{510}\ddot{\theta}_0 + g_5 \\
\tau_{rr} &= f_{61}\ddot{\theta}_{dl} + f_{62}\ddot{\theta}_{dr} + f_{63}\ddot{\theta}_{fl} + f_{64}\ddot{\theta}_{fr} + f_{65}\ddot{\theta}_{rl} + f_{66}\ddot{\theta}_{rr} + f_{67}\ddot{P}_h + f_{68}\ddot{P}_{vl} + f_{69}\ddot{P}_{vr} + f_{610}\ddot{\theta}_0 + g_6 \\
F_{ph} &= f_{71}\ddot{\theta}_{dl} + f_{72}\ddot{\theta}_{dr} + f_{73}\ddot{\theta}_{fl} + f_{74}\ddot{\theta}_{fr} + f_{75}\ddot{\theta}_{rl} + f_{76}\ddot{\theta}_{rr} + f_{77}\ddot{P}_h + f_{78}\ddot{P}_{vl} + f_{79}\ddot{P}_{vr} + f_{710}\ddot{\theta}_0 + g_7 \\
F_{pvl} &= f_{81}\ddot{\theta}_{dl} + f_{82}\ddot{\theta}_{dr} + f_{83}\ddot{\theta}_{fl} + f_{84}\ddot{\theta}_{fr} + f_{85}\ddot{\theta}_{rl} + f_{86}\ddot{\theta}_{rr} + f_{87}\ddot{P}_h + f_{88}\ddot{P}_{vl} + f_{89}\ddot{P}_{vr} + f_{810}\ddot{\theta}_0 + g_8 \\
F_{pvr} &= f_{91}\ddot{\theta}_{dl} + f_{92}\ddot{\theta}_{dr} + f_{93}\ddot{\theta}_{fl} + f_{94}\ddot{\theta}_{fr} + f_{95}\ddot{\theta}_{rl} + f_{96}\ddot{\theta}_{rr} + f_{97}\ddot{P}_h + f_{98}\ddot{P}_{vl} + f_{99}\ddot{P}_{vr} + f_{910}\ddot{\theta}_0 + g_9 \\
\tau_0 &= f_{101}\ddot{\theta}_{dl} + f_{102}\ddot{\theta}_{dr} + f_{103}\ddot{\theta}_{fl} + f_{104}\ddot{\theta}_{fr} + f_{105}\ddot{\theta}_{rl} + f_{106}\ddot{\theta}_{rr} + f_{107}\ddot{P}_h + f_{108}\ddot{P}_{vl} + f_{109}\ddot{P}_{vr} \\
&\quad + f_{1010}\ddot{\theta}_0 + g_{10}
\end{aligned}$$

Where τ_{dl} , τ_{dr} are the torques applied on the left and right driving wheels; τ_{fl} , τ_{fr} , τ_{rl} , τ_{rr} are the torques on the left and right side of the front and rear caster arms. F_{ph} is the horizontal force applied on the horizontal movement of driving wheel axis. F_{pvl} , F_{pvr} are the vertical forces applied on driving wheels axis. τ_0 is the torque acting on the passenger body posture. Moreover, f and g are the functions of all the variables as follows:

$$f_{ij} = f_{ij}(\theta_{dl}, \theta_{dr}, \theta_{fl}, \theta_{fr}, \theta_{rl}, \theta_{rr}, \theta_0, P_h, P_{vl}, P_{vr})$$

$$g_{ij} = g_{ij}(\theta_{dl}, \theta_{dr}, \theta_{fl}, \theta_{fr}, \theta_{rl}, \theta_{rr}, \theta_0, P_h, P_{vl}, P_{vr})$$

6.3.4 Control Development

If the body is kept nearly upright, $\sin \theta_0 \approx \theta_0$, $\cos \theta_0 \approx 1$. The dynamic model could be further linearized based on the assumptions to below state equation

$$\frac{d}{dt}X = AX + Bu$$

Where

$$X = \left[\underbrace{\int \theta_0 dt \quad \dot{\theta}_0}_{\text{Posture angle}} \quad \underbrace{\int P_{vl} dt \quad \int P_{vr} dt \quad P_{vl} \quad P_{vr} \quad \dot{P}_{vl} \quad \dot{P}_{vr} \quad \Delta P_h \quad \Delta \dot{P}_h}_{\text{Vertical move}} \quad \underbrace{\theta_{fl} \quad \theta_{fr} \quad \theta_{rl} \quad \theta_{rr}}_{\text{Caster arm angle}} \quad \underbrace{\dot{\theta}_{dl} \quad \dot{\theta}_{dr}}_{\text{Driving wheel speed}} \right]^T$$

$$u = [\tau_{dl} + g_1' \quad \tau_{dr} + g_2' \quad \tau_{fl} + g_3' \quad \tau_{fr} + g_4' \quad \tau_{rl} + g_5' \quad \tau_{rr} + g_6' \quad F_{ph} + g_7' \quad F_{pvl} + g_8' \quad F_{pvr} + g_9']^T$$

$g_1' \sim g_9'$ are mainly consists of gravity which are not dependent on state variables. More detailed information about A, B and $g_1' \sim g_9'$ are omitted due to space limitations.

Represented by a controllable system, because it is also observable state variables, this can be stabilized by state feedback. In this case, the control law is represented by the following equation.

$$u = K(X_{ref} - X)$$

Where

$$X_{ref} = [0 \quad 0 \quad 0 \quad 0 \quad P_{vlref} \quad P_{vrref} \quad \dot{P}_{vlref} \quad \dot{P}_{vrref} \quad \Delta P_h \quad 0 \quad \theta_{flref} \quad \theta_{frref} \quad \theta_{rlref} \quad \theta_{rrref} \quad \dot{\theta}_{dlref} \quad \dot{\theta}_{drref}]^T$$

K is the state feedback gain matrix, derived by PID theory. When the PerMMA II drives in the acceleration/deceleration state, horizontal movement of the driving wheels can compensate

for the passenger's posture (**Fig. 6-7-a**). When the PerMMA II climbs the stairs, it uses the front and rear caster arm and the vertical and the horizontal movement of driving wheels simultaneously (**Fig. 6-7-b**). When the PerMMA II drives on an up-down slope, caster arm movement up and down can compensate for the passenger's posture (**Fig. 6-7-c**). The passenger's posture can keep the same as the horizontal state with respect to the inclination driving on cross slope by using the vertical movement of the driving wheel axis (**Fig. 6-7-d**).

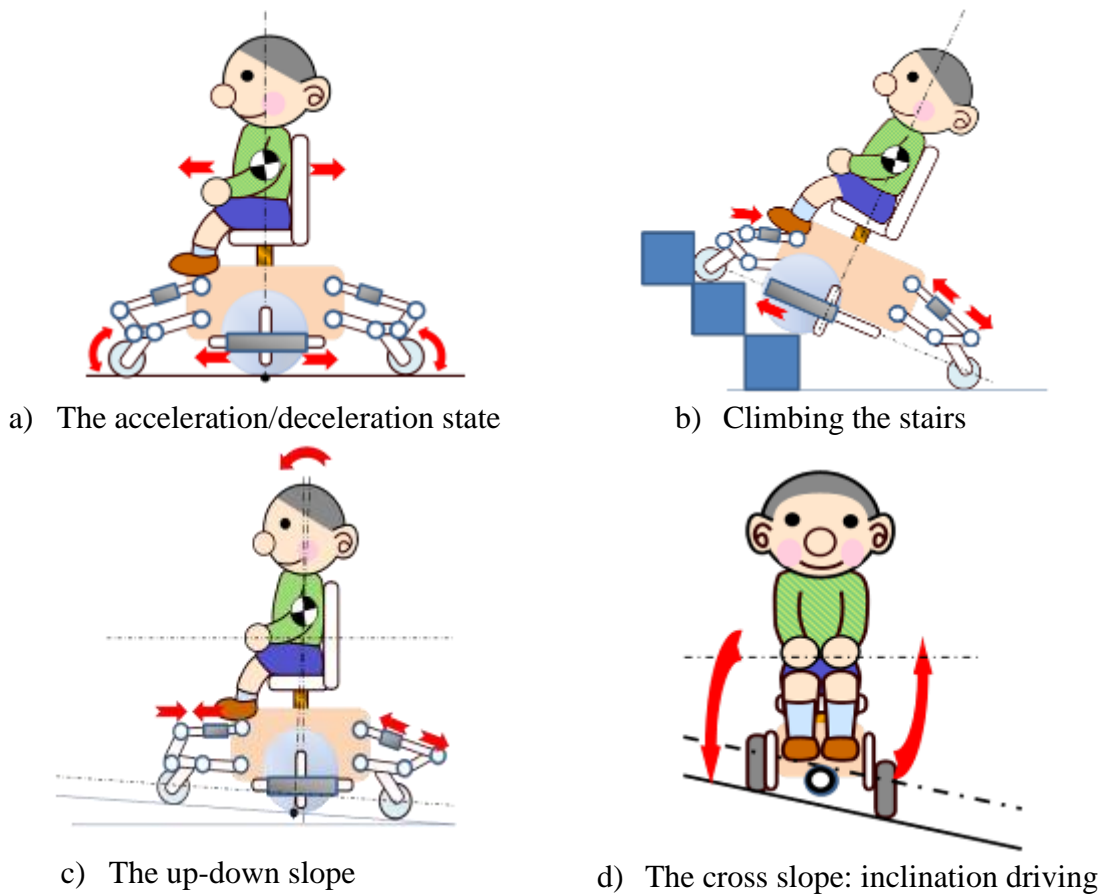


Figure 6-7: PerMMA Gen II control states

In addition, $\dot{\theta}_0$ is measured using the pitch-axis gyroscope of the attached inertia sensor. Thus θ_0 is estimated from the accelerometer and the integrated value of the pitch-axis gyroscope. The posture control for PerMMA Gen II consists of the feed-forward compensator and the feedback compensator. The feedback controller is used for regulating the state deviation between the desired state X_{ref} and the actual state X of the wheelchair. The feedback gain K is determined by using the PID control theory [136]. The feed-forward controller is used for regulating the influence element of gravity with respect to the posture of PerMMA II. The control system block diagram is shown in **Figure 6-8**.

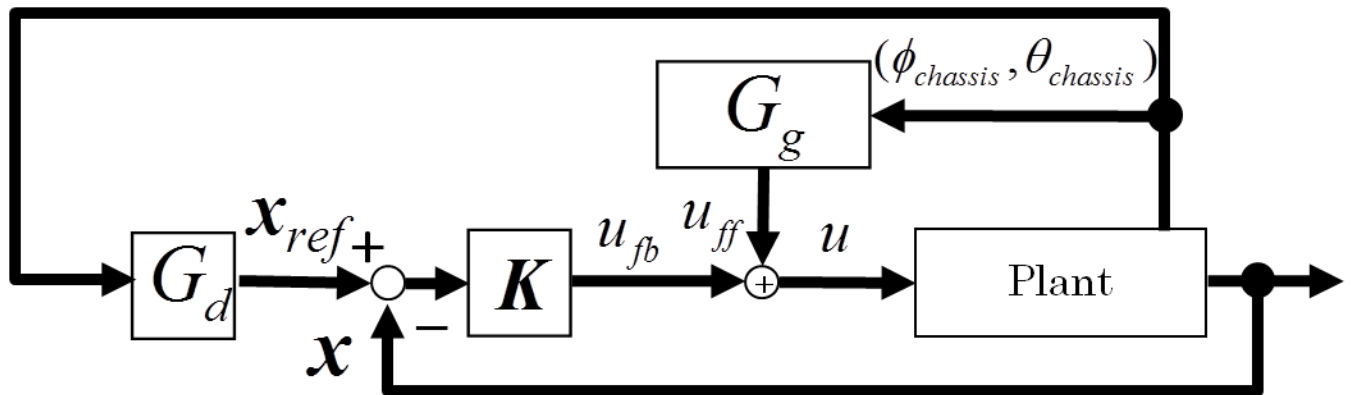


Figure 6-8: Block diagram of the state feedback feed-forward controller

6.4 SIMULATIONS AND RESULTS

A working prototype of PerMMA Gen II has been built as shown in **Figure 6-1**. The kinematic information about PerMMA II is:

- PerMMA Gen II is 200lbs, has a 14” driving wheel tire diameter, and has a maximum speed of 6 miles per hour. The dimensions are listed in **Table 6-1**.

Table 6-1: Wheelchair dimension comparison

Wheelchair Model	Base Length	Overall Width
Permobil C500	49.5”	25.5”
PerMMA2	40”	26”
Invacare TDX	35.25”	25.5”
Overall RESNA dimensions	47.24”	27.56”

- PerMMA Gen II has two driving wheels, two front caster arms, two rear caster arms, and four caster wheels.
- PerMMA Gen II has 5 degrees of freedom: the longitudinal, the vertical, the yaw, the pitch and roll motion. Each caster and driving wheel has 3 degree of freedom.
- To measure posture, PerMMA Gen II includes a 3axes gyro sensor and a 3axes accelerate sensor.

To confirm the effectiveness of the control law obtained in the previous section and the stability performance by using the proposed controller, a simulation in the Open Dynamics Engine (ODE) was conducted [137]. **Figure 6-9** shows a three-dimensional model-based simulation of the behavior of the PerMMA Gen II test unit represented by rigid drawing.

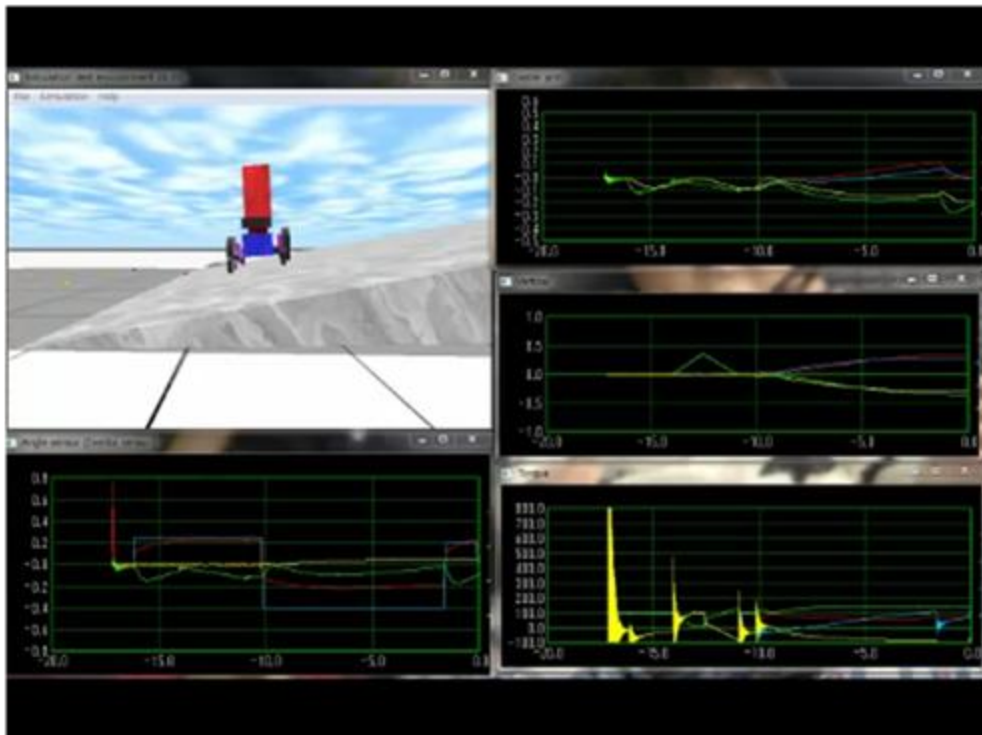
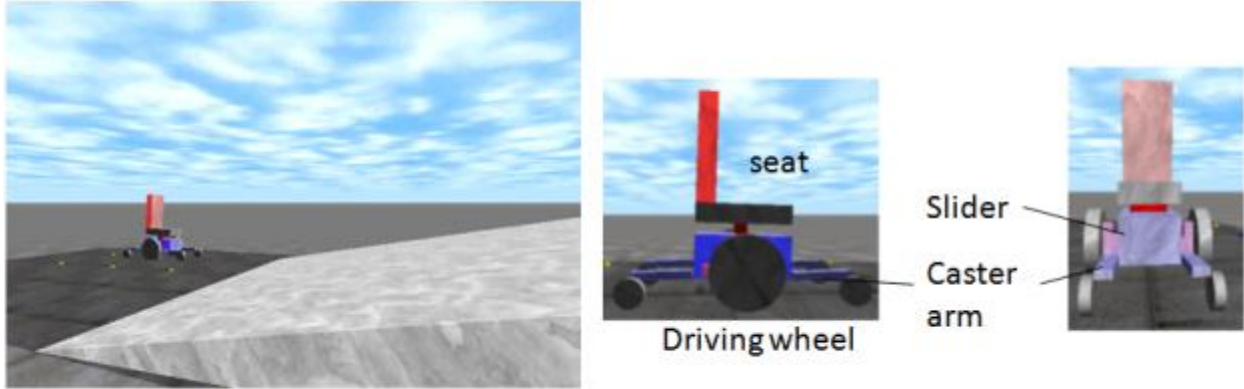


Figure 6-9: 3-D simulation environment of PerMMA Gen II on a slope using ODE

In the test simulation of stability performance with the developed control law, the wheelchair was driven with the maximum speed of 1.38 m/s. The wheelchair was driven straight. Then the vehicle entered a gap of 5cm. After overcoming a step to reach the target speed, the target speed was changed to 0 m/s for simulating sudden braking. For the slope driving simulation, the slope angle was set to 10 degrees with maximum speed of 1.38m/s.



Slope Angle: 10deg;Maximum Speed: 5km/h

Figure 6-10: Simulation setup for PerMMA Gen II posture control

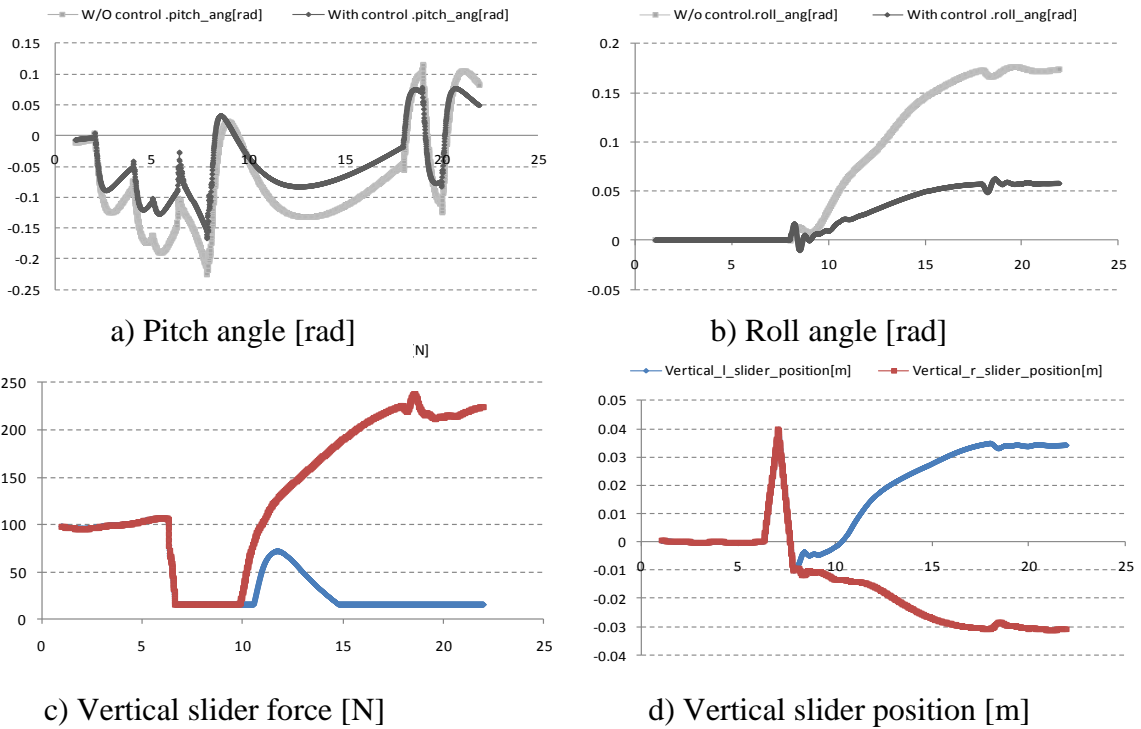


Figure 6-11: Simulation results for PerMMA Gen II posture control

Figure 6-10 shows how PerMMA Gen II performed during the simulation. **Figure 6-11** shows the change in the behavior of each joint.

Simulation results show that with the controller applied, there is less pitch and roll motion than by controlling the vertical driving wheel position and the caster arms simultaneously without the control (**Figure 6-11 a, b**). The dark line represents the result with the control applied and the light line represents angles without control. There is less deviation for the pitch angle with the control applied than without the control. When the wheelchair is driven on a slope, the roll angle is within 3 degrees with the control applied, while without the control the roll angle is more than 8 degrees. Concerning the vertical forces applied on the left (blue) and right (red) driving wheels (**Fig. 6-11-c**), different forces are applied to change the vertical position of the left and right driving wheels (**Fig. 6-11-d**) to react to the slope the wheelchair is driven on. From the simulation results, the controller successfully keeps the posture.

6.5 SUMMARIES

The PerMMA Gen II mobile base prototype has dimensions comparable to current commercially available power wheelchairs, within the range of RESNA/ANSI wheelchair standard [37, 38]. After finishing the integration of caster wheel brakes, more tests will be performed on the PerMMA Gen II mobile base based on the standards, such as turning radius, static and dynamic stabilities (Section 8 of the durability test will not be performed). Due to the adjustable caster and position of the driving wheels, the overall test results – especially stability - are expected to be better than most of the other power wheelchairs. Since PerMMA Gen II can drive underneath regular 26-inch high office desks, this may lead to more working opportunities for power wheelchair users and reduce the costs of rebuilding the working environment.

PerMMA Gen II's climbing sequence models can be applied to any curb height of 8 inches or less. This is important as standard curb height is 8 inches, but curb height tends to decrease due to deterioration. Multiple interfaces for users to switch between different driving modes will be used, since users may have different capabilities and preferences for changing the mode, either by themselves or by the controller.

The ODE software and the Single Board Computer of the PerMMA Gen II wheelchair use the same programming language, C/C++, which makes the algorithm transition to the wheelchair controller simpler. The ODE simulation results demonstrate the effectiveness of the posture control algorithm. However, the control gain K is decided by trials and errors which could be improved by applying the linear quadratic regulator (LQR) method which was used to improve the stability of a two-leg-wheeled inverted-pendulum-type vehicle equipped with a slider [138]. Since PerMMA Gen II was built from scratch, a very good model of the system is available, and because of PerMMA Gen II's advanced sensory system, all of the states are available for feedback and stability will be guaranteed when using LQR. In addition, the controller is automatically generated by simply selecting a couple of parameters (no need to do loop-shaping).

In addition, with independently controlled casters and driving wheels for PerMMA Gen II, the left and right side height of the wheelchair could be adjustable independently therefore lateral pressure relief could be performed to prevent pressure ulcers and increase the comfort of the wheelchair users. Seeking lateral support is one of many strategies in normal sitting behavior that users may develop to cope with (long-time) sitting. The efficiency of lateral support is closely related to the (lateral) support surface built in the backrest. Even minor lateral adjustments can have positive effects on function, weight distribution and mealtime management

[139]. And raising comfort level [140]. There are also examples of case studies showing that lateral tilt-in-space has applications in difficult seating problems in the areas of gastric emptying, pressure relief, hip pain relief, head and trunk balance, oral secretion control, progression of scoliosis, need for repositioning, posture induced tone, and sitting tolerance [141]. But active lateral tilt in wheelchairs is, however, seldom used. One possible reason for the rare usage of lateral tilt in wheelchairs is the lack of available lateral tilt capabilities for wheelchairs or seating systems currently on the market. PerMMA Gen II could provide up to 10 degrees of dual lateral tilt. More evaluations of the lateral tilt function of PerMMA Gen II regarding to pressure relief will be conducted.

A future goal is to evaluate the control simulation of the step climbing sequence by applying it to PerMMA Gen II. A secondary goal is to be able to climb up to three steps; however, this will require some modification to the current wheelchair. The ability of lifting up/down each wheel independently allows PerMMA Gen II to perform other applications such as lateral pressure relief and automatic seat leveling while driving over uneven surfaces. These applications can be performed manually with the use of switches; however, more work is in progress to perform these applications automatically. The features of PerMMA Gen II will be used in combination with another project that recognizes different terrains and change acceleration and velocity according to these terrains [142]. The safety of the user is the highest priority during the development and simulation of the step climbing.

7.0 RECOMMENDATIONS FOR FUTURE WORK

Electric powered wheelchairs (EPWs) have gained increasing popularity among people with disabilities as well as with aged populations because they provide functional mobility, the ability to participate in activities, and better health and improved quality of life for people with lower and upper extremity impairment. They are becoming increasingly important as more users – such as those with progressive conditions, with high levels of impairment, and with aging-related loss of physical strength and functional ability – transition from manual mobility to power mobility. . Great advances have been made in the past years on the design, control, and user interfaces of EPWs. Examples of this are many EPWs now come with power seating functions to provide users with enhanced posture support and comfort; EPWs often include multiple control inputs based on users’ requirements; and much research has been done on navigation, obstacle avoidance, and advanced control interfaces such as voice control, eye control and brain control (using a brain-computer interface). However, EPW users are still experiencing difficulty maneuvering on various terrains, such as curbs, side slope, dirt, gravel, snow and sand. EPWs lack functions such as robust motion control, traction control, and anti-tipping control which are available for automobiles but not for EPWs. In addition, for EPW, there is no standard in the field of wheelchair-use analysis like the SmartWheel for manual wheelchairs. Although many EPWs come with several drives or profiles, they might not be appropriately used by the service

provider or end-users. Lastly, most off-road or outdoor-use EPWs are not able to be used indoors, which means insurance companies will not reimburse for their use, and therefore users cannot afford them.

For our approaches, we first investigated what the problems were and what had been developed to address the problems. Focus group studies with wheeled mobility device prescription professionals and active EPW users provided us with important information about the problems for both indoor and outdoor EPW usage. User strategies are mostly experience-based and/or just avoiding going out entirely which may cause decreased community participation and quality of life. We then investigated whether the durability of EPW dropped and led to some of the problems. Though we did not find quality changes of EPWs, further rigorous research might need to look at how the durability of EPWs affect users' indoor and outdoor driving activities, since people who use EPWs reported significantly more repairs and adverse consequences compared with manual wheelchair users.

We then worked on development and evaluations of the advanced real-time EPW controller. With the developed controller platform, experimental tests on model-based speed control, real-time slip detection and traction control, and real-time tip-over prevention were conducted. The experimental findings together with the user studies were then combined to develop a terrain-dependent EPW driver assistance system for current EPWs. Driving rules for different terrains were developed based on quantitative feedback of slip ratios, number of direction changes during straight driving and time needed to complete a test. The driving rules were further validated by 10 able-bodied users who provided feedback on safety, comfort and ease of operation, and the results of quantitative variables. For some barriers such as curbs, three or four steps, deep gravel, and slippery grass or snow we were limited by the mechanical design

of current EPWs and were unable to drive through even with the driving rules applied. Therefore in the last part of our studies, a new mobile base for PerMMA Gen II with position-able driving and caster wheels were developed. With this new feature, PerMMA Gen II is able to climb up to 8” curbs and go through uneven terrains more safely and easily. In addition, it has comparable dimensions to current EPWs for indoor usage, but also allows users to drive underneath regular 26-inch high office desks which may lead to more working opportunities for power wheelchair users and help to reduce the costs of rebuilding the working environment. It also supports lateral tilt, which will reduce the risk of pressure ulcers and increase the quality of life of power wheelchair users.

Our work differs from others’. Firstly, we use a participatory action design method in which end-users, clinicians, and caregivers are all involved during the overall design and development. Secondly, great emphasis has been put on user evaluation. For each of our developments, we not only conduct modeling, simulation and experimental tests, but we also collect users’ feedback in the forms of focus group studies, case studies, and clinical trials. Last but not the least, we investigate the improvement of current EPWs but also develop state-of-the-art products to advance the current EPWs.

Future directions are threefold. First, system synergization: 1) finishing the modification and redesign of the PerMMA Gen II mobile base; integrating the caster brakes into the current system; testing the system with climbing 8” curbs; validating the simulation results of driving on slopes with posture compensation algorithms; designing a testing course with both indoor and outdoor environmental scenarios; implementing and preliminarily testing the stair climbing sequences developed by simulation; integrating the terrain classification and terrain dependent driving rules and conducting subject tests to evaluate the whole system; integrating PerMMA

Gen I and PerMMA Gen II to develop PerMMA Gen III with enhanced manipulation and mobility. 2) Integrating the terrain classification system; implement the terrain dependent EPW driver assistance system on different types of EPWs; conducting EPW user studies on the developed systems.

Second, as we mentioned above, the SmartWheel sets the standard in the field of manual wheelchair use analysis. SmartWheel facilitates justification of the proper wheelchair, optimal set-up, and propulsion training, all of which serves to reduce incidence of pain and injury and improves quality of life for manual wheelchair users. The SmartWheel measures push forces, frequency, length, smoothness, speed, etc. It has multiple sizes available for different manual wheelchairs. EPW prescription, on the other hand, is observation based by clinician-subjective ratings. This approach is lacking of objective, comprehensive assessment batteries to provide clinicians with guidelines when evaluating driving proficiency and safety in EPW use. Although a number of nonstandard checklists are available for evaluating safe driving proficiency and/or identifying the driving skills needed to attain safe proficiency, they do not meet the established requirement of a scientifically sound measurement tool. With our terrain dependent EPW driver assistance system and advanced real-time controller platform, a “SmartWheel” for EPW (SmartBox) that measures the speed, acceleration/deceleration, times, number of direction changes, driving patterns, etc. could be developed. These data could provide baseline information to help clinicians determine or evaluate driving proficiency and/or develop service plans aimed at addressing those skills that need improvement or compensation to ensure driving proficiency. In addition, like the virtual seating coach system, the SmartBox could be used to understand how users use their EPWs and provide valuable feedback to clinicians (and the users themselves) on necessary adjustments of the driving parameters for safe and comfortable driving.

Moreover, the SmartBox is compact (the current controller could mount on several EPWs; we may not need all the sensors and computation power from the advanced real-time controller to further reduce the size and cost), and could be mounted on most EPWs.

Third, for training purpose: new EPW drivers and clinicians refer to the Power-Mobility Community Driving Assessment and The Powered Wheelchair Training Guide tools. However, many incidents stem from a lack of insufficient training. With the SmartBox, focus group studies, and driving rules, an evidence-based training protocol could be developed to provide better training and evaluation of the effects of training. Furthermore, the controller could be used as an education platform for design classes due to its rich interface, its sensor package (as well as available expansions), and its flexible software.

APPENDIX A

Questionnaires of Demographics

Below were the questionnaires of demographics used for the subject test for the driving rules development for Phase 2 of terrain dependent driving

Gender: Male Female **Age:** _____

1. What is your highest level of education?

- No formal education
- Less than high school graduate
- High school graduate/GED
- Vocational training
- Some college/Associate's degree
- Bachelor's degree (BA, BS)
- Master's degree (or other post-graduate training)
- Doctoral degree (PhD, MD, EdD, DDS, JD, etc.)

2. Current marital status (check one)

- Single
- Married

- Separated
- Divorced
- Widowed
- Other (please specify) _____

3. How would you describe your primary racial group?

- No primary group
- White Caucasian
- Black/African American
- Asian
- American Indian/Alaska Native
- Native Hawaiian/Pacific Islander
- Multi-racial
- Other (please specify) _____

4. Is English your primary language?

- Yes
- No

4a. If “No”, what is your primary language? _____

5. What is your primary occupational status? (Check one)

- Work full-time
- Work part-time
- Student
- Homemaker
- Retired

- Volunteer worker
- Seeking employment, laid off, etc
- Other (please specify) _____

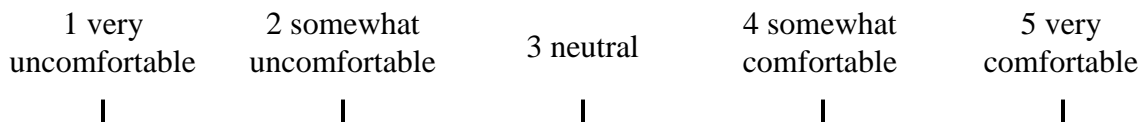
APPENDIX B

Self-Scoring Sheet

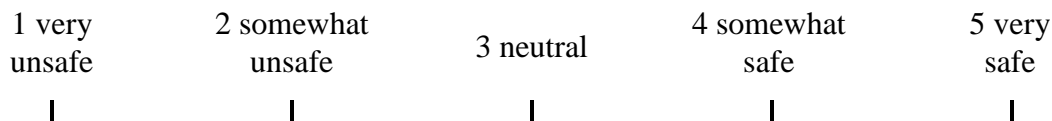
Below was the self-scoring sheet used for collecting the data when users driving one different terrains about their feelings including comfort level, how safe they are feeling and how easy and difficult about operating the EPW.

___ Setting 1

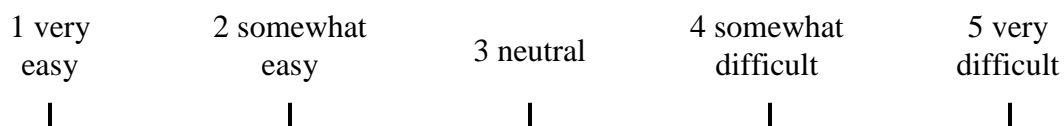
Please rate your **comfort** level regarding **this** driving task:



Please rate how **safe** you feel regarding **this** driving task:

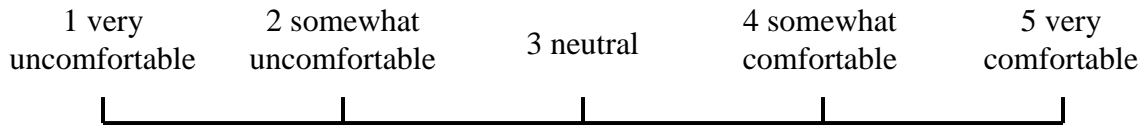


Please rate how **easy or difficult** on operating the wheelchair regarding **this** driving task:

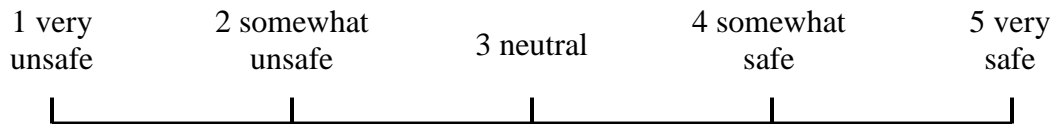


___ **Setting 2**

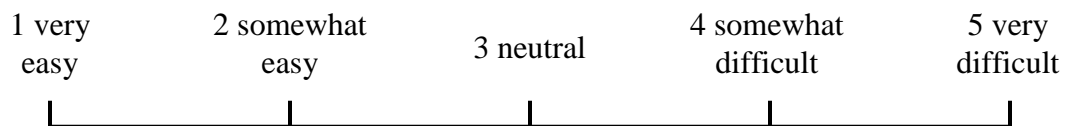
Please rate your **comfort** level regarding **this** driving task:



Please rate how **safe** you feel regarding **this** driving task:

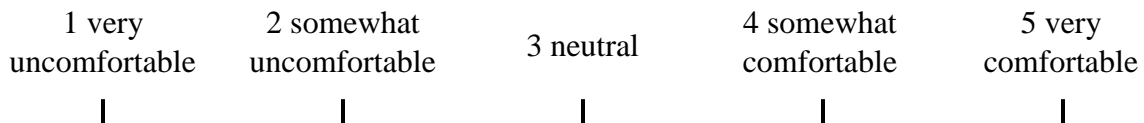


Please rate how **easy or difficult** on operating the wheelchair regarding **this** driving task:

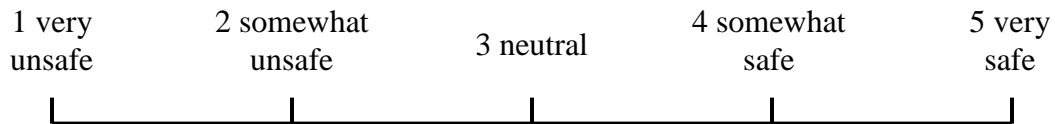


___ **Setting 3**

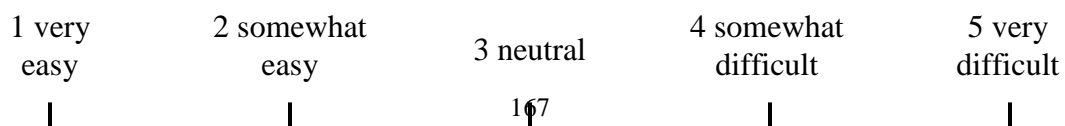
Please rate your **comfort** level regarding **this** driving task:



Please rate how **safe** you feel regarding **this** driving task:

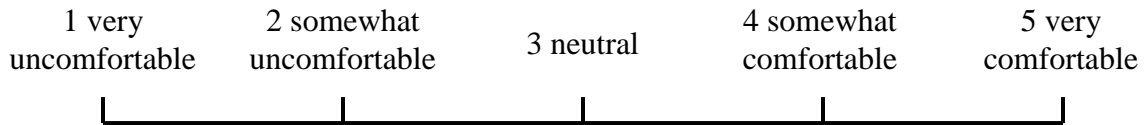


Please rate how **easy or difficult** on operating the wheelchair regarding **this** driving task:

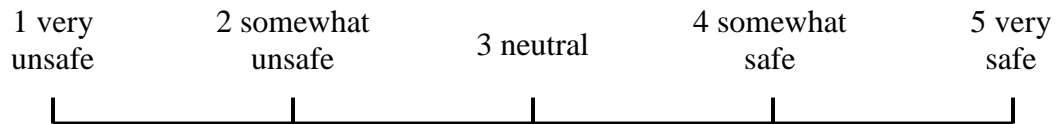


___ **Setting 4**

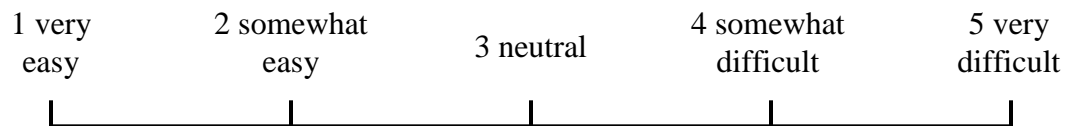
Please rate your **comfort** level regarding **this** driving task:



Please rate how **safe** you feel regarding **this** driving task:



Please rate how **easy or difficult** on operating the wheelchair regarding **this** driving task:



The order of the four driving settings was randomized selected for the user. Both users and investigators who analyze the data were blinded about what setting users were using.

BIBLIOGRAPHY

- [1] Cooper RA, Cooper R, Boninger ML (2008). Trends and issues in wheelchair and seating technologies. *Assistive Technology*, 20(2): 61-72

- [2] 20th Anniversary of Americans with Disabilities Act: July 26. Retrieved from http://www.census.gov/newsroom/releases/archives/facts_for_features_special_editions/cb10-ff13.html

- [3] Goodwin J, Nguyen-Oghalai T, Kuo Y, Ottenbacher K (2007). Epidemiology of Medicare abuse: the example of wheelchairs. *Journal of the American Geriatrics Society*, 55(2): 221-226

- [4] Bottos M, Bolcati C, Sciuto L, Ruggeri C, Feliciangeli A (2001). Powered wheelchairs and independence in young children with tetraplegia. *Developmental Medicine and Child Neurology*, 43(11): 769-777

- [5] Deitz J, Swinth Y, White O (2002). Powered mobility and preschoolers with complex developmental delays. *American Journal of Occupational Therapy*, 56(1): 86-96

- [6] Nilsson LM, Nyberg PJ (2003). Driving to learn: A new concept for training children with profound cognitive disabilities in a powered wheelchair. *American Journal of Occupational Therapy*, 57: 229-233

- [7] Pettersson I, Tornquist K, Ahlstrom G (2006). The effect of an outdoor powered wheelchair on activity and participation in users with stroke. *Disability and Rehabilitation: Assistive Technology* 1(4): 235-243

- [8] Pettersson I, Ahlstrom G, Tornquist K (2007). The value of an outdoor powered wheelchair with regard to the quality of life of persons with stroke: A follow-up study. *Assistive Technology*, 19(3):143-153
- [9] Evans S, Neophytou C, De Souza L, Frank A O (2007). Young people's experiences using electric powered indoor - outdoor wheelchairs (EPIOCs): potential for enhancing users' development. *Disability and rehabilitation*, 29(16): 1281-1294
- [10] Evans S, Frank AO, Neophytou C, De Souza L (2007). Older adults' use of and satisfaction with Electric Powered Indoor/outdoor Wheelchairs (EPIOCs). Oxford University Press, 36(4):431-435
- [11] Tan YK, Sasidhar S (2009). Engineering Better Electric-Powered Wheelchairs To Enhance Rehabilitative and Assistive Needs of Disabled and Aged Populations. *Rehabilitation Engineering*, Tan Yen Kheng (Ed.), ISBN: 978-953-307-023-0, INTECH, Available from: <http://sciyo.com/articles/show/title/engineering-better-electric-powered-wheelchairs-to-enhance-rehabilitative-and-assistive-needs-of-dis>
- [12] Nitz JC (2008). Evidence from a cohort of able bodied adults to support the need for driver training for motorized scooters before community participation. *Patient Education and Counseling*, 70(2): 276-80
- [13] Nilsson L, Eklund M (2006). Driving to Learn: Powered wheelchair training for those with cognitive disabilities. *International Journal of Therapy and Rehabilitation*, 11(13): 517- 527
- [14] Cooper RA (1995). Intelligent control of power wheelchairs. *IEEE Engineering in Medicine and Biology Magazine*, 15(4): 423-431
- [15] Ding D, Cooper RA, Guo S, Corfman TA (2004). Analysis of Driving Backwards in an Electric-Powered Wheelchair. *IEEE Transactions on Control Systems Technology*, 12(6): 934-943
- [16] Kirby RL, Ackroyd-Stolarz SA (1995). Wheelchair safety--adverse reports to the United States Food and Drug Administration. *American Journal of Physical Medicine & Rehabilitation*, 74(4): 308-312

- [17] Xiang H, Chany AM, Smith GA (2006). Wheelchair related injuries treated in US emergency departments. *Injury Prevention*, 12(1): 8-11
- [18] Van Drongelen A, Roszek B, Hilbers-Modderman E, Kallewaard M, Wassenaar C (2002). Wheelchair incidents. RIVM, Bilthoven
- [19] Power Wheelchairs and User Safety (2003) by the National Institute for Rehabilitation Engineering. Retrieved from: <http://www.agis.com/Document/492/power-wheelchairs-and-user-safety.aspx>
- [20] Brose S, Weber D, Salatin B, Grindle GG, Wang H, Vazquez JJ, Cooper RA (2010). The Role of Assistive Robotics in the Lives of Persons with a Disability. *American Journal of Physical Medicine and Rehabilitation*, 89(6): 509-521
- [21] Simpson RC (2005). Smart Wheelchairs: A Literature Review. *Journal of Rehabilitation Research and Development*, 42(4): 423-436
- [22] Simpson RC, LoPresti E, Cooper RA (2008). How Many People Would Benefit From a Smart Wheelchair? *Journal of Rehabilitation Research and Development*, 45(1): 53-72
- [23] TAO-7 Intelligent Wheelchair Base for the Development of Autonomous Wheelchair (2008). Retrieved from: http://www.aai.ca/robots/tao_7.html
- [24] CALL Center Smart Wheelchair. Retrieved from: <http://www.smilerehab.com/index.php>
- [25] TopChair. Retrieved from http://www.topchair.fr/en/index_en.php
- [26] Wiart L, Darrah J, Hollis V, Cook, L, May L (2004). Mothers' perceptions of their children's use of powered mobility. *Physical and Occupational Therapy in Pediatrics*, 24(4): 3-21.
- [27] McGarry S, Girdler S (2011). Powered mobility as an intervention for children with cerebral palsy: A systematic review. *Disability And Rehabilitation: Assistive Technology* (under review)

- [28] Erren-Wolters CV, van Dijk HA, de Kort AC, IJzerman MJ, Jannink MJ (2007). Virtual reality for mobility devices: training applications and clinical results: a review. *International Journal of Rehabilitation Research*, 30(2): 91–96
- [29] Montesano L, Diaz M, Bhaskar S, Minguez J (2010). Towards an Intelligent Wheelchair System for Users with Cerebral Palsy. *IEEE Transactions on Neural Systems and Rehabilitation Engineering*, 18(2): 193-202
- [30] Trahanias P, Lourakis M, Argyros S, Orphanoudakis S (1997). Navigational support for robotic wheelchair platforms: an approach that combines vision and range sensors. *International Conference on Robotics and Automation*, Vol. 2: 1265-1270
- [31] Nakanishi S, Kuno Y, Shimada N, Shirai Y (1999). Robotic Wheelchair Based on Observations of Both User and Environment. *Proceedings of the 1999 IEEE/RSJ International Conference on Intelligent Robots and Systems*, Vol. 2: 912-917
- [32] Salatin B (2010). Electrical powered wheelchair driving outdoors: user needs evaluation and the development of an advanced controller. Master thesis, University of Pittsburgh
- [33] Tolerico ML, Ding D, Cooper RA, Spaeth DM, Fitzgerald SG, Cooper R, Kelleher A, Boninger ML (2007). Assessing the Mobility Characteristics and Activity Levels of Manual Wheelchair Users. *Journal of Rehabilitation Research and Development*, 44 (4): 561-572
- [34] Xiang H, Chany AM, Smith GA (2006). Wheelchair related injuries treated in US emergency departments. *Injury Prevention*, 12(1): 8-11
- [35] Cooper RA, Cooper R, Boninger ML (2008). Trends and issues in wheelchair and seating technologies. *Assistive Technology*, 20(2): 61-72
- [36] Fitzgerald SG, Collins DM, Cooper RA, Tolerico ML, Kelleher A, Hunt P, Martin S, Impink B, Cooper R (2005). Issues in maintenance and repairs of wheelchairs: A pilot study. *Journal of Rehabilitation Research and Development*, 42:853–862

- [37] ANSI/RESNA (1998). American National Standard for Wheelchairs-- Volume 2: Additional Requirements for Wheelchairs (Including Scooters) With Electrical Systems. Virginia: Rehabilitation Engineering and Assistive Technology Society of North America; 1998
- [38] ANSI/RESNA (1998). American National Standard for Wheelchairs-- Volume 1: Requirements and Test Methods for Wheelchairs (Including Scooters). Virginia: Rehabilitation Engineering and Assistive Technology Society of North America; 1998
- [39] Fass MV, Cooper RA, Fitzgerald SG, Schmeler M, Boninger ML, Algood SD, Ammer WA, Rentschler AJ, Duncan J (2004). Durability, Value, and Reliability of Selected Electric Powered Wheelchairs. *Archives of Physical Medicine and Rehabilitation*, 85(5):805-814
- [40] Rentschler AJ, Cooper RA, Fitzgerald SG, Boninger ML, Guo S, Ammer WA, Vitek M, Algood D (2004). Evaluation of Selected Electric-Powered Wheelchairs Using the ANSI/RESNA Standards. *Archives of Physical Medicine and Rehabilitation*, 85(4):611-619
- [41] Karmarkar A, Cooper RA, Liu HY, Connor S, Puhlman J (2008). Evaluation of Pushrim-Activated Power Assisted Wheelchairs (PAPAW) Using ANSI/RESNA Standards. *Archives of Physical Medicine and Rehabilitation*, 89(6): 1191-1198
- [42] Cooper, RA, Robertson RN, Lawrence B, Heil T, Albright SJ, VanSickle DP, Gonzalez J (1996). Life-Cycle Analysis of Depot Versus Rehabilitation Manual Wheelchairs. *Journal of Rehabilitation Research and Development*, 33(1):45-55
- [43] Fitzgerald SG, Cooper RA, Boninger ML, Rentschler AJ (2001). Comparison of Fatigue Life for 3 Types of Manual Wheelchairs. *Archives of Physical Medicine and Rehabilitation*, 82(10):1484-1488
- [44] Kwarciak AM, Cooper RA, Ammer WA, Boninger ML, Cooper R (2005). Fatigue Testing of Selected Suspension Manual Wheelchairs Using ANSI/RESNA Standards. *Archives of Physical Medicine and Rehabilitation*, 86(1):123-129
- [45] Liu H, Cooper RA, Pearlman J, Cooper RM, Connor S (2008). Evaluation of Titanium Ultralight Manual Wheelchairs Using ANSI/RESNA Standards, *Journal of Rehabilitation Research and Development*, 45(9): 1251-1268.

- [46] Wright M (2006). Pay Attention To Wheelchair Safety - Things To Look Out For. Retrieved from: <http://ezinearticles.com/?Pay-Attention-To-Wheelchair-Safety---Things-To-Look-Out-For&id=385017>
- [47] Ding D, Cooper RA, Guo S, Corfman TA (2004). Analysis of Driving Backwards in an Electric-Powered Wheelchair. *IEEE Transactions on Control Systems Technology*, 12(6): 934-943
- [48] Ding D, Cooper RA, Guo S, Corfman TA (2003). A study on modeling an electric-powered wheelchair. *RESNA 26th International Annual Conference*
- [49] Ding D, Cooper RA, Guo S, Corfman TA (2003). Robust velocity control simulation of a power wheelchair, *RESNA 26th International Annual Conference*
- [50] Shung JB, Stout G, Tomizuka M, Auslander DM (1983). Dynamic modeling of a wheelchair on a slope. *Journal of Dynamic Systems, Measurement, and Control*, 105(2): 101-106
- [51] Shung JB, Tomizuka M, Auslander DM, Stout G (1983). Feedback control and simulation of a wheelchair. *Journal of Dynamic Systems, Measurement, and Control*, 105(2): 96-100
- [52] Wolf EJ (2006). Evaluation of Electric Powered Wheelchairs and Exposure to Whole-Body Vibration. *Doctoral Dissertation, University of Pittsburgh*
- [53] Friction Factors: Coefficient of frictions. Retrieved from: http://www.roymech.co.uk/Useful_Tables/Tribology/co_of_friect.htm
- [54] Cooper RA (1993). Stability of a wheelchair controlled by a human pilot. *IEEE Transactions on Rehabilitation Engineering*, 1(4):193–206
- [55] Asensio JR, Montano L (2002). A Kinematic and Dynamic Model-Based Motion Controller for Mobile Robots. *15th Triennial World Congress, Barcelona, Spain, 2002*
- [56] Urbano J, Terashima K, Miyoshi T, Kitagawa H (2005). Velocity control of an omni-directional wheelchair considering user's comfort by suppressing vibration.

IEEE/RSJ International Conference on Intelligent Robots and Systems, 2005, pp. 2385 – 2390

- [57] Yoshiyuki M, Kohei K, Ryo S (2003). Vibration Simulation Model of Passenger-Wheelchair System in Wheelchair-Accessible Vehicle. *Journal of Mechanical Design*, 125(4): 779-785

- [58] Ervin SF (2006). *A Course of Practical Physics for Students of Science and Engineering* [online]. Available: <http://books.google.com/>

- [59] Griffiths IW, Watkins J, Sharpe D (2005). Measuring the moment of inertia of the human body by a rotating platform method. *American Journal of Physics*, 73(1): 85-92

- [60] Yamamoto Y, Yun X (1992). Coordinating Locomotion and manipulation of a mobile manipulator. *Proceedings of 31st IEEE Conference Decision and Control*, Tucson, AZ, pp. 2643-2648

- [61] Cooper RA (1995). Intelligent Control of Power Wheelchairs. *IEEE Engineering in Medicine & Biology Magazine*, 14(4): 423-430

- [62] Ding D, Cooper RA (2005) A review of the current state of electric powered wheelchairs. *IEEE Control Systems Magazine*, 25(2): 22-34

- [63] Gustafsson F (1997). Slip-based tire-road friction estimation. *Automatica*, 33(6): 1087-1099

- [64] Ojeda L, Reina G, Borenstein J (2004). Experimental results from FLEXnav: An expert rule-based dead-reckoning system for Mars rovers. *IEEE Aerospace Conference*

- [65] Ojeda L, Cruz D, Reina G, Borenstein J (2006). Current-based slippage detection and odometry correction for mobile robots and planetary rovers. *IEEE Transactions on Robotics*, 22(2): 366-378

- [66] Tan H, Chin Y (1992). Vehicle antilock braking and traction control: a theoretical study. *International Journal of Systems Science*, 23(3): 351-365

- [67] Automotive Handbook (2000). 5th edition, Robert Bosch GmbH, Germany
- [68] Sukkariéh S, Nebot E, Durrant-Whyte H (1999). A high integrity IMU/GPS navigation loop for autonomous land vehicle applications. IEEE Transactions on Robotics and Automation, 15(3): 572-578
- [69] Hofmann-Wellenhof B, Lichtenegger H, Collins J (2001). Global Positioning System: Theory and Practice, 5th ed., Springer-Verlag, Wien
- [70] GPS 16/17 Series Technical Specifications (2005). Garmin Intl., Inc
- [71] Ward C, Iagnemma K (2007). Model-based wheel slip detection for outdoor mobile robots. IEEE International Conference on Robotics and Automation
- [72] Ward C, Iagnemma K (2007) Classification-based wheel slip detection and detector fusion for outdoor mobile robots. IEEE International Conference on Robotics and Automation
- [73] Ding D, Cooper RA, Guo S, Corfman TA (2003). A study on modeling an electric-powered wheelchair. RESNA 26th International Annual Conference
- [74] Ding D, Cooper RA, Guo S, Corfman TA (2003). Robust velocity control simulation of a power wheelchair, RESNA 26th International Annual Conference
- [75] Craig JJ (2004). Introduction to Robotics: Mechanics and Control. Prentice Hall, 3rd edition
- [76] Rizzoni G (2000). Principles and Applications of Electrical Engineering. McGraw-Hill
- [77] Tadano S, Tsukada A (2000). Some mechanical problems to use electric wheelchairs in a snowy region. Human Biomechanics and Injury Prevention, page: 199-204

- [78] Makki A, Siy P (1993). A robust traction controller design using the theory of variable structure systems. Proceedings of the 36th Midwest Symposium on Circuits and Systems, page: 356-359
- [79] Tan HS, Tomizuka M (1990). Discrete-Time Controller Design For Robust Vehicle Traction. IEEE Control Systems Magazine, 10(3): 107-113
- [80] U.S. Department of Health and Human Services (2000). Healthy people 2010: Understanding and improving health. 2nd ed. Washington (DC): U.S. Department of Health and Human Services
- [81] Cooper RA, Cooper R, Boninger ML (2008). Trends and issues in wheelchair and seating technologies. Assistive Technology, 20(2): 61-72
- [82] Salatin B, Wang H, Grindle GG, Ding D, Cooper RA (2009). Electric powered wheelchair driving strategies over difficult outdoor terrain: A focus group study. Proceedings of the Rehabilitation Engineering and Assistive Technology Society of North America Conference, CD-ROM, June 23-27
- [83] Salatin B, Wang H, Grindle GG, Cooper RA (2008). Quantifying forward tipping characteristics of a front wheel drive electric powered wheelchair. Proceedings of the Rehabilitation Engineering and Assistive Technology Society of North America Conference, CD-ROM, June 26-30
- [84] Kaye SH, Kang T, LaPlante MP (2002). Wheelchair use in the United States, San Francisco: Disability Statistics Center
- [85] U.S. Access Board Washington, DC. Available from <http://www.ap.buffalo.edu/idea/Anthro/spacerequirementsforwheeledmobility.htm>
- [86] Auger C, Demers L, G elinas I, Jutai J, Fuhrer MJ, DeRuyter F (2008). Powered mobility for middle-aged and older adults: systematic review of outcomes and appraisal of published evidence, American Journal of Physical Medicine and Rehabilitation, 87(8): 666-80

- [87] Evans S, Frank AO, Neophytou C, De Souza L (2007). Older adults' use of and satisfaction with Electric Powered Indoor/outdoor Wheelchairs (EPIOCs). Oxford University Press, 36(4):431-435
- [88] Ding D, Cooper RA, Guo S, Corfman TA (2004). Analysis of Driving Backwards in an Electric-Powered Wheelchair, IEEE Transactions on Control Systems Technology, 12(6): 934-943
- [89] Van Drongelen A, Roszek B, Hilbers-Modderman E, Kallewaard M, Wassenaar C (2002). Wheelchair incidents. RIVM, Bilthoven
- [90] Kirby RL, Ackroyd-Stolarz SA (1995). Wheelchair safety--adverse reports to the United States Food and Drug Administration. American Journal of Physical Medicine & Rehabilitation, 74(4): 308-312
- [91] Xiang H, Chany AM, Smith GA (2006). Wheelchair related injuries treated in US emergency departments. Injury Prevention, 12(1): 8-11
- [92] Brose S, Weber D, Salatin B, Grindle GG, Wang H, Vazquez JJ, Cooper RA (2010). The Role of Assistive Robotics in the Lives of Persons with a Disability, American Journal of Physical Medicine and Rehabilitation, 89(6): 509-521
- [93] Wang H, Salatin B, Grindle GG, Ding D, Cooper RA (2009). Real-Time Model Based Electrical Powered Wheelchair Control, Medical Engineering and Physics, 31(10): 1244-1254
- [94] Wang H, Salatin B, Grindle GG, Ding D, Cooper RA (2009). Real-time Slip Detection and Traction Control of Electrical Powered Wheelchairs, Proceedings of the Rehabilitation Engineering and Assistive Technology Society of North America Conference, CD-Rom, June 23-27, 2009
- [95] Wang H, Salatin B, Grindle GG, Bachman E, Ding D, Cooper RA (2010). Real-Time Forwarding Tipping Detection and Prevention of a Front Wheel Drive Electric Powered Wheelchair, Proceedings of the Rehabilitation Engineering and Assistive Technology Society of North America Conference, Las Vegas, NV, CD-Rom, June 26-30, 2010

- [96] Cooper RA, Cooper R, Boninger ML (2008). Trends and issues in wheelchair and seating technologies, *Assistive Technology*, 20(2): 61-72
- [97] Wang H, Coyle E, Chung C, Bates W, Ding D, Collins E, Cooper RA (2011). How Driving Parameters Affect an Electrical Powered Wheelchair's Slip on Different Terrains, Proceedings of the Rehabilitation Engineering and Assistive Technology Society of North America Conference, Toronto, ON, Canada, CD-ROM, June 5-8, 2011
- [98] Vanderwerp D (2005). What does terrain response do? Retrieved from: <http://www.caranddriver.com/features/what-does-terrain-response-do>
- [99] Ford Media: 2011 Ford Explorer Terrain Management System (2010), available from http://media.ford.com/images/10031/2011_Explorer_TMS.pdf
- [100] Jeep.Com: 2012 Jeep Grand Cherokee Selec-Terrain System (2011), available from http://www.jeep.com/en/2012/grand_cherokee/capability/off_road_performance/#
- [101] ADA Accessibility Guidelines for Buildings and Facilities (ADAAG) (2002), available from: <http://www.access-board.gov/adaag/html/adaag.htm#4.8>
- [102] Cooper RA, Thorman T, Cooper R, Dvorznak MJ, Fitzgerald SG, Ammer W, Song-Feng G, Boninger ML (2002). Driving Characteristics of Electric Powered Wheelchair Users: How Far, Fast, and Often do People Drive? *Archives of Physical Medicine and Rehabilitation*, 83(2): 250-255
- [103] Salatin B, Wang H, Grindle GG, Cooper RA, Quantifying Forward Tipping Characteristics of a Front Wheel Drive Electric Powered Wheelchair, Proceedings of the Annual RESNA Conference, Arlington VA, CD-ROM, June 26-30, 2008
- [104] Buning ME, Angelo JA, Schmeler MR (2001). Occupational performance and the transition to powered mobility: a pilot study. *American Journal of Occupational Therapy* 55(3):339-344
- [105] Brandt A, Iwarsson S, Stahle A (2004). Older people's use of powered wheelchairs for activity and participation. *Journal of Rehabilitation Medicine*, 36(2):70-77

- [106] Evans R (2000). The effect of electrically powered indoor/outdoor wheelchairs on occupation: a study of users' views. *British Journal of Occupational Therapy*, 63(11):547-553
- [107] Wressle E, Samuelsson K (2004). User satisfaction with mobility assistive devices. *Scandinavian Journal of Occupational Therapy*, 11(3):143-150
- [108] Mortenson WB, Miller WC, Boily J, Steele B, Odell L, Crawford EM, Desharnais G (2005). Perceptions of power mobility use and safety within residential facilities. *Canadian Journal of Occupational Therapy*, 72(3):142-152
- [109] Cooper RA (1999). Engineering manual and electric powered wheelchairs. *Critical Reviews™ in Biomedical Engineering*, 27(1-2):27-73
- [110] Cooper RA, Dicianno BE, Brewer B, LoPresti E, Ding D, Simpson RC, Grindle GG, Wang H (2008). A Perspective on Intelligent Devices and Environments in Medical Rehabilitation, *Medical Engineering and Physics*, 30(10): 1387-1398
- [111] Edlich RF, Nelson KP, Foley ML, Buschbacher RM, Long WB, Ma EK (2004). Technological advances in powered wheelchairs. *Journal of Long-Term Effects of Medical Implants*, 14(2): 107-130
- [112] Field D (1999). Powered mobility: a literature review illustrating the importance of a multifaceted approach. *Assist Technology*, 11(1):20-33
- [113] McClain L, Cram A, Wood J, Taylor M (1998). Wheelchair accessibility- living the experience: function in the community. *Occupational Therapy Journal of Research*, 18(1):25-43
- [114] de KortYAW, Midden CJH, van Wagenberg AFGM (1998). Predictors of the adaptive problem solving of older persons in their homes. *Journal of Environmental Psychology*, 18(2):187-197
- [115] Lawton MP (1989). Environmental proactivity. In Spacapan S, Oskamp S, eds. *The course of later life*. New York: Springer Publishing Company; 1989

- [116] Fange A, Iwarsson S, Persson A (2002). Accessibility to the public environment as perceived by teenagers with functional limitations in a south Swedish town centre. *Disability and Rehabilitation*, 24(6): 318-326
- [117] Evans S, Neophytou C, De Souza L, Frank A O (2007). Young people's experiences using electric powered indoor - outdoor wheelchairs (EPIOCs): potential for enhancing users' development. *Disability and rehabilitation*, 29(16): 1281-1294
- [118] Evans S, Frank AO, Neophytou C, De Souza L (2007). Older adults' use of and satisfaction with Electric Powered Indoor/outdoor Wheelchairs (EPIOCs). Oxford University Press, 36(4):431-435
- [119] Laffont I, Guillon B, Fermanian C, Pouillot S, EvenSchneider A, Boyer F, Ruquet M, Aegerter P, Dizen O, Lofaso F (2008). Evaluation of a stair-climbing power wheelchair in 25 people with tetraplegia. *Archives of physical medicine and rehabilitation*, 89(10):1958-1964
- [120] Kemcare Ltd, 2005. Available from <http://www.kemcare.co.nz/>
- [121] Cooper RA, Boninger ML, Cooper R, Fitzgerald SG, Kellerher A (2004). Preliminary assessment of a prototype advanced mobility device in the work environment of veterans with spinal cord injury. *Neurological Rehabilitation*, 19 (2):161-170
- [122] Uustal H, Minkel JL (2004). Study of the Independence IBOT 3000 Mobility System: an innovative power mobility device, during use in community environments. *Archives of physical medicine and rehabilitation*, 85(12):2002-2010
- [123] Giuseppe Q, Franco W, Oderio R (2011). Wheelchair.q, a motorized wheelchair with stair climbing ability. *Mechanism and Machine Theory* (August 2011)
- [124] Giuseppe Q, Franco W, Oderio R. 2009. Wheelchair.q, a mechanical concept for a stair climbing wheelchair. In *Proceedings of the 2009 international conference on Robotics and biomimetics (ROBIO'09)*. IEEE Press, Piscataway, NJ, USA, 800-805
- [125] Morales R, Feliu V, González A, Pintado P (2003). A New Staircase Climbing Wheelchair. 13th International Symposium on Measurement and Control in Robotics, ISMRC'03, Madrid, December 2003

- [126] Morales R, Feliu V, González A, Pintado P (2005). A Prototype of a New Staircase Climbing Wheelchair. 14th International Congress on Computing, CIC05, Mexico City, September 2005
- [127] Morales R, Feliu V, González A, Pintado P (2004). Kinematics of a New Staircase Climbing Wheelchair. 7th International Conference on Climbing and Walking Robots, CLAWAR 2004, Madrid, September 2004
- [128] Morales R, Feliu V, Gonzalez A, Pintado P (2006). Coordinated motion of a new staircase climbing wheelchair with increased passenger comfort. Robotics and Automation, 2006. ICRA 2006. Proceedings 2006 IEEE International Conference on, on page(s):3995 – 4001, May 2006
- [129] Morales R, Feliu V, Gonzalez A, Pintado P (2006). Kinematic Model of a New Staircase Climbing Wheelchair and its Experimental Validation. The International Journal of Robotics Research, 25(9):825-841
- [130] Morales R, Gonzalez A, Feliu V, Pintado P (2007). Environment adaptation of a new staircase-climbing wheelchair, Autonomous Robots, 23(4):275-292
- [131] Gonzalez A, Morales R, Feliu V, Pintado P (2007). Improving the mechanical design of a new staircase climbing wheelchair. Industrial Robot: An International Journal, 34(2):110-115
- [132] Chen CT, Pham HV (2008). Enhanced development and stability analysis of a new stair-climbing robotic wheelchair. IEEE International Conference on Advanced Robotics and its Social Impacts, Taipei, Taiwan, Aug. 23-25, 2008 page: 1-6
- [133] Galileo Mobility, 2011, available from http://www.galileomobility.com/?page_id=39
- [134] Nakajima Lab, 2010, available from <http://www.nakajima-lab.it-chiba.ac.jp/research/mover.html>

- [135] Grindle GG, Wang H, Salatin B, Vazquez JJ, Cooper RA (2011). Design and Development of the Personal Mobility and Manipulation Appliance (PerMMA). *Assistive Technology*, 23(2): 81-92
- [136] Astrom KJ, Hagglund T (1995). *PID controllers: Theory, Design and Tuning*, 342pp. Instrument Society of America
- [137] Open Dynamics Engine, available from <http://www.ode.org/>
- [138] Tomokuni N, Shino M, Kamata M (2008). Improving stability for a two-legged inverted-pendulum-type vehicle equipped with a slider, in *Proceedings of 17th Annual Conference on Japan Society of Mechanical Engineering, Transportation and Logistics Division*, 2008, pp. 373-376
- [139] Clements K, Geddes J, Bebb M, Reeves J (2004). Lateral tilt in space: an innovative design for a unique problem. 2004. <http://e-bility.com/arataconf/papers/doc/clements.doc>
- [140] Hardwick K, Stewart S (1994). Raising the comfort level. *Teamrehab Report*, 11:27-31
- [141] Cooper D (2004). A retrospective of three years of lateral tilt-in-space. *Proceedings of the International Seating Symposium*, 2004, 205-209
- [142] ABA Accessibility Guidelines for Buildings and Facilities <http://www.access-board.gov/adaag/html/adaag.htm>